Universidad de Valladolid


UNIVERSIDAD DE VALLADOLID

ESCUELA DE INGENIERIAS INDUSTRIALES

Grado en Ingeniería Química

# Diseño de procesos catalíticos con la utilización de $CO_2$

Autor:

Rodrigues De Freitas, Jesús

Bolado Rodríguez, Silvia

Universiteit Gent

Valladolid, Septiembre 2018

TFG REALIZADO EN PROGRAMA DE INTERCAMBIO

---

TÍTULO: Design of $CO_2$ utilization catalytic processes

ALUMNO: Jesús Rodrigues De Freitas

FECHA: 06/09/2018

CENTRO: Laboratory of Chemical Technology (LCT)

TUTOR: César Urbina Blanco

## Resumen en Castellano

El diseño y estudio de dos importantes procesos catalíticos usando $CO_2$ han sido realizados: su acoplamiento reductivo con etileno y su metanación.

Por un lado, para el primer proceso se han desarrollado cálculos DFT usando Gaussian 16 para definir el mecanismo de reacción constituido por el acoplamiento oxidativo y la β-eliminación. Se han diseñado dos mecanismos acoplando un etileno y dos etilenos a cada ligando usado en este proyecto, obteniéndose un resultado más favorable a partir del mecanismo planteado con el primero.

Por otro lado, el estudio de metanación de $CO_2$ indica que la influencia de la presión y la temperatura es significativa sobre que la de parámetros como la conversión de los reactivos y la producción de metano. Las condiciones ideales para el proceso son: una temperatura de 550 K y altas presiones. La relación molar de los reactantes debe ser estimada a través de un balance de energía.



## Palabras Clave

Dióxido de carbono, metanación, acoplamiento reductivo, DFT y catálisis homogénea.

# Design of $CO_2$ utilization catalytic processes

Jesús Rodrigues De Freitas

Supervisors: Prof. dr. ir. Mark Saeys
Counsellor: César Alejandro Urbina Blanco

Dissertation submitted in order to obtain the academic degree of Degree of Chemical Engineering

Faculty of Engineering and Architecture
Academic year 2017-2018

GHENT UNIVERSITY

Universidad de Valladolid

# Confidentiality notice

This master dissertation contains confidential information and/or confidential research results proprietary to Ghent University. It is strictly forbidden to publish, cite or make public in any way this master dissertation or any part thereof without the express written permission of Ghent University. Under no circumstance this master dissertation may be communicated to or put at disposal of third parties. Photocopying or duplicating it in any other way is strictly prohibited. Disregarding the confidential nature of this master dissertation may cause irremediable damage to Ghent University. The stipulations above are in force until the embargo date 12/31/9999.

Jesús Rodrigues De Freitas

August 2018

# Acknowledgements

First of all, I want to thank Professor César Urbina Blanco, for his dedication, time and work so I could continue with the present project. He has been who has guided me and facilitated me every of the tools that have been necessary to study all aspects for the design of carbon dioxide processes. He has served as the basis, in addition to the present project, to learn new programs and have new experiences with the world of organometallic chemistry, with which I had never had contact.

Secondly, I want to thank Professor Andrés León, for helping me in everything he could and for clarifying my doubts about the program and thanks to this experience, I have applied the knowledge that I acquired.

To the University of Ghent, and specifically to Professor Mark Saeys, for giving me the opportunity to live this experience in my Erasmus, which has served me not only to grow professionally, but to train me in my career and to live so many moments that I take with me, strengthening me as a person and helping me mature in different facets.

To the University of Valladolid, for allowing me to live this experience, for its help from many perspectives and for training me as a future chemical engineer, to my professors and colleagues, from whom I have learned so many things and could not be more grateful.

To my family, for supporting me at all times, and despite the distance, even though they are not physically with me in this experience, they have motivated me when necessary and have encouraged me to move forward.

To Venezuela, because it is my seed, the place where I was born and where I feel proud to be. Grateful for taking the name of my country and being able to leave the name on high, because at this moment we are going through a so hard situation that it cannot be explained.

Having nothing else to add, thank you very much.

UNIVERSITEIT GENT

FACULTY OF **ENGINEERING AND ARCHITECTURE**

**Laboratory for Chemical Technology**
Director: Prof. Dr. Ir. Guy B. Marin

Laboratory for Chemical Technology

# Declaration concerning the accessibility of the master thesis

Undersigned,

*Jesús Rodrigues De Freitas*

Erasmus student in Ghent University, academic year 2017-2018 and is author of the thesis with title:

*Design of $CO_2$ utilization catalytic processes*

The author gives permission to make this master dissertation available for consultation and to copy parts of this master dissertation for personal use. In the case of any other use, the copyright terms have to be respected, in particular with regard to the obligation to state expressly the source when quoting results from this master dissertation.

August 10th, 2018

Jesús Rodrigues De Freitas

# Design of $CO_2$ utilization catalytic processes

Author: Jesús Rodrígues De Freitas

Supervisors: Prof. dr. ir. Mark Saeys
Counsellor: dr. César Alejandro Urbina Blanco

Dissertation submitted in order to obtain the
academic degree of Chemical Engineering

Department Of Materials, Textiles And Chemical Engineering
Academic year 2017-2018
Faculty of Engineering and Architecture
Ghent University

***Abstract***

A design and study for two important $CO_2$ utilization catalytic processes: its reductive coupling with ethylene to produce acrylic acid and its methanation to produce methane.

From one hand, DFT calculations have been done using Gaussian 16 to define the reaction mechanism constituted by the oxidative coupling and the β-hydride elimination, considered the most limiting step in the reaction, which has a more favorable mechanism from the *cis* conformer. N-Heterocyclic carbenes have been used as ligands to study two different reaction mechanisms depending on nickel chemical properties. The first mechanism starts with one ethylene and the second mechanism with two ethylenes. They differ in the way the oxidative coupling takes place, obtaining later a different intermediate and in the fact one ethylene might be dissociated. Different causes as the squared plannar geometry in the metallic center, possible agostic interactions and so more on bring a better stability in the structures. The most optimal ligands are the ones with better steric control as it is found in the literature.

On the other hand, $CO_2$ methanation study has indicated that the influence of pressure and temperature is significantly over different parameters as reagents conversion, methane production and carbon monoxide production. The ideal conditions to obtain a higher hydrogen conversion and methane production are: a temperature of 550 K and high pressures. However, a complete energy balance might be done considering the different machines as compressors, heat exchangers and separators to determine which is specifically the best molar ratio for this process and to verify how high the pressure needs to be without affecting the energetic cost.

---

***Keywords*** Reductive coupling, Density Functional Theory, homogenous catalysis, N-Heterocyclic carbenes, nickel, $CO_2$ methanation.

# Design of $CO_2$ utilization catalytic processes

Jesús Rodrigues De Freitas

Supervisor(s): Mark Saeys

Coach(s): César Urbina Blanco

***Abstract*: This article studies two different $CO_2$ utilization catalytic processes: its reductive coupling with ethylene to produce acrylic acid and its methanation to produce methane. The first has been studied through Gaussian 16 using nine N-heterocyclic carbenes with different steric and electronic properties, obtaining that the β-elimination is the limiting step in two reaction mechanisms. For the second process, there have been done different simulations using Aspen Plus, resulting low temperatures and low pressures as optimal conditions. However, the molar ratio between reactants might be chosen after a complete energy balance.**

***Keywords*: Reductive coupling, Density Functional Theory, homogenous catalysis, N-Heterocyclic carbenes, nickel, $CO_2$ methanation.**

## I. Introduction

Carbon dioxide ($CO_2$) is considered today to be the major cause of climate change, due to its greenhouse properties and its continuous accumulation in the atmosphere.[1] At the same time, the atmospheric concentration of this compound rose from 278 ppm during the preindustrial times to a current level of approximately 411.68 ppm,[2]meaning that the use of carbon based fossil fuels in human activities (representing almost 80-85% of the world's energy sources) could increase more causing worse effects.[3] However, carbon is not the only source of $CO_2$, because it can be originated from petroleum or even gas combustion, so the problem comes from several causes.[4]

For this reason, it must be found measures to reduce $CO_2$ emissions and with them it would be possible to attack some threats that are kept being a disadvantage for the world, such as the global warming and so on. Carbon dioxide could take a different pathway in comparison with the ones used nowadays. Due to its reactivity, two possible examples are the reductive coupling between carbon dioxide and ethylene in which the acrylic acid is obtained. Secondly, the methanation process consisting in the reaction between this gas and hydrogen to produce methane. For the first case, it is a potential alternative route to acrylic acid or acrylate, because they have been studied employing various (transition) metal complexes.[5] In the second one, the Sabatier process or also called methanation, can also be used to reduce $CO_2$ generated in a space habitat to reclaim the oxygen for recycle.

The reductive coupling between carbon dioxide and ethylene can be studied through N-heterocyclic carbenes. This type of complex compounds is now widespread[6]; these exciting species have found applications in transition metal chemistry[7], as organocatalysts.[8]and as reagents to stabilize geometries and oxidation states of main group elements.[7] At the same time, their recognized popularity can be attributed to several factors as their highly molecular leading to their large structural and stereoelectronic diversity and the fact of being prepared easily with strong metal-NHC bonds.[9] Besides, NHC have two important characteristics that might be considered at the time of deciding to use them as catalysts: their electronic properties and their steric properties.[10]

## II. Methods

Computational programs have been used to design and study the $CO_2$ utilization catalytic processes.

### *A. Method for the reductive coupling of carbon dioxide with ethylene*

The program used to study the reductive coupling between $CO_2$ and ethylene is Gaussian 16, starting from the following mechanism found in Figure 1.

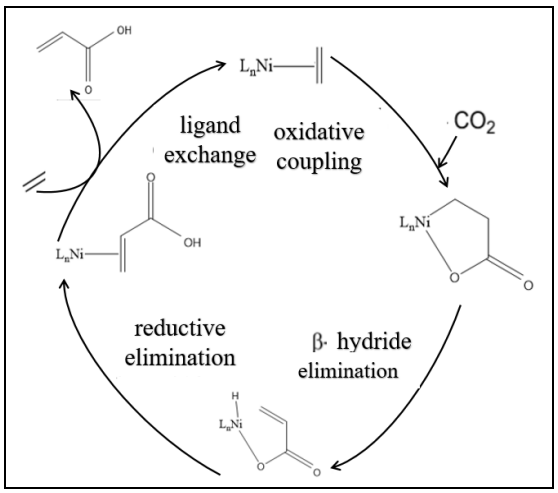


Figure 1. Reaction mechanism proposed by Hollering et al.[5]

Each intermediate was built in Gaussian 16, sent to optimize and after it has converged, it has been performed a rotational scan study through a 360º rotation in a dihedral scan, consisting in sweeps of 36 steps of 10º each, with the aim of studying the conformer with the lowest energy and from this obtaining the structure the most stable as possible. Once each of them has been obtained, then there have been done diverse types of bond scans to look for possible transition states for the oxidative coupling (the approaching of $CO_2$ carbon to each of the ethylene carbons) and for the β-hydride elimination (the approaching of the β-hydrogen to the metallic atom).

Using these scans, when a possible result is found, it is sent as a possible transition state (TS) and if it shows an imaginary frequency associated with the reaction mechanism and it converges in all the aspects, an IRC is performed (Intrinsic Reaction Coordinate) in both directions (forward and reverse) to determine that it is precisely the searched transition state.

Then, based on this energy values, the partial Gibbs free energy diagrams have been built for each ligand and then it is determined how these ligands participate in the steps such as the oxidative coupling and the most limiting step: β-hydride elimination.

In addition, for these calculations it has been applied the functional PBE1BE, based on the functional PBE. The polarized divided valence (SVP) has been applied through the base Def2SVP considering the equations that approximate to the Schrödinger equation according to Koch et al.[11].

The nine ligands used for this investigation are shown in Figure 2.

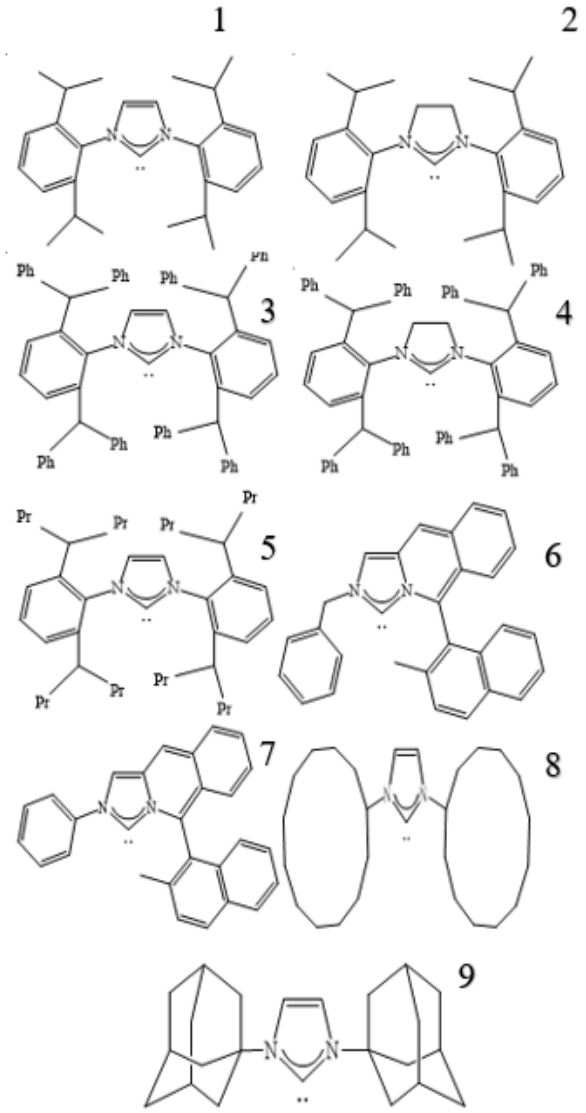


Figure 2. N-Heterocyclic carbenes used as ligands. IPr (1), SIPr (2), IPr* (3), SIPr* (4), IHept (5), Isoqui (6), ISO (7), IDD (8) and IAd (9)

All these ligands are constituted by an ylidene ring and they have been chosen due to the clasiffication studied by Gómez-Álvarez et al.[12] about these ligands in N-alkyl and N-aryl ligands according to their electronic and steric properties.

### *B. Method for carbon dioxide methanation*

$CO_2$ methanation takes place in the following raction:

$$CO_2 + 4H_2 \leftrightarrows CH_4 + 2H_2O \qquad \Delta H = -206.28 \text{ kJ mol}^{-1} \quad (1)$$

At the same time, there is a secondary reaction called Water Gas Shift (WGS):

$$CO + H_2O \leftrightarrows CO_2 + H_2 \qquad \Delta H = -41.16 \text{ kJ mol}^{-1} \quad (2)$$

Aspen Plus has been the main tool to study $CO_2$ methanation starting from some initial conditions that CATCO2RE has estimated for their process: **methanation catalysts**: supported Ni, Ru or Co; **conditions**: pressure of 1 atmosphere and a temperature equals or higher than 550 K, to prevent the formation of volatile Ni-carbonyls; **selectivity**: 100% for stoichiometric feeds (will depend on feed composition); **conversion**: as higher as possible, but it is better if it is 100%.; **reactor dimensions & catalyst amount**: 1 cm diameter, ~0.5 g of 15 wt.% Ni on y-$Al_2O_3$ (75% conversion, no heat or mass transfer limitations and negligible pressure drop) and **catalyst stability**: sulfur, water and so on.

In this case, it has been used a Gibbs reactor to minimize the Gibbs Free energy for each reaction, without considering the kinetics involved in them. Using this reactor and the thermodynamic model chosen for the study: Peng-Robinson (PR), several sensitivity analyses have been done to study the influence of the temperature, pressure and $H_2/CO_2$ molar ratio over different parameters as reactants conversion, methane production, methane yield, methane molar fraction and carbon monoxide production.

Thus, an energy balance has been estimated using the simulations results and a design process has been proposed to detail this balance. Then, diverse types of waste (household waste, wastewater treatments and waste of agrifood) have been considered as feed for the reactor with different compositions, as it is shown in Table 1.

Table 1. Feed compositions according to the type of waste

| Compound | Household Waste (average) (feed molar fraction %) | Household Waste (higher) (feed molar fraction %) | Household Waste (lower) (feed molar fraction %) | Wastewater treatment (average) (feed molar fraction %) | Wastewater treatment (higher) (feed molar fraction %) | Wastewater treatment (lower) (feed molar fraction %) | Waste of agrifood industry (feed molar fraction %) |
|---|---|---|---|---|---|---|---|
| **$CH_4$** | 55.27 | 50.5 | 60.00 | 67.50 | 60.00 | 75.00 | 68.00 |
| **$CO_2$** | 36.19 | 38.38 | 34.00 | 26.00 | 33.00 | 19.00 | 26.00 |
| **$N_2$** | 2.51 | 5.05 | 0.00 | 0.50 | 1.00 | 0.00 | 0.00 |
| **$H_2O$** | 6.03 | 6.06 | 6.00 | 6.00 | 6.00 | 6.00 | 6.00 |

## III. Results and Discussion

### *A. Results for the reductive coupling of carbon dioxide with ethylene*

The different ligands used for this investigation have been divided into three groups considering their steric control studied by Gómez-Álvarez et al.[12]: IHept, IPr* and SIPr* (first group), IPr, SIPr and IAd (second group) and finally IDD, ISO and Isoqui (third group). There have been studied two different reaction mechanisms: the first constituted by one

ethylene and the second constituted by two ethylenes, owing to the stability the metallic center (nickel) acquires with 16 electrons counted in accordance with the 18-electron rule for organometallic compounds. In Figure 3, it is shown the first proposed reaction mechanism and in Figure 4, it is shown the correspondent partial energy diagram for the first group.

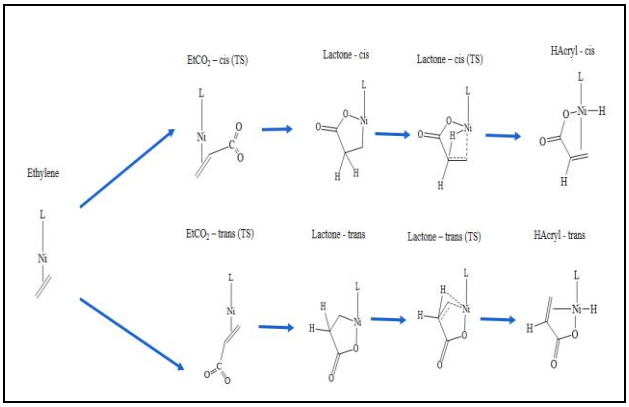


Figure 3. First reaction mechanism

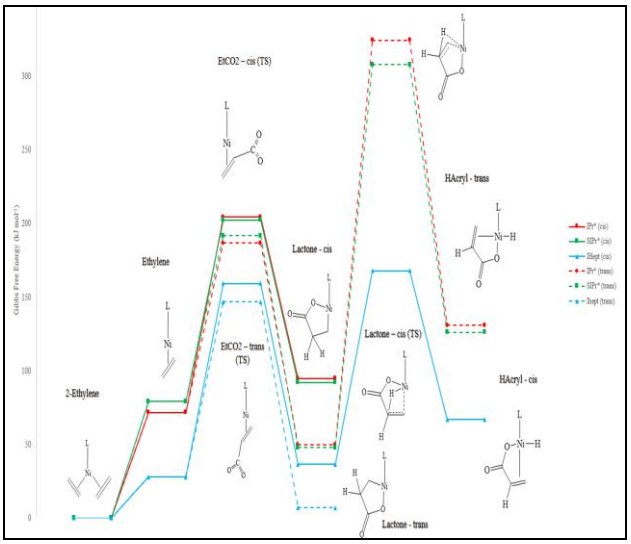


Figure 4. Partial energy diagram for first group in the first reaction mechanism (IPr* (red), SIPr* (green) and IHept (blue); solid line (*cis* mechanism) and dashed line (*trans* mechanism)

The first aspect that may be mentioned is referred to the presence of the two ethylenes bound to the organometallic compound in the diagrams. The latter is more stable than the one with just one ethylene, so that is why it has been used as the reference to estimate the Gibbs Free energy for each step in the mechanism. In the three groups, as it happens in Figure 4, in the first step (the oxidative coupling), it has been obtained that the β-coupling gets higher energies than the α-coupling, due to the high energetic cost it takes to obtain the *cis*-lactone in comparison with the *trans*-lactone, which at the same time are more stable than the others.

The limiting step in the proposed mechanism is the β-elimination, as it has been stablished by Buntine et al.[13] due to the high kinetic barrier that it might be beaten. The transition state from the *trans*-lactone to the hydride acrylate-trans is too high, taking values of almost 350 kJ $mol^{-1}$, which is practically undesired and impossible to develop in real life. Nevertheless, while it is true that the *cis*-lactone (transition state) is more stable but with high energies too, at the time of looking for the ideal mechanism, this becomes the key step to choose between one or the another.

Regarding ligands, IDD represents the ligand with the highest Gibbs Free energies in almost all the steps, which coincides with the study done by Gómez et al.[12] and the definition of this ligand as the one with less steric control among the studied in this investigation.

Thus, IHept represents the ligand with more stability, mentioned by Gómez et al.[12] as the bulkiest among the studied, which can be seen in the previous Figure through the energies in comparison with IPr* and SIPr*. At the same time, the ligands not study by them, Isoqui and ISO have shown a favorable result for this reaction, due among other reasons to the electronic cloud coming from the aromatic rings that provides greater stability to the reagent.

The second reaction mechanism is shown in Figure 5 and the correspondent partial energy diagram for the first group, it is shown in Figure 6.

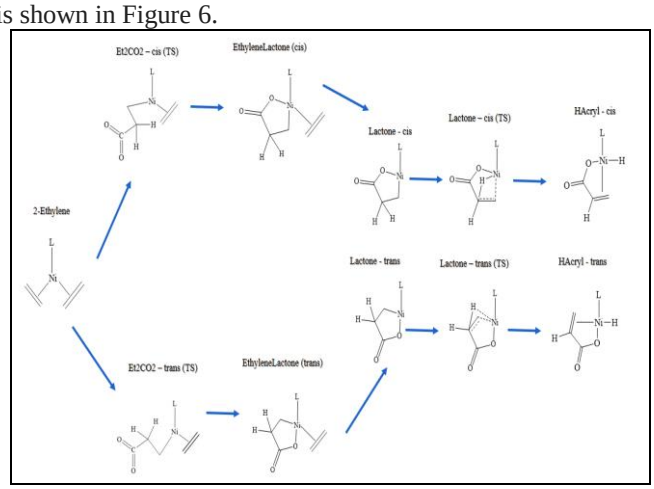


Figure 5. Second reaction mechanism

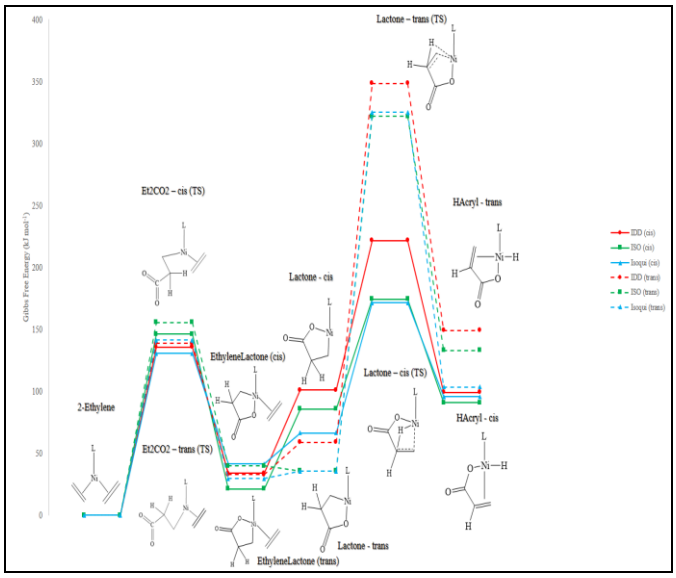


Figure 6. Partial energy diagram for first group in the first reaction mechanism (IDD* (red), ISO (green) and Isoqui (blue)); solid line (*cis* mechanism) and dashed line (*trans* mechanism)

It has been found that the transition state in the coupling has not a specific trend to be more convenient in terms of stability for the α or β carbon bond. At the same time, owing to the mistakes found in the IRC for some of the ligands, it is necessary to verify their validity. Furthermore, this mechanism becomes important when the following intermediate

conformed by an ethylene and lactone is more stable than the proper lactones, owing to the electrons the ethylene could contribute (2 electrons) to the compound, that brings more stability, besides the geometry that the metallic center acquires.

Then, both mechanisms have the same pathway starting from the β-elimination, that might occur with one ethylene. For this reason, for the second mechanism it has been found that it is not possible to produce this step with another ethylene, so this means the one not forming part of the lactone might be dissociated, as it was found by Grubbs et al.[14] and the necessary structure for which the β-elimination takes place, where the M–C–C–H unit must be able to take up a roughly syn-coplanar conformation, which brings the β hydrogen close to the metal.[15]

Hence, the importance of having lower energies in the oxidative coupling is given due to the high energies in the β-elimination. As it has been already shown, both proposed mechanisms follow the same steps after the dissociation. Energetically, the transition state for the *trans*-lactone involves an unattainable way that would not take place easily, and it also results unreal to develop in the laboratory. At the same time, the transition state after the *cis*-lactone, despite of having high energies, allow to produce the hydride acrylate that is necessary to continue to the following steps to produce acrylic acid.

## *B. Results for methanation*

### *B.1. Influence of the temperature and pressure*

The study of the influence of pressure and temperature has been done using different sensitivity analysis in Aspen Plus. In the following Figures, there are shown the effect of both parameters over the most important criterions for the study: hydrogen conversion and methane production.

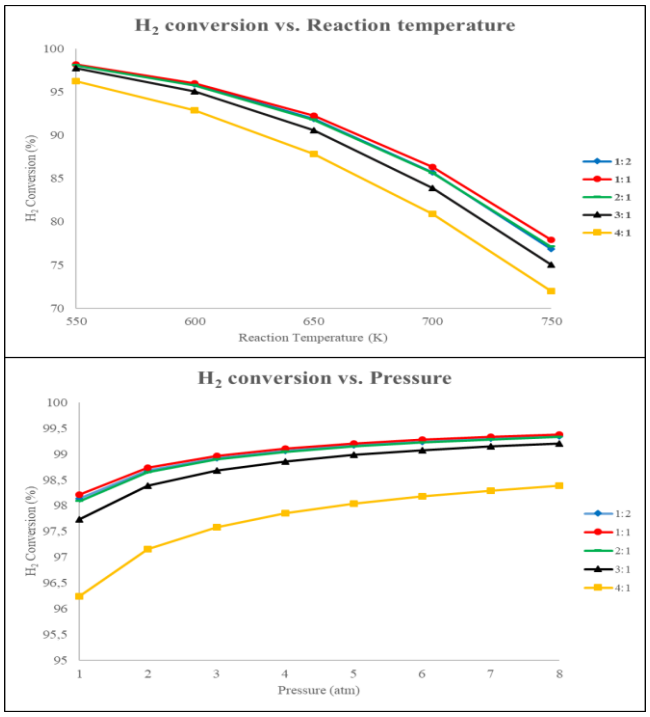


Figure 7. $H_2$ conversion vs. reaction temperature and pressure

As it is shown, $H_2$ conversion shows higher values for a equimolar ratio at low temperatures, due to the fact that when the temperature increases, the equilibrium constant decreases and the equilibrium reaction moves to the left, producing higher reactants flow and having a lower conversion. In the case of pressure, an amount of pressure involves a higher conversion, because the total of moles in the product side is lower than in the reactants, which means that the reversible reaction moves to the right.

In the case of the methane production, in Figure 8 there are shown the same parameters.

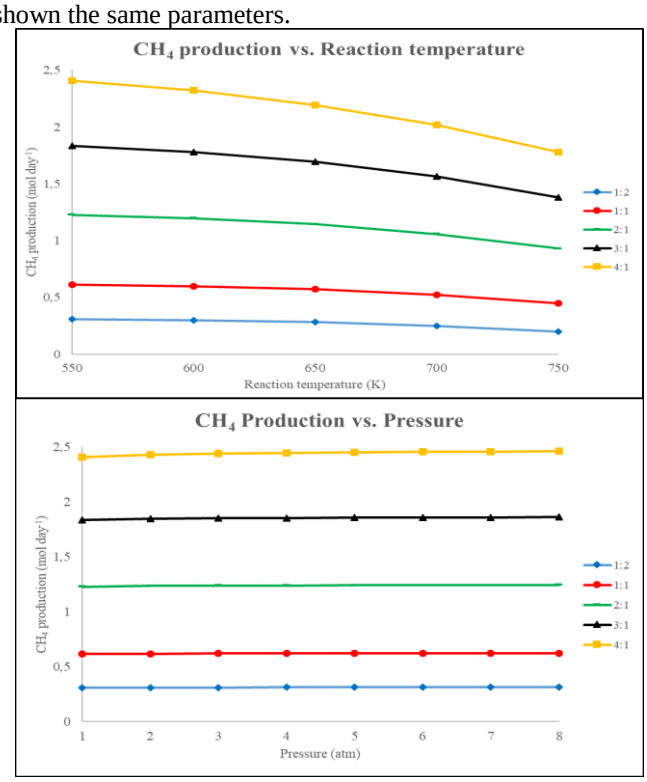


Figure 8. $CH_4$ production vs. reaction temperature and pressure

For methane production, it has been found that the stoichiometric molar ratio is more favourable in comparison with others at low temperatures, while the production increases through an amount in the pressure.

Regarding other parameters, $CO_2$ conversion is higher at low temperatures and high pressures. Water Gas Shift reaction starts at 650 K, increasing CO production while the temperature increases. The pressure does not represent a crucial factor for WGS, because it has the same number of moles in each side of the reaction. Finally, $CH_4$ yield is representantly higher regarding $CO_2$, which will be determinant for this production.

After these results, it has been concluded that the methanation needs to take place at the minimum temperature stablished in the conditions (550 K) and at high pressures. However, the molar ratio results a dilemma due to the result obtained for each criterion that becomes a contradiction. For this reason, it has been done an energy balance to determine the preference among the molar ratios.

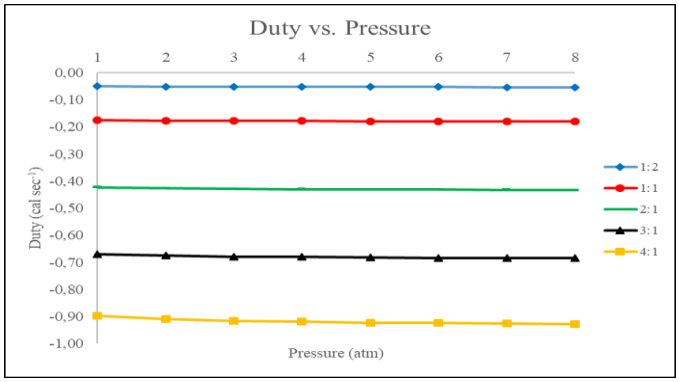


Figure 9. Duty reactor vs. Pressure

Figure 9 shows that the Gibbs reactor produces a higher duty when there are high pressures and the molar ratio increases, due to the two effects already mentioned (the increasing of reagents flow and an amount in the pressure, which generate a displacement in the reaction to the right, promoting the formation of products). According to the objectives already mentioned, this energy balance should not be focused exclusively in the reactor, because at the end it is preceded and followed by other machines and equipment which are extremely important due to the energy they use or produce in the process.

Due to this characteristic, the election of any specific pressure or molar ratio basing just on Figure 9 is not enough to rule out other conditions.

Therefore, it has been created a flow diagram considering a compressor, two heat exchangers and a separator as it has been proposed by Porubova et al.[16], to indicate how the energy may be estimated for different cases.

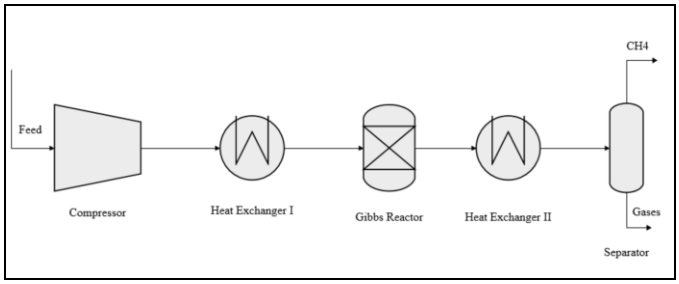


Figure 10. Proposed flow diagram

In the separator, the energy separation has been estimated using the Gibbs energy of separation (2)

$$Separation\ energy_{gases} = -R * T * \sum x_i * \ln(x_i) \quad (2)$$

which works for ideal gases using molar fractions in dry basis, because water is easier to separate in comparison with the rest of gases. This is not the exactly case, but it brings an idea on how the energetic behavior is. In Figure 11, it is shown the result of this calculation.

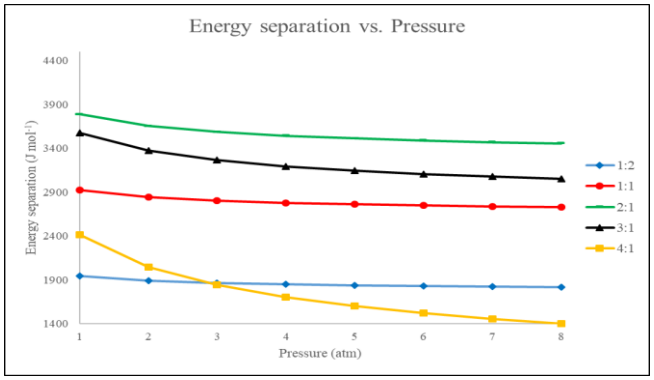


Figure 6.10 Energy separation vs. pressure

Differing from the previous case, energy separation seems to acquire the lowest values at high pressures and a stoichiometric ratio. For this reason, it is needed to do a total energy balance considering each energy to stablish a final judgement about the optimal conditions, because energy separation is just a part of the entire calculation.

*B.2. Study of types of waste*

It has been determined that wastewater treatments have a more adequate result for the methanation, owing to the kinetics and thermodynamics involved in the reaction that is favorized when $H_2$ molar ratio:the rest of gases in the feed is necessary to not exceed the determined boundaries shown in the methods (hydrogen molar fraction is even higher for household water treatments).

## IV. Conclusions

First, the reductive coupling of $CO_2$ with ethylene has been studied through homogeneous catalysis. There have been proposed two different mechanism reactions: the first starting with one ethylene and the second with two ethylenes, to complete the stability of 16 electrons in nickel complex. The studied steps, the oxidative coupling and the β-elimination have been considered following two different pathways depending on which $CO_2$ carbon is bound: *cis* (for β-ethylene carbon) and *trans* (for α- ethylene carbon).

The β-elimination produced via the *trans*-lactone has been found practically impossible to put in practice, because the Gibbs Free Energy have resulted to be even 350 kJ $mol^{-1}$, which is unattainable in the experimental design. Therefore, the pathway considered for the reaction to take place starts from the α-coupling through the first reaction mechanism, because it has not been determined how it would be the ethylene dissociation for the second mechanism that could involve higher energetic costs. Finally, the most optimal ligands according to the results have been IHept, Isoqui and ISO, which have registered favorable energies in the process and this is desired in terms of the reaction, that might be completed to verify its validity until the acrylic acid production.

Secondly, the study of the $CO_2$ methanation done through the design of a Gibbs reactor in Aspen Plus has allowed to determine that the preferred temperature according to the exothermic behaviour of the reactions is 550 K, precisely the one stablished as the minimum, because higher temperatures would imply lower hydrogen conversions and worse methane production. In addition, pressure is a magnitude that would favorize this reaction when it acquires higher values than the atmospheric one. Regarding the reactants molar ratio, from the

beginning it is hard to determine a specific relation according to the goals, in view they have opposite effects if they are taken higher or lower values than the stoichiometric ratio, what leads to do an energy balance.

The separation energy has been estimated from the supposition of working with ideal gases and it just brings an idea on how much energy would be obtained from determined pressures and molar ratios. It is obtained that for the stoichiometric ratio brings the most optimal energy, without taking a complete analysis. Finally, it has been found that wastewater treatments have a more adequate result for the methanation, owing to the kinetics and thermodynamics involved in the reaction that is favorized when $H_2$ molar ratio/the rest of gases is necessary to not exceed the determined boundaries shown in the methods, in comparison with household and agrifood wastes.

## ABBREVIATIONS

| | |
|---|---|
| **DFT** | Density Functional Theory |
| **IAd** | 1,3-Diadamantylylimidazol-2-ylidene |
| **IDD** | 1,3-Dicyclododecylimidazol-2-ylidene |
| **IHept** | 1,3-Bis(2,6-di(4-heptyl)phenyl)imidazol-2-ylidene |
| **IPr** | 1,3-Bis(2,6-di-iso-propylphenyl)imidazol-2-ylidene |
| **IPr*** | 1,3-Bis(2,6-bis(diphenylmethyl)-4-methylphenyl)imidazol-2-ylidene |
| **ISO** | 2-p-5-(2-methylnaphthalen-1-yl)imidazo[1,5-b]-isoquinolinium |
| **Isoqui** | 2-Benzyl-5-(2-methylnaphthalen-1-yl)imidazo[1,5-b]-isoquinolinium |
| **NHC** | N-Heterocyclic Carbene |
| **SIPr** | 1,3-Bis(2,6-di-iso-propylphenyl-4,5-dihydroimidazol-2-ylidene |
| **SIPr*** | 1,3-Bis(2,6-bis(diphenylmethyl)-4,5-dihydroimidazol-2-ylidene |
| **WGS** | Water-Gas Shift |

## REFERENCES


[1] S. K. Ritter, *Chemical Engineering & NEWS*, 2009, **87**, 11-21.

[2] $CO_2$-earth (2018). Are we stabilizing yet?. Daily $CO_2$. Consulted on 3 June 2018 via https://www.co2.earth/daily-co2.

[3] Aresta, M. (2010, first edition). *Carbon dioxide as a Chemical feedstock.* Weinheim: Wiley-VCH.

[4] Metz, B. & Davidson, O. (2005, first edition). *Carbon capture and storage.* Cambridge: WMO.

[5] M. Hollering, B. Dutta and F. Kühn, *Coordination Chemistry Reviews*, 2016, **309,** 51-67.

[6] M. N. Hopkinson, C. Richter, M. Schedler and F. Glorius, Nature, 2014, **510**, 485–496

[7] S. Díez-González, N. Marion and S. P. Nolan, Chem. Rev., 2009, **109**, 3612–3676.

[8] D. M S. Flanigan, F. Romanov-Michailidis, N. A. White and T. Rovis, Chem. Rev., 2015, **115**, 9307–9387.

[9] M. Jomon, K. Nobuaki and C. H. Suresh, *Organometallic*s, 2008, **27**, 4666–4670.

[10] Schlosser, M. (2013, first edition). *Organometallic in Synthesis: Third Mannual.* Wiley: Oxford.

[11] Koch, W., & Holthausen, M. (2015). *A Chemist's Guide to Density Functional Theory.* Weinheim: Wiley-VCH.

[12] A. Gómez-Suárez, D. J. Nelson and S. P. Nolan, *Chem. Commun*, 2017, **53**, 2650.

[13] D.C. Graham, C. Mitchell, M.I. Bruce, G.F. Metha, J.H. Bowie and M.A. Buntine, *Organometallics*, 2007, **26**, 6784–6792.

[14] R. Grubbs, A. Miyashita, M. Liu and P. Burk, *J. Am. Chem. Soc*, 1978, **100**, 2418–2425.

[15] Crabtree, R. (2007). The organometallic chemistry of the transition metals, Yale University: Wiley.

[16] J. Porubova, G. Bazbauers and D. Markova, 2011, Scientific Journal of Riga Technical University, 2011, **6**, 79-84.

# Table of contents

List of Figures……iii

List of Tables..……v

List of Symbols……..…….....vii

Chapter 1. Introduction..... 1

1.1. Aim…….....2

1.2. Structure of this work…….....3

1.3. References…….....4

Chapter 2. Reductive coupling of carbon dioxide with ethylene ..... 6

2.1. State of the art ……..…….....7

2.2. References……..……...…….....16

Chapter 3. Methanation ..... 19

3.1. State of the art ……..…….....20

3.2. References……..……...…….....25

Chapter 4. Methods ..... 27

4.1. Method for reductive coupling of carbon dioxide with ethylene……..…….....27

4.1.1. Description……..……...……...…….....27

4.1.2. Gibbs free energy change……...……...……...…….....31

4.2. Method for carbon dioxide methanation…….……..…….....35

4.3. References……..…….……..…….....39

Chapter 5. Reductive coupling of carbon dioxide with ethylene results ..... 41

5.1. Reaction mechanisms…….…….……..…….....41

5.1.1. Ethylene study.....41

5.1.2. Two ethylenes study.....47

5.1.3. Comparison between both mechanisms.....52

5.2. Intermediates comparison…….…….……..…….....53

5.2.1. *Cis*-Lactone vs. *Trans*-Lactone.....53

5.2.2. *Cis*-EthyleneLactone vs. *Trans*-EthyleneLactone.....55

5.2.3. *Cis*-Hydride acrylate vs. *Trans*-Hydride acrylate…….....56

5.3. Most favorable mechanism and ligand.....57
5.4. Conclusions.....58
5.5. References.....59
Chapter 6. Methanation results.....61
6.1. Study of temperature and pressure.....61
6.1.1. Influence of the reaction temperature.....61
6.1.1.1. Reactants conversion.....61
6.1.1.2. Molar aspects.....64
6.1.1.3. Methane yield.....67
6.2.1. Influence of the pressure in the methanation reactor.....68
6.1.1.1. Reactants conversion.....68
6.1.1.2. Molar aspects.....69
6.1.1.3. Methane yield.....71
6.2. Energy balance.....73
6.3. Types of waste for methanation reaction.....75
6.3.1. L-gas network study.....76
6.3.2. H-gas network study.....78
6.4. Conclusions.....80
6.5. References.....81
Chapter 7. Conclusions and future work..... 83
7.1. Conclusions.....83
7.2. Future work.....84

# List of Figures

Figure 2.1: Production of acrylic acid in Hoberg et al. Papers……... 7

Figure 2.2: Ni mediated catalytic cycle proposed by Walther et al……..... 7

Figure 2.3: Pathways: a) Desired for the Reductive Elimination Resulting in Production of the Acrylate and Regeneration of the Active Catalyst; (b) Proposed Intramolecular H-Transfer Reaction to produce acrylate …… 8

Figure 2.4: Proposed mechanism to obtain acrylic acid by Buntine et al……..... 9

Figure 2.5: Proposed mechanism for catalytic coupling of $CO_2$ and ethylene to acrylic acid employing metal (M) complexes……. ……10

Figure 2.6: Reaction energy diagrams using different ligands by Blug et al…….. ……..11

Figure 2.7: Energy profiles for the ($Ni(Mdbu)_2$+$CO_2$+$C_2H_4$) from DFT calculations by Buntine et al……. 12

Figure 2.8: Proposed mechanism for the group B molecules…… 14

Figure 2.9: Diagram energy for molecules in Group C by Flores……..... 15

Figure 3.1: Process designed for carbon dioxide conversion to solar fuels emphasizing the methanation reactor……. ……..20

Figure 3.2: Simulation results obtained by Gao et al. of mole fraction for each compound against temperature…….....21

Figure 3.3: Effect of pressure and temperature in $CO_2$ methanation obtained by Gao et al. in different aspects (left) and effect of $H_2/CO_2$ molar ratio obtained by Gao et al. in different aspects (right)…….....…….22

Figure 3.4: Simulation results obtained by Er-rbib et al. Compared to the experimental data obtained by Kopyscinski (2010) ……..….23

Figure 3.5: Gibbs reactor model ellaborated in Aspen Plus……..…… 24

Figure 3.6: Theoretical conversion of $CO_2$ for different values of pressure……..…… 25

Figure 4.1: Reaction mechanism used in this project, proposed by Hollering et al……... 28

Figure 4.2. Imidazol-2-ylidene ring……... 28

Figure 4.3. Ligands IPr (left) and SIPr (right) ……..29

Figure 4.4. Ligands IPr* (left) and SIPr* (right)……... 29

Figure 4.5. Ligand IHept…… 30

Figure 4.6. Ligand Isoqui (left) and ISO (right) ……..…… 30

Figure 4.7. Ligand IAd (left) and IDD (right) ……..…… 31

Figure 4.8: Tool to obtain the ideal thermodynamic model for a simulation in Aspen Plus..... 37

Figure 4.9: Sensitivity analysis in Aspen Plus……...39

Figure 5.1: First reaction mechanism ……..…….....42
Figure 5.2:Diagram energy for ligands IPr*, SIPr* and IHept with the first reaction mechanism…….……..…….…….... ..43
Figure 5.3: Partial diagram energy for ligands IPr, SIPr and IAd with the first reaction mechanism……...…..……..... 44
Figure 5.4: Partial diagram energy for ligands IDD, ISO and Isoqui with the first reaction mechanism…….……..…….. 45
Figure 5.5: Inner attack of $CO_2$ to IDD (left) and external attack to IAd (right)……46
Figure 5.6: Second reaction mechanism……..... 48
Figure 5.7: Partial diagram energy for ligands IPr*, SIPr* and IHept with the second reaction mechanism……..... 49
Figure 5.8: Partial diagram energy for ligands IPr, SIPr and IAd with the second reaction mechanism……..... 50
Figure 5.9: Partial diagram energy for ligands IDD, ISO and Isoqui with the second reaction mechanism……..... 51
Figure 5.10: *Cis*-lactone (left) and *Trans*-lactone (right) for ligand IHept…… 54
Figure 5.11: Possible agostic interaction found for lactone-trans in IDD……. 55
Figure 5.12: *Cis*-EthyleneLactone (left) and *Trans*-EthyleneLactone (right) for ligand ISO……56
Figure 5.13: *Cis*-Hydride acrylate and *Trans*-Hydride acrylate for ligand IDD……... 57
Figure 6.1: Graphic representation of the hydrogen conversion vs. reaction temperature…… 62
Figure 6.2: Graphic representation of the carbon dioxide conversion vs. reaction temperature…….... 63
Figure 6.3: Graphic representation of the methane production vs. reaction temperature……..65
Figure 6.4: Graphic representation of the methane production vs. reaction temperature……. 66
Figure 6.5: Graphic representation of the carbon monoxide production vs. reaction temperature……66
Figure 6.6: Graphic representation of methane yield regarding $H_2$ vs. reaction temperature…… 67
Figure 6.7: Graphic representation of methane yield regarding $CO_2$ vs. reaction temperature……. 67
Figure 6.8: Graphic representation of the hydrogen conversion vs. methanation reactor pressure….. 68
Figure 6.9: Graphic representation of the carbon dioxide conversion vs. methanation reactor pressure……...69
Figure 6.10: Graphic representation of the methane production vs. methanation reactor pressure….. 70
Figure 6.11: Graphic representation of the methane molar fraction vs. methanation reactor pressure..70
Figure 6.12: Graphic representation of the carbon monoxide production vs. methanation reactor pressure…….. 71

Figure 6.13: Graphic representation of methane yield regarding $H_2$ vs. pressure……..72
Figure 6.14: Graphic representation of methane yield regarding $CO_2$ vs. pressure……... 72
Figure 6.15: Graphic representation of reactor duty vs. pressure……...73
Figure 6.16: Flow diagram for methanation process…… 74
Figure 6.17: Graphic representation of energy separation vs. pressure……..75

# List of Tables

Table 4.1: Conditions for the reactor according to components and its possible waste……...…….... 35

Table 4.2: Specifications and conditions for L and H-gas network……..... 36

Table 4.3: Feed composition for several types of waste……... 36

Table 4.4: Mathematic formulas for parameters calculated in Aspen Plus……..... 38

Table 5.1: Gibbs Free Energies for *Cis*-Lactone and *Trans*-Lactone in all ligands……..... 53

Table 5.2: Gibbs Free Energies for *Cis*-EthyleneLactone and *Trans-Ethylene*Lactone-trans in all ligands…… 55

Table 5.3: Gibbs Free Energies for *Cis*-Hydride acrylate and *Trans*-Hydride acrylate in all ligands... 56

Table 6.1: Maximum $H_2$ conversion found for each molar ratio at T=550 K and P=1 atm…… 63

Table 6.2: Product composition in dry basis for L-gas network according to the types of waste……. 76

Table 6.3: $H_2$ and $CH_4$ flows for L-gas network according to the types of waste……... 76

Table 6.4: $H_2$ and $CO_2$ conversion for L-gas network according to the types of waste…… 77

Table 6.5: Summary for parameters for L-gas network according to the type of waste……... 77

Table 6.6: Product composition in dry basis for H-gas network according to the types of waste…..... 78

Table 6.7: $H_2$ and $CH_4$ production flow for H-gas network according to the types of waste.. 78

Table 6.8: $H_2$ and $CO_2$ conversion for H-gas network according to the types of waste…….. 79

Table 6.9: Summary for parameters for H-gas network according to the type of waste……..79

# List of Symbols

## Acronyms

| *Acronym* | *Description* |
|---|---|
| **B3LYP** | Becke, three-parameter, Lee-Yang-Parr |
| **DBU** | 1,8-Diazabicyclo[5.4.0]undec-7-ene |
| **DFT** | Density Functional Theory |
| **EES** | Electrical energy storage |
| **IAd** | 1,3-Diadamantylylimidazol-2-ylidene |
| **IDD** | 1,3-Dicyclododecylimidazol-2-ylidene |
| **IHept** | 1,3-Bis(2,6-di(4-heptyl)phenyl)imidazol-2-ylidene |
| **IPr** | 1,3-Bis(2,6-di-iso-propylphenyl)imidazol-2-ylidene |
| **IPr*** | 1,3-Bis(2,6-bis(diphenylmethyl)-4-methylphenyl)imidazol-2-ylidene |
| **ISO** | 2-p-5-(2-methylnaphthalen-1-yl)imidazo[1,5-b]-isoquinolinium |
| **Isoqui** | 2-Benzyl-5-(2-methylnaphthalen-1-yl)imidazo[1,5-b]-isoquinolinium |
| **NHC** | N-Heterocyclic Carbene |
| **SIPr** | 1,3-Bis(2,6-di-iso-propylphenyl-4,5-dihydroimidazol-2-ylidene |
| **SIPr*** | 1,3-Bis(2,6-bis(diphenylmethyl)-4,5-dihydroimidazol-2-ylidene |
| **WGS** | Water-Gas Shift |

## Roman Symbols

| *Symbol (Unit)* | *Description* |
|---|---|
| $C_e$ (kJ mol$^{-1}$) | Electronical contribution for heat capacity |
| $C_r$ (kJ mol$^{-1}$) | Rotational contribution for heat capacity |
| $C_t$ (kJ mol$^{-1}$) | Transitional contribution for heat capacity |
| $C_v$ (kJ mol$^{-1}$) | Vibrational contribution for heat capacity |
| $E_{el}$ (kJ mol$^{-1}$) | Energy due to electronical motion |
| $E_{rot}$ (kJ mol$^{-1}$) | Energy due to rotational motion |
| $E_{tot}$ (kJ mol$^{-1}$) | Total energy |
| $E_{tran}$ (kJ mol$^{-1}$) | Energy due to transitional motion |
| $E_{vib}$ (kJ mol$^{-1}$) | Energy due to vibrational motion |
| $G_{corr}$ (kJ mol$^{-1}$) | Correction for Gibbs Free Energy |
| $H$ (J s) | Planck´s constant = 6.626176x10$^{-34}$ J s |
| $H_{corr}$ (kJ mol$^{-1}$) | Correction for Enthalpy |
| $k_B$ (J K$^{-1}$) | Boltzmann constant = 1.380662x 10$^{-23}$ J/K |
| $m$ (kg) | Mass of the molecule |
| $P$ (atm) | Pressure (as default its value is 1 atmosphere) |
| $q_e$ | Electronic partition function |
| $q_r$ | Rotational partition function |
| $q_t$ | Transitition partition function |
| $R$ (J mol$^{-1}$ K$^{-1}$) | Gas constant (8.31441 J/(mol*K)) |
| $S_{el}$ (kJ mol$^{-1}$ K$^{-1}$) | Entropy due to electronical motion |
| $S_{rot}$ (kJ mol$^{-1}$ K$^{-1}$) | Entropy due to rotational motion |
| $S_{tot}$ (kJ mol$^{-1}$ K$^{-1}$) | Total entropy |
| $S_{tran}$ (kJ mol$^{-1}$ K$^{-1}$) | Entropy due to transitional motion |
| $S_{vib}$ (kJ mol$^{-1}$ K$^{-1}$) | Entropy due to vibrational motion |
| $T$ (K) | Reaction temperature (K), default is 298.15 K |
| $V$ (m$^3$) | Volume |
| $\sigma_r$ | Symmetry number for rotation |
| $\ominus_r$ | Characteristic temperature for rotation (referred to the moment of inertia) |
| $\ominus_{r,x}\ominus_{r,y}\ominus_{r,z}$ | Characteristic temperature for rotation (referred to the moment of inertia in the x, y and z plane) |
| $\frac{\ominus_{v,K}}{T}$ | Characteristic temperature for vibration K |

## Greek Symbols

| *Symbol* | *Description* |
|---|---|
| **α** | Carbon in α-position |
| **β** | Carbon in β-position |

# Chapter 1
# Introduction

Carbon dioxide ($CO_2$) is considered today to be the major cause of climate change, due to its greenhouse properties and its continuous accumulation in the atmosphere.[1] At the same time, the atmospheric concentration of this compound rose from 278 ppm during the preindustrial times to a current level of approximately 411.68 ppm,[2] meaning that the use of carbon based fossil fuels in human activities (representing almost 80-85% of the world's energy sources) could increase more causing worse effects.[3] However, carbon is not the only source of $CO_2$, because it can be originated from petroleum or even gas combustion, so the problem comes from several causes.[4]

For this reason, it must be found measures to reduce $CO_2$ emissions and with them it would be possible to attack some threats that are still being a disadvantage for the world, such as the global warming and so more on. Society can contribute with this fact, but this contribution is not enough,[3] so that is why technologies must be created or developed to significantly reduce the concentration of $CO_2$ in the atmosphere. It is not affordable to delete it completely, due to the excessive cost this requires, thus this would not be a solution.[6] Furthermore, the feasible options that are still available lay down in the use of carbon dioxide as a raw material for chemical compounds and fuels. However, the creation of new pathways for several processes in its sustainability and $CO_2$ employment could be an absolutely crucial step.[6]

Nevertheless, the use of carbon dioxide as a raw material for chemical synthesis is one of the biggest scientific challenges nowadays.[7-8] In addition, the capture and use of carbon dioxide has been recognized by important organisms as the European Chemical Council and the European Union as one of the most relevant researches to achieve the climate objectives established for 2050.[9] Due to its chemistry, carbon dioxide has a high oxidation state[7], giving an acceleration of its thermodynamics, causing a difficulty to be a raw material for the industry. On the contrary, the activation of carbon dioxide needs a high amount of energy, which can be obtained through various sources such as electricity, heat or even with the use of high energy substrates, as well as active, selective, stable and economic catalysts.[10]

Then, as it has already been mentioned, carbon dioxide could take a different pathway in comparison with the ones used nowadays. Due to its reactivity, two possible examples are the reductive coupling between carbon dioxide and ethylene in which the acrylic acid is obtained. Secondly, the methanation process consisting in the reaction between this gas and hydrogen to produce methane. For the first case, it is a potential alternative route to acrylic acid or acrylate, because they have been studied using various (transition) metal complexes.[11] In the second one, the Sabatier process or also called methanation, can also be used to reduce $CO_2$ generated in a space habitat to reclaim the oxygen for recycle.

The reductive coupling between carbon dioxide and ethylene can be studied through N-heterocyclic carbenes. This type of complex compounds is now widespread[12]; these exciting species have found applications in transition metal chemistry[13], as organocatalysts[14] and as reagents to stabilize geometries and oxidation states of main group elements.[13] At the same time, their recognized popularity can be attributed to several factors as their highly molecular leading to their large structural and stereoelectronic diversity and the fact of being prepared easily with strong metal-NHC bonds.[15] Besides, NHC have two important characteristics that might be considered at the time of deciding to use them as catalysts: their electronic properties and their steric properties.[16]

From one hand, the first parameter involves major contributions from σ- or π-donation as well as π-accepting properties. Besides, the donating ability is associated with the energy level of the highest occupied molecular orbital (HOMO) meaning that the higher the HOMO energy of a ligand, the stronger is its electron donating ability. When it is considered the lowest unoccupied molecular orbital (LUMO), it is referred to the electron acceptor capability of a ligand, meaning in this case that the lower the LUMO energy, the better is the accepting property of a ligand.[15] On the other hand, the second parameter requires the concept of percent buried volume, defined as the percentage of a sphere (with a radium of approximately 3.5 Å) around the metallic center that is occupied by a given ligand.[16]

## 1.1 Aim

The aim of this thesis is to design two uses currently attributed for the carbon dioxide catalytic processes: its reductive coupling with ethylene to obtain acrylic acid and the methanation process in which methane is the main product. From one hand, there is a proposed mechanism for the first reaction composed by 4-steps (oxidative coupling, β-hydride elimination, reductive elimination and ligand exchange). Through the use of organometallic ligands, new strategies to create optimal conditions for the β-Hydride elimination via activation of the M-O bond seem to be a viable strategy that could be studied using these compounds. On the other hand, a Gibbs reactor will be designed in Aspen Plus considering some initial conditions such as pressure, temperature and conversion.

Furthermore, the thermodynamic methodology applied in this program will allow to define which is the molar ratio that must be used for the methanation reactants according to the goal drawn from the beginning.

## 1.2 Structure of this work

Chapter 2 presents a state of the art of $CO_2$ reductive coupling with ethylene. The aim of this literature study is to provide an overview of the different projects that have similarly worked with this reaction employing the same or similar programs. According to the different catalysts used by other authors, there will be shown the different contributions coming from them.

Chapter 3 presents a state of the art for $CO_2$ methanation. The aim of this literature study is to provide an overview of all the parameters studied by several authors depending on different conditions such as temperature, pressure and conversion, and what it has implied from the computational point of view.

Chapter 4 presents the computational methods applied for each of the catalytic processes mentioned before. In addition, the essential thermodynamic concepts, the explanation of each of the data used to do the calculations in Gaussian 16 and the methodology applied in Aspen Plus to study the methanation process.

Chapter 5 presents the results obtained from the reductive coupling, considering the discussion for the intermediate and transition states obtained, and their correspondent energy diagrams created from Gaussian 16.

Chapter 6 presents the results obtained from the methanation study, evaluating the different parameters involved in the reaction, contemplating several types of waste used as feed flows and the discussion for the best option according to the conditions stablished in the methodology and proposing an energy balance for the most optimal values that the parameters could acquire at the time of designing the process.

Chapter 7 presents the conclusions and future work determined from the development of this project.

## 1.3 References


1. S. K. Ritter, *Chemical Engineering & NEWS,* 2009, **87**, 11-21.

2. $CO_2$-earth (2018). Are we stabilizing yet?. Daily $CO_2$. Consulted on 3 June 2018 via https://www.co2.earth/daily-co2.

3. Aresta, M. (2010, first edition). *Carbon dioxide as a Chemical feedstock.* Weinheim: Wiley-VCH.

4. Metz, B. & Davidson, O. (2005, first edition). *Carbon capture and storage.* Cambridge: WMO.

5. Williams, J. (1978, first edition). *Carbon Dioxide, Climate and Society.* Oxford: Pergamon.

6. Zenguelis, D. (2014). *How much will it cost to cut global greenhouse gas emissions?***.** Consulted on 2 May 2018 via http://www.lse.ac.uk/GranthamInstitute/faqs/how-much-will-it-cost-to-cutglobal-greenhouse-gas-emissions/.

7. Neelameggham, N. (2018). *Carbon Dioxide Reduction Technologies: A Synopsis of the Symposium at TMS.* Consulted on 1 May 2018 via http://www.tms.org/pubs/journals/jom/0802/neelameggham-0802.html.

8. J. Klankermayer, S.Wesselbaum, K. Beydoun and Leitner, W, *Angew Chem Int Ed Engl*, Angewandte Chemie International Edition, 2017, **55**, 7296- 7343.

9. Kuckshinrichs, W., & Hake, J. (2015). *Carbon Capture, Storage and Use*. Weinheim: Springer.

10. M, Pérez-Fortes, J. Schöneberger, A. Boulamanti, G. Harrison and E. Tzimas, *International Journal of Hydrogen Energy*, 2016, **37**, 16444- 16462.

11. M. Hollering, B. Dutta and F. Kühn, *Coordination Chemistry Reviews*, 2016, **309,** 51-67.

12. M. N. Hopkinson, C. Richter, M. Schedler and F. Glorius, Nature, 2014, **510**, 485–496

13. S. Díez-González, N. Marion and S. P. Nolan, Chem. Rev., 2009, **109**, 3612–3676.

14. D. M S. Flanigan, F. Romanov-Michailidis, N. A. White and T. Rovis, Chem. Rev., 2015, **115**, 9307–9387.

15. M. Jomon, K. Nobuaki and C. H. Suresh, *Organometallic*s, 2008, **27**, 4666–4670.

16. Schlosser, M. (2013, first edition). *Organometallic in Synthesis: Third Mannual.* Wiley: Oxford.

# Chapter 2
# Reductive coupling of carbon dioxide with ethylene

A possible pathway to improve the carbon dioxide conversion can be found in its catalytic coupling reaction with ethylene for the production of acrylic acid. The latter is a chemical with high importance in the industry that exceeds a demand of 4 Mt/year.[1] In addition, this oxidative coupling could be done through several homogeneous transition metal complexes such as titanium, iron, nickel, molybdenum and others.[2,3]

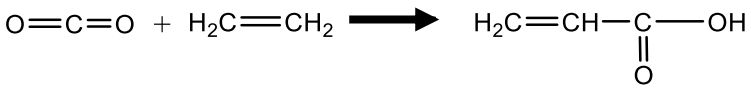

(1)

Based on this, it is important to detail how the study of this reaction has evolved over time, considering all the contributions given by different authors and detailing its state of the art. It must be considered some important investigations with a similar work in comparison with this project.

## 2.1 State of the art

In the 1980s, Hoberg et al.[5-8] disclosed the origin of nickel-based work and from which many studies were done basing them on this one, considering the research on acrylate production from metal assisted coupling of $CO_2$ with alkenes or alkynes originated from the nickel-based work of Hoberg and co-workers. Their papers detailed the formation of saturated and unsaturated carboxylic acids (i.e., acrylates) via the coupling of $CO_2$ with a variety of alkenes, among its found ethylene. This coupling reaction was obtained due to a stoichiometric amount of nickel bis(diazabicyclo[5.4.0]undec-7-ene) ($Ni(DBU)_2$) formed in situ from $Ni(COD)_2$ and DBU as it can be shown in Figure 2.1.[4]

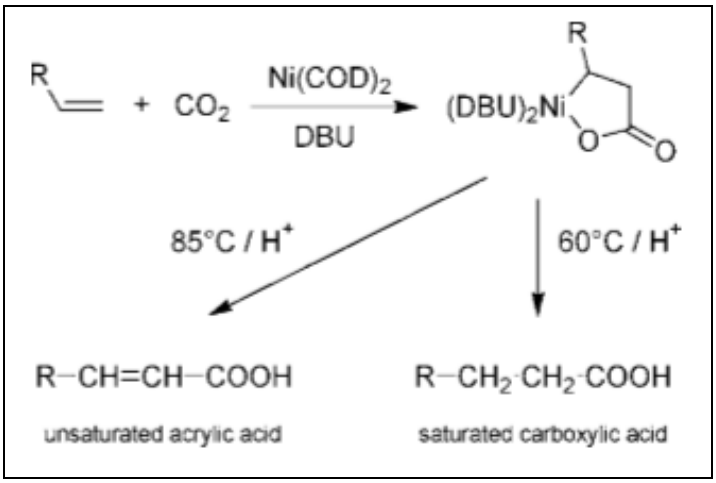


**Figure 2.1. Production of acrylic acid in Hoberg et al. papers.[4]**

In 2006, Walther et al.[9] presented a temporary catalytic cycle (shown in Figure 2.2) of Ni mediated coupling of $CO_2$ and ethene involving the γ-lactone as an intermediate, leading to acrylic acid as a product. Then, the first evidence of an β-hydride transfer was described in their report during attempts of reacting nickelalactones with donor ligands, in order to show the potential activators of the β-hydride elimination reaction.[9]

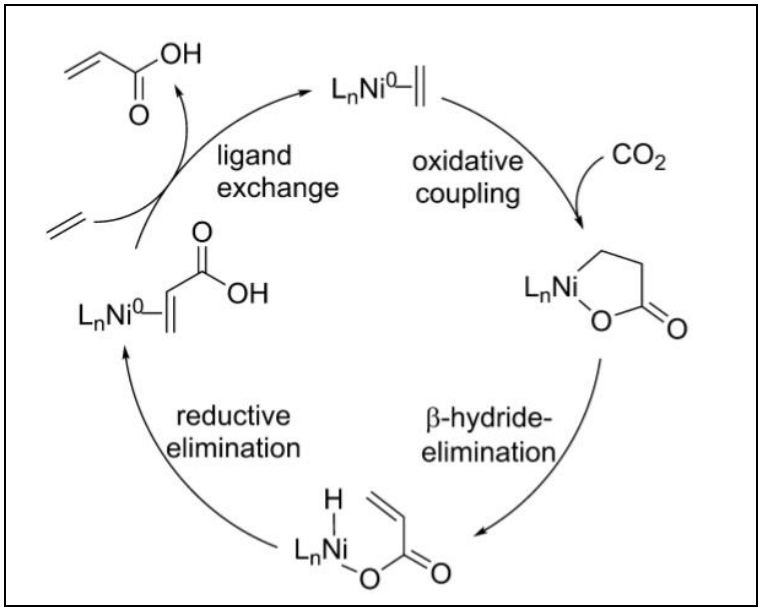


**Figure 2.2. Ni mediated catalytic cycle proposed by Walther et al.[9]**

In 2007, Buntine et al.[10] focused their study in the production of acrylic acid via homogeneous nickel-mediated coupling of ethylene and carbon dioxide using DFT with the aim of describing the potential energy surface for both the nickel-mediated coupling reaction and an intramolecular deactivation reaction that was reported to hinder the desired catalytic activity.[10] After Hoberg et al. suggestion about the lack of catalytic activity in the acrylate case owing to a hydride transfer reaction of the hydride ligand from the nickel center to DBU, they mentioned two pathways for the

reaction employing it. Based on this, the reaction would prevent the possibility of reductive elimination, thus it could be possible to inhibit both the formation of acrylic acid and regeneration of the zerovalent nickel catalyst. In Figure 2.3, both reactions are shown.

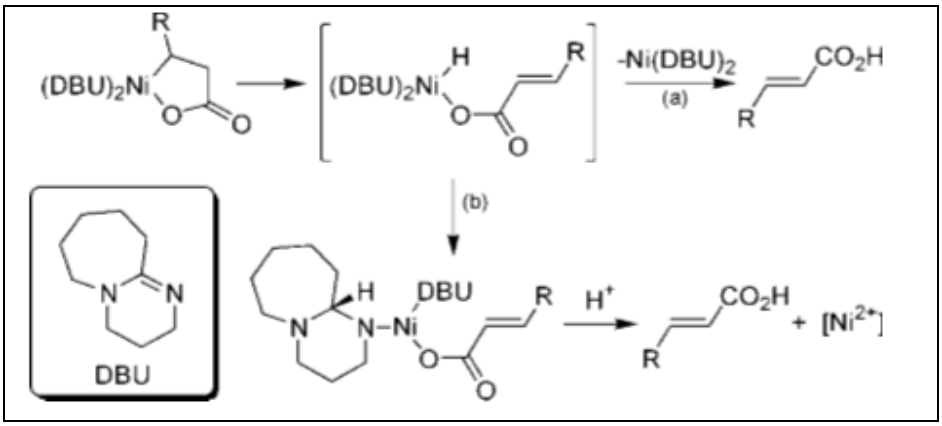


**Figure 2.3. Pathways: a) Desired for the Reductive Elimination Resulting in Production of the Acrylate and Regeneration of the Active Catalyst; (b) Proposed Intramolecular H-Transfer Reaction to produce acrylate.[10]**

The computational calculations were focused on geometry optimizations using the B3LYP [11-13] density functional, and the LANL2DZ[14,15], consisting on nickel basis set and 6-31+G(d,p)[16-19], basis set for the rest of atoms), where the compound basis set with pure d functions (5D) was used in the whole calculations.[10]

Buntine et al.[10] considered three important sections: the *nickelacycle formation:* after having used $Ni(DBU)_2$ as a catalyst, the resulting energies make them conclude that this section occurs in a single step via the reaction of nickel-coordinated of ethylene with an incoming $CO_2$.[10] Nickelacycle is shown in Figure 2.4 through the symbol *a.*

Secondly, from *nickelacycle to nickel acrylate* (shown through symbol *b* in Figure 2.4*)*, they determined that the mechanism beyond this sector is still unknown, but basing their ideas on Hoberg reports, they concluded the β-hydride elimination occurred from the nickelacycle, the resulting intermediate would directly contain both hydride and acrylate ligands.[10] Finally, *liberation of acrylic acid* (shown through symbol *c* in Figure 2.4), concluding that this requires reductive elimination of the acrylate and hydride ligands.[10] The proposed mechanism by these authors employing their catalyst is shown in Figure 2.4.

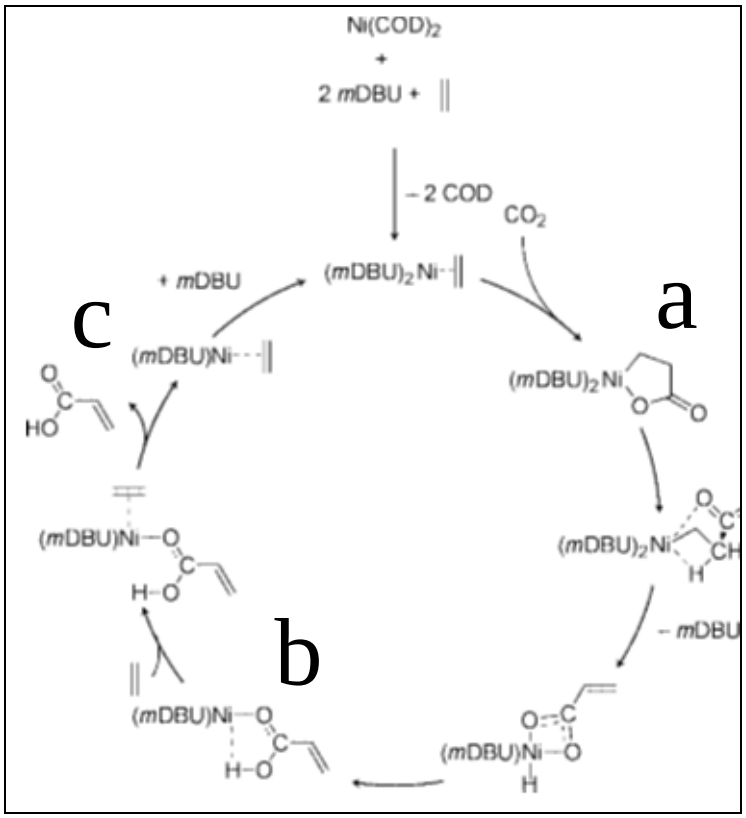


**Figure 2.4. Proposed mechanism to obtain acrylic acid by Buntine et al.[10]**

Furthermore, Blug et al.[20] studied the mechanistic aspects of $CO_2$ coupling with ethylene to acrylic acid in the presence of homogeneous nickel catalysts employing bidentate phosphorous ligands, considering density functional theory calculations (DFT). The mechanism that they proposed involves six important steps: the cycle is initiated by the sequential coordination of ethylene and carbon dioxide to the Ni-complex followed by a facile coupling step resulting in the formation of a stable nickelalactone intermediate. Then, the formation of acrylic acid proceeds via a dual- step process involving highly unfavorable β-H transfer resulting then in the Ni-hydrido acrylate complex followed by the reductive elimination of acrylic acid.[23] In the Figure 2.5 is shown the whole mechanism.[20]

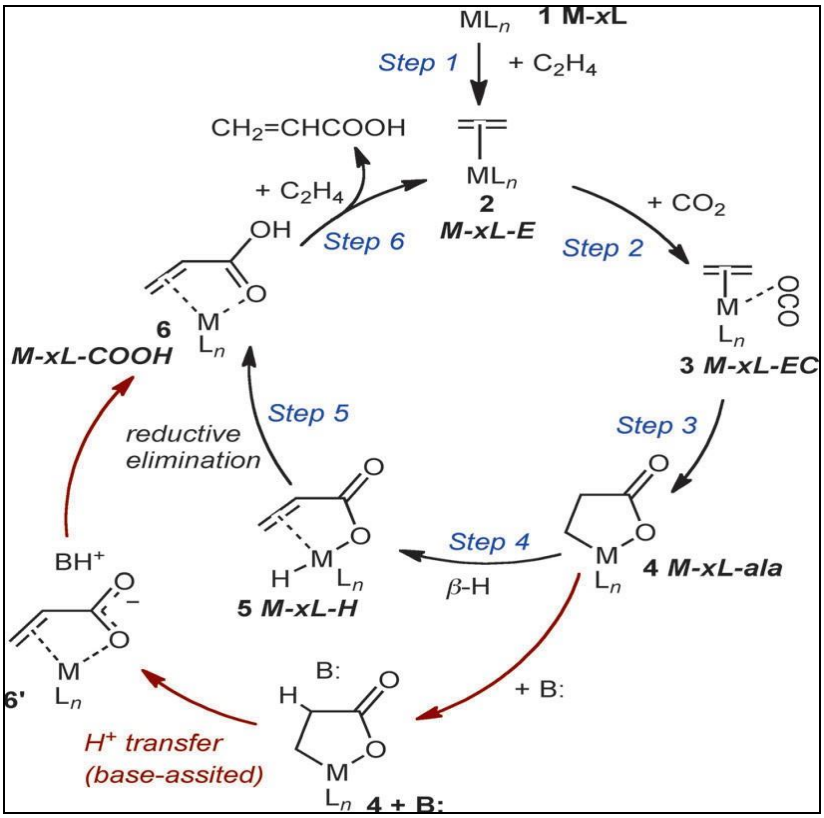


**Figure 2.5. Proposed mechanism for catalytic coupling of $CO_2$ and ethylene to acrylic acid employing metal (M) complexes.[20]**

This mechanism acquires more importance via a metalalactone intermediate. According to several studies, stoichiometric formation of such complexes has been observed during this reaction with metals such as nickel, molybdenum and tungsten-complexes.[21-23]

Moreover, all calculations done by Blug et al.[20] were obtained thank to Gaussian 09 suite of programs. Similar to Buntine et al.[10] they obtained their results through 6-31+G(d) basis set for nickel, while the rest of atoms were studied with 6-31G(d) basis set. They determined that all the structural parameters for Ni-complexes have a congruency with those structures found in X-ray crystallized.[20]

One of the most important conclusions given by Blug et al.[20] remains on the idea of the stability of niclekalactone, considering it the key intermediate in this catalytic reaction. Its stability is to be assumed to be a critical factor that is completely decisive to find the possibly to perform the coupling in a certain way.[20]

Regarding to the electronic and steric effects, they found through their results that it is not possible to promote the coupling just adjusting these parameters. In the Figure 2.6 there are shown the different energy diagrams obtained by Blug et al.[20] considering suddenly their analysis for this point.[20,24,25]

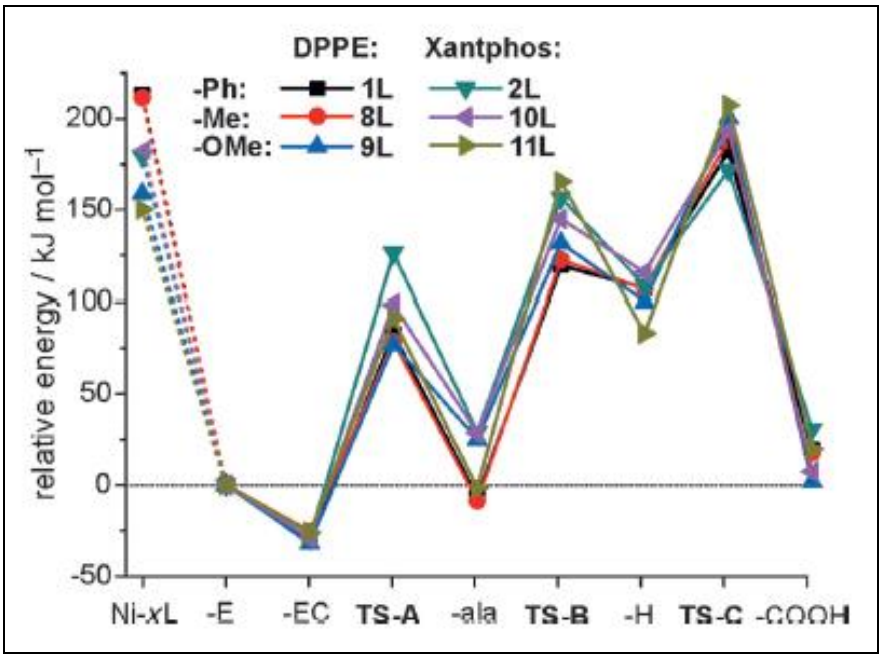


**Figure 2.6. Reaction energy diagrams using different ligands by Blug et al.[20]**

Although some of the substituents in the ligands are found to decrease the steric hindrance imposed by the bidentate ligand onto the Ni center, this does not lead to notable changes in the calculated energy profiles for the catalytic reactions.

Similarly, Hollering et al. considered a research for renewable alternative energy sources and energy storing due to the possibilities that have been gaining a significant importance during the last years looking forward to a solution that could avoid the depleting fossil carbon sources.[26] Besides, they determined that conversion of $CO_2$ and alkenes to acrylate could not be regarded as a breakthrough for industrial applications.[27] According to them, an efficient study about a catalytic cycle for this reaction has not been found yet.[26]

However, several groups have been focusing their investigations on strategies to overcome the most crucial step in the mechanism shown above: the β-hydride elimination. They have been looking forward to appropriate reagents that could facilitate this process, among the use of excess methylating agents or even the use of Lewis acidic reagents.[26]

Rieger et al.[28] employed directly methylation to apply the β-hydride elimination to liberate acrylate. Based on this, they studied this reaction using the nickelalactone that comes from Walther et al.[9] study. In here, the main aim was to activate the Ni-O bond considering an electrophilic attack of the Me cation, and then produce the reductive elimination of HX.[26]

Furthermore, all these experimental studies using a Lewis acid have proved that an electron who accepts cocatalyst could trigger a catalytic acrylate formation. This idea has been shown by

further jobs done by Bernskoetter et al.[29], which showed that the presence of the Lewis acid additive sodium cation lowers the overall reaction energy of a γ-to-β isomerization of nickelalactones.[26]

Corresponding to the computational calculations, the reaction mechanism of the transition metal which are part of the coupling between ethylene and carbon dioxide, has been investigated using theoretical calculations as it has been shown previously. For example, Dedieu et al.[30] studied their project on bisamine Ni systems comparing pathways of an alkene attacking a $CO_2$-coordinated moiety and a $CO_2$ attack on a precoordinated alkene, as the first step in the coupling reaction.[30.] For both cases the attacked ligand undergoes a different number of coordination. Thus, it was concluded that a $C_2H_4$ attack on a $CO_2$-coordinated system is the energetically favored pathway, as the $\eta_2$-$C_2H_4$ transforming to a $\eta_1$-$C_2H_4$ is not as possible as other options. On the contrary, this investigation was contradicted by a more comprehensive DFT study done by Pápai et al.[31] on the intermediacy of a carbon dioxide coordinated Ni complex in the coupling mechanism, obtaining that toward a $CO_2$ attack on the ethene bound species and the C-C coupling taking place in a single step.[31]

The most important conclusion obtained by Buntine et al.[10] and Pápai et al.[31] focused on the fact that Ni-catalyzed coupling of carbon dioxide and ethylene is possibly hindered due to thermodynamic reasons. In Figure 2.7, it is shown the diagram energy obtained by them.

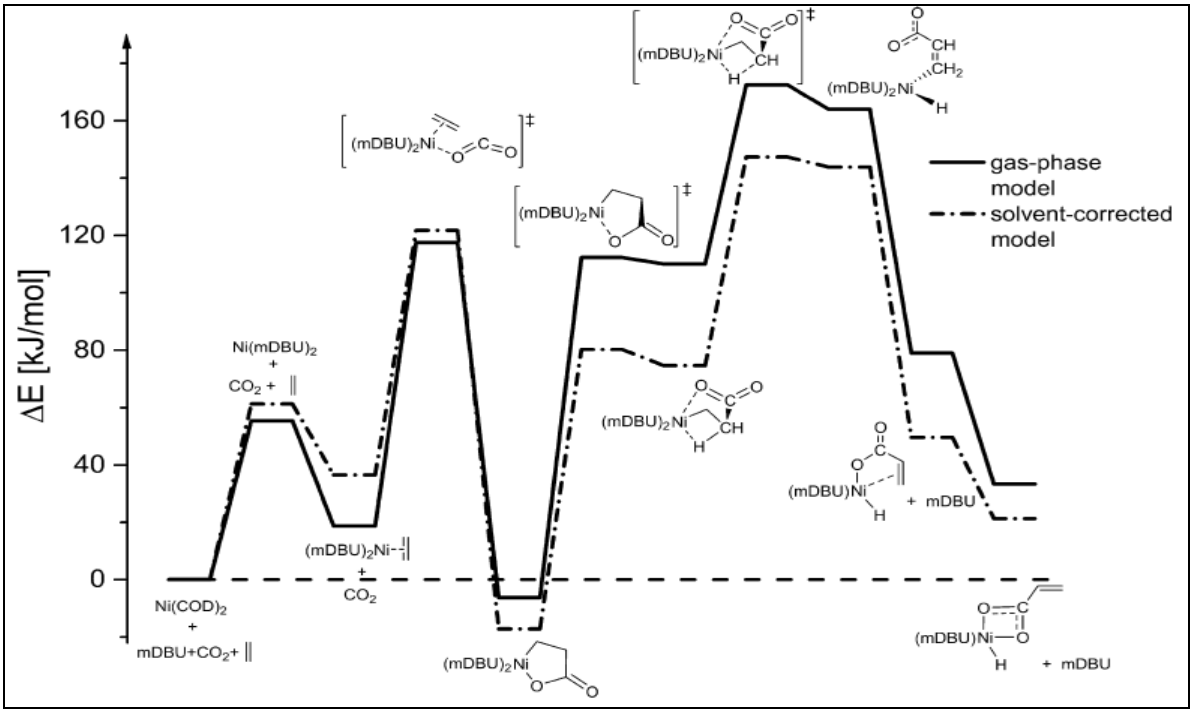


**Figure 2.7. Energy profiles for the (Ni(Mdbu)$_2$+$CO_2$+$C_2H_4$) from DFT calculations by Buntine et al.[10]**

Then, Pidko et al.[22] investigated this reaction with bisphosphine ligands using DFT. They optimized structures of nickelalactones employing a different variety of bidentate ligands that were obtained and they studied the effect of the ligand's bite angle on the stability of these molecules

concluding that it affects their stability but it does not affect the catalytic pathway that is needed for geometric, electronic or even steric properties of the ligand. At the same time, they confirmed several ideas: the β-transfer is the determining step and reductive decomposition of nickelalactone is energetically unfavorable for the coupling.[22]

In 2017, Flores[32] developed a project about the design and evaluation of a catalyst for the reductive coupling of $CO_2$ with olefins. She based her study on homogeneous catalysis in the mechanism proposed by other authors such as Hollering et al, considering the four important steps: oxidative coupling of reactants to form a metalalactone, β-elimination of hydrogen to produce an hydride-acrylate, reductive elimination of this acrylate and ligand exchange to regenerate the initial active complex.[32] At the same time, she focused her study, besides the previous authors already mentioned, in the results obtained by Grubbs et al.[33] whose main input was that bidentate ligands are not ideal for the mechanism, due to the fact that β–elimination is only performed by the monodentate ligands.[32]

Flores[32] employed as a methodology the Gaussview program (Gaussian 09 version) building a different list of catalysts in gas phase. It was considered that the homogeneous catalysis has the advantage in the time spent to evaluate a particular catalyst, owing to the variables involved in the calculations, comparing with the heterogeneous one.[32] As a molecular modeling it was employed the functional PBE1PBE, based at the same time in the functional PBE. It was developed by authors like Perdew, Burke and Ernzerhof in 1996 and it can correct properly the electronic density gradient.[34] For the approximation calculations it was used the SVP (Split Valence Polarized), developed by Schafer, Horn and Alhrichs, specifically the base Def2SVP that represents equations which aim is to facilitate the approximation for Schrödinger equation.[35]

From this, Flores[32] proposed taking Grubbs et al.[33] investigation the use of monodentate ligands to habilitate the β–hydride elimination emphasized on N-Heterocyclic carbenes. There were created three groups called A, B and C. The first indicated which is the type of intern ring ideal for the reaction, while B and C indicated the steric control ideal for it. After its building, there were done the 360 degrees rotation for the ligands and the reactants bound to the metallic center, using steps of 10 degrees turns in the complex catalytic to determine if the intermediary compound obtained was a local or absolute minimum energetically.

These sweeps considerated the increasing or decreasing in the atoms distances to reproduce the behavior of molecular bonds during the reaction.[33] Due to this methodology, it was possible to achieve the production of intermediate and transition state molecules, being them with lower and higher energy respectively. Then, the best catalyst was chosen according to the Free energy

diagrams, when it was found the one with less levels of this parameter, facilitating the reaction development.[32]

Results obtained by Flores[32] in the group A reflected that the β–hydride elimination did not produce in *trans* configuration, because it was not possible to look for any intermediate enough stable. For this reason, it was calculated an intermediate between *cis* and *trans* to check if this rearrangement signified an additional kinetic barrier.[32] Regarding groups B (mechanism shown in Figure 2.8) and C, they were created according to the results of the first group to deepen in their study in the energetic and kinetic dimension. Simultaneously, steric control was covered through a change in the substituents for a higher size in compounds such as phenyls.[32]

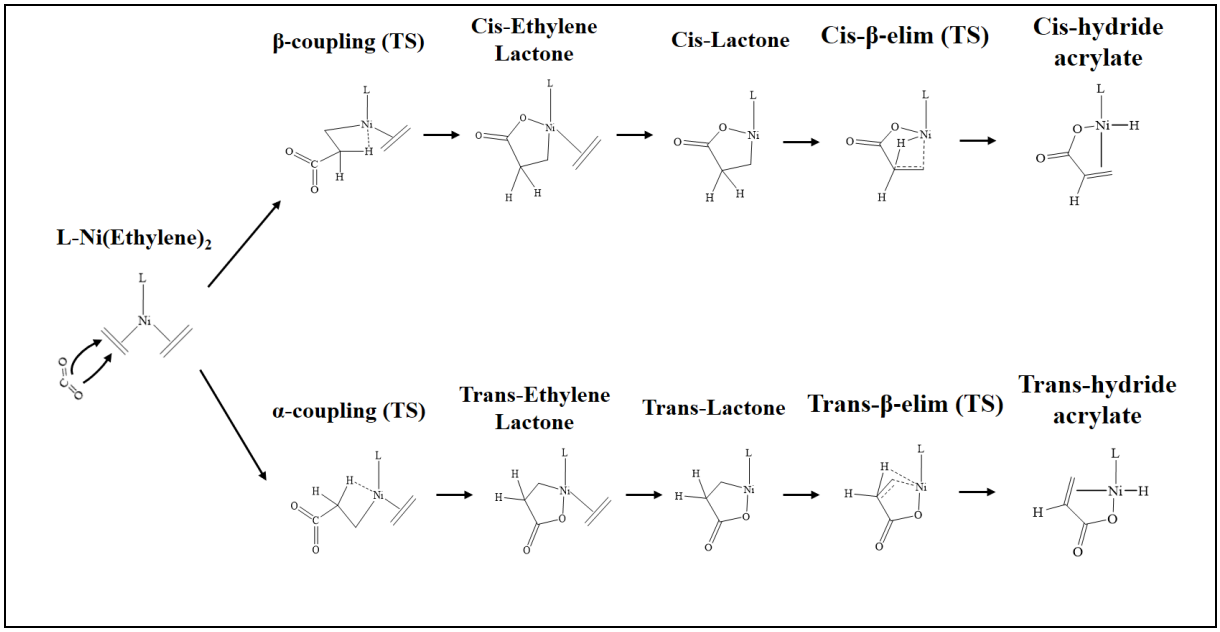


**Figure 2.8. Proposed mechanism for the group B molecules.[32]**

However, it was appreciated a partial shielding in the upper part of the metallic center that gives certain stability to the catalytic complex in comparison with those ligands employed in the group A. In this case, with the group B and C (which diagram energy is shown in Figure 2.9), it was concluded that the intermediate cis-trans previously mentioned was not necessary to use and the β-hydride elimination happens without considering this one. In the last group, there were considered ligands with the most steric control reported by literature, finding that the partial reaction mechanism had to be modified due to the high shielding caused by the substituents. For this reason, Flores[32] accomplished that with these type of ligands, produced lactones are more stable, which means that the reaction is favored, owing to the decreasing in the kinetic barriers for the previous steps in the mechanism proposed by Walther et al.[9,32]

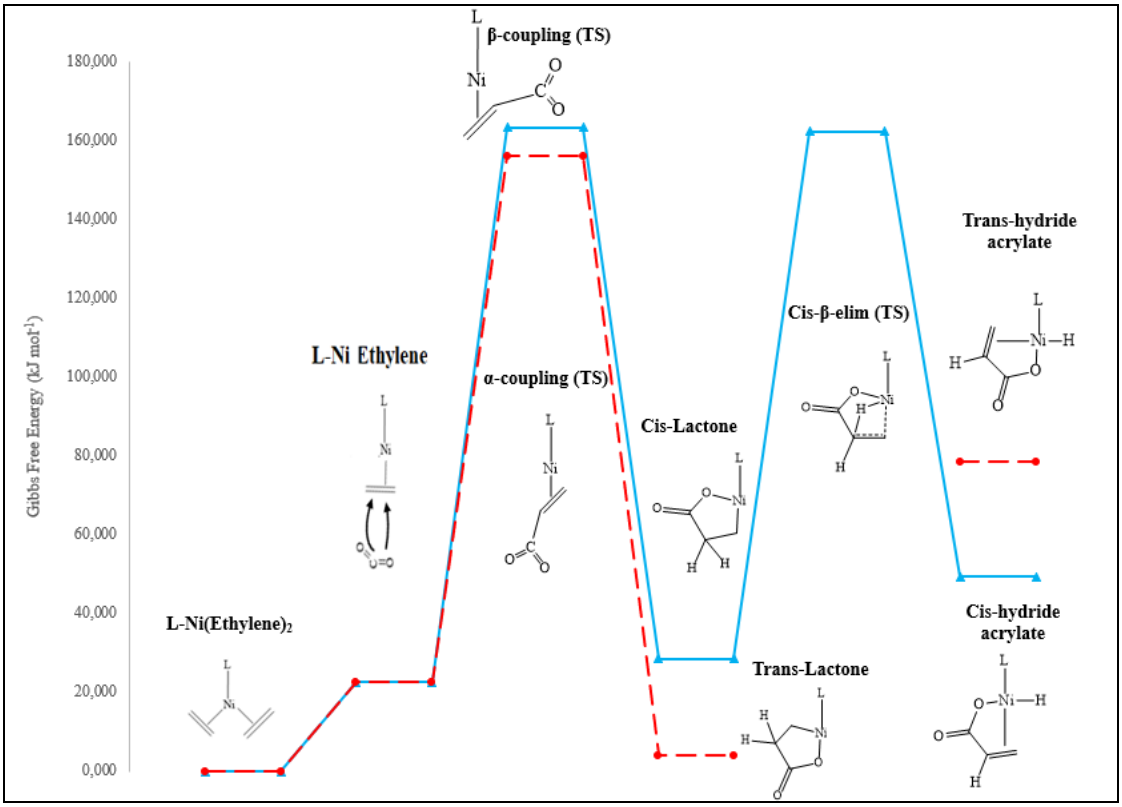


**Figure 2.9. Diagram energy for molecules in Group C by Flores[32]**

## 2.2 References


1.J. Glauser, M. Blagoev and T. Kumamoto, *CEH Marketing Research Report*, 2011.

2. R. Alvarez, E. Carmona, A. Galindo, E. Gutierrez, J. M. Marin, A. Monge, M. L. Poveda, C. Ruiz and J. M. Savariault, *Organometallics,* 1989, **8**, 2430.

3. A. Galindo, A. Pastor, P. J. Perez and E. Carmona, *Organometallics*, 1993, **12**, 4443.

4. H. Hoberg, K. Sümmermann, A. Milchereit, *Angew. Chem*, 1985, **97**, 320–321.

5. Burkhart, G and Hoberg, H, *Angew. Chem., Int. Ed. Engl*, 1982, **21**, 76–76.

6. Hoberg, H and Schaefer, D. J, *Organomet. Chem*, 1982, **236**, C28– C30.

7. Hoberg, H and Schaefer, D. J, *Organomet. Chem*, 1983, **251**, C51– C53.

8. Hoberg, H, Peres, Y and Milchereit, A, J. *Organomet. Chem,* 1986, **307**, C38–C40.

9. R. Fischer, J. Langer, A. Malassa, D. Walther, H. Gorls and G. Vaughan, *Chem. Com-mun*, 2006, **6**, 2510–2512.

10. D.C. Graham, C. Mitchell, M.I. Bruce, G.F. Metha, J.H. Bowie and M.A. Buntine, *Organometallics*, 2007, **26**, 6784–6792.

11. A. D. Becke, J. *Chem. Phys*. 1993, **98**, 5648–5652.

12. A. D. Becke, *Phys. ReV.A*, 1988, **38**, 3098–3100.

13. C. Lee, W. Yang and R. G. Parr, *Phys. ReV*, 1988, **37**, 785–789.

14. T. H. Dunning and P.J. Hay (1976, third edition). *Modern Theoretical Chemistry*. Plenum: New York.

15. P.J. Hay, P. J and W.R. Wadt, *J. Chem. Phys*. 1985, **82**, 299.

16. W.J. Hehr, R. Ditchfie and J.A. Pople, *J. Chem. Phys*. 1972, **56**, 2257-ff.

17. P.C. Hariharan and J.A. Pople. *Theor. Chim. Acta*, 1973, **28**, 213– 222.

18. G.W. Spitznagel, T. Clark, J. Chandrasekhar, P. Schleyer, P, *J. Comput. Chem*. 1982, **3**, 363–371.

19. T. Clark, J. Chandrasekhar, G.W. Spitznagel and P. Schleyer, *J. Comput. Chem.* 1983, **4**, 294–301.

20. G. Yang, B. Schäffner, M. Blug, E.J.M. Hensen, E.A. Pidko, *ChemCatChem*, 2014, **6**, 800–807.

21. S. Y. T. Lee, M. Cokoja, M. Drees, Y. Li, J. Mink, W. A. Herrmann and F. E. Kuhn, *ChemSusChem,* 2011, **4**, 1275.

22. G.A. Filonenko, E.J.M. Hensen and E.A. Pidko, *Catal. Sci. Technol.* **2014**, ***4***, 3474.

23. M. L. Lejkowski, R. Lindner, T. Kageyama, P. N. Plessow, I. B.M_ller, A. Sch_fer, F. Rominger, P. Hofmann, C. Futter, S. A. Schunk and M. Limbach, *Chem. Eur. J*, 2012, **18,** 14017.

24. D. Jin, T. J. Schmeier, P. G. Williard, N. Hazari and W. H. Bernskoetter, *Organometallics* 2013, **32**, 2152.

25. J. Li, G. Jia and Z. Lin, *Organometallics*, 2008, **27**, 3892.

26. M. Cokoja, C. Bruckmeier, B. Rieger, W.A. Herrmann and F.E. Kühn, *Angew. Chem.Int. Ed*, 2011, **50**, 8510–8537.

27. M. Hollering, B. Dutta and F. Kühn, *Coordination Chemistry Reviews*, 2016, **309,** 51-67.

28. C. Bruckmeier, M.W. Lehenmeier, R. Reichardt, S. Vagin and B. Rieger, *Organometallics*, 2010, **29**, 2199–2202.

29. D. Jin, P.G. Williard, N. Hazari and W.H. Bernskoetter, *Chem. Eur*. J, 2014, **20**, 3205–3211.

30. A. Dedieu and F. Ingold, *Angew. Chem. Int. Ed*. 1989, **28**, 1694–1695.

31. I. Pápai, G. Schubert, I. Mayer, G. Besenyei and M. Aresta, *Organometallics*, 2004, **23**, 5252–5259.

32. Flores, M. (2017). *Diseño y evaluación de un catalizador para el acoplamiento reductor de $CO_2$ con olefinas.* Caracas: Simón Bolívar University.

33. R. Grubbs, A. Miyashita, M. Liu and P. Burk, *J. Am. Chem. Soc*, 1978, **100**, 2418–2425.

34. Jen-Shiang, Y. (2013). Density Functional (DFT) Methods.1, nr.1, pp. **1-10.** Consulted on 6 May 2018 via http://wild.life.nctu.edu.tw/~jsyu/compchem/g09/g09ur/k_dft.htm/

35. Koch, W., & Holthausen, M. (2015). *A Chemist's Guide to Density Functional Theory*. Weinheim: Wiley-VCH.

# Chapter 3

# Methanation

Another alternative to fight against the increasing of atmospheric carbon dioxide is found through many renewable sources of energy, such as wind power and solar energy that provides energy in a fluctuating manner.[1] To exemplify this, a technology called Electrical energy storage (EES) is considered as a valuable tool that can potentially smooth the variability in power flow from renewable generation and store renewable energy.[2] In this process, compounds like carbon dioxide and hydrogen are introduced into a methanation reactor where they are converted into methane and water. There are considered two essential reactions in which can also be called as the Sabatier and Senders discovering[3], considering as the main important the following one:

$$CO_2 + 4H_2 \leftrightharpoons CH_4 + 2H_2O \qquad \Delta H = -206.28 \text{ kJ/mol} \quad (1)$$

Nevertheless, there is another reaction called Water Gas Shift (WGS) which occurs simultaneously when an active catalyst is used.

$$CO + H_2O \leftrightharpoons CO_2 + H_2 \qquad \Delta H = -41.16 \text{ kJ/mol} \quad (2)$$

Looking through this reaction, there is a project called CATCO2RE which target is to investigate the conversion of $CO_2$ to solar fuels (methane and methanol) integrating new developments in the production of solar hydrogen, with the design and synthesis of selective active catalysts at milder reaction conditions, and effective $CO_2$ capture and purification technologies. Scientists from Flanders, Belgium have designed a plant, shown in Figure 3.1, in which it is necessary to design a methanation reactor.

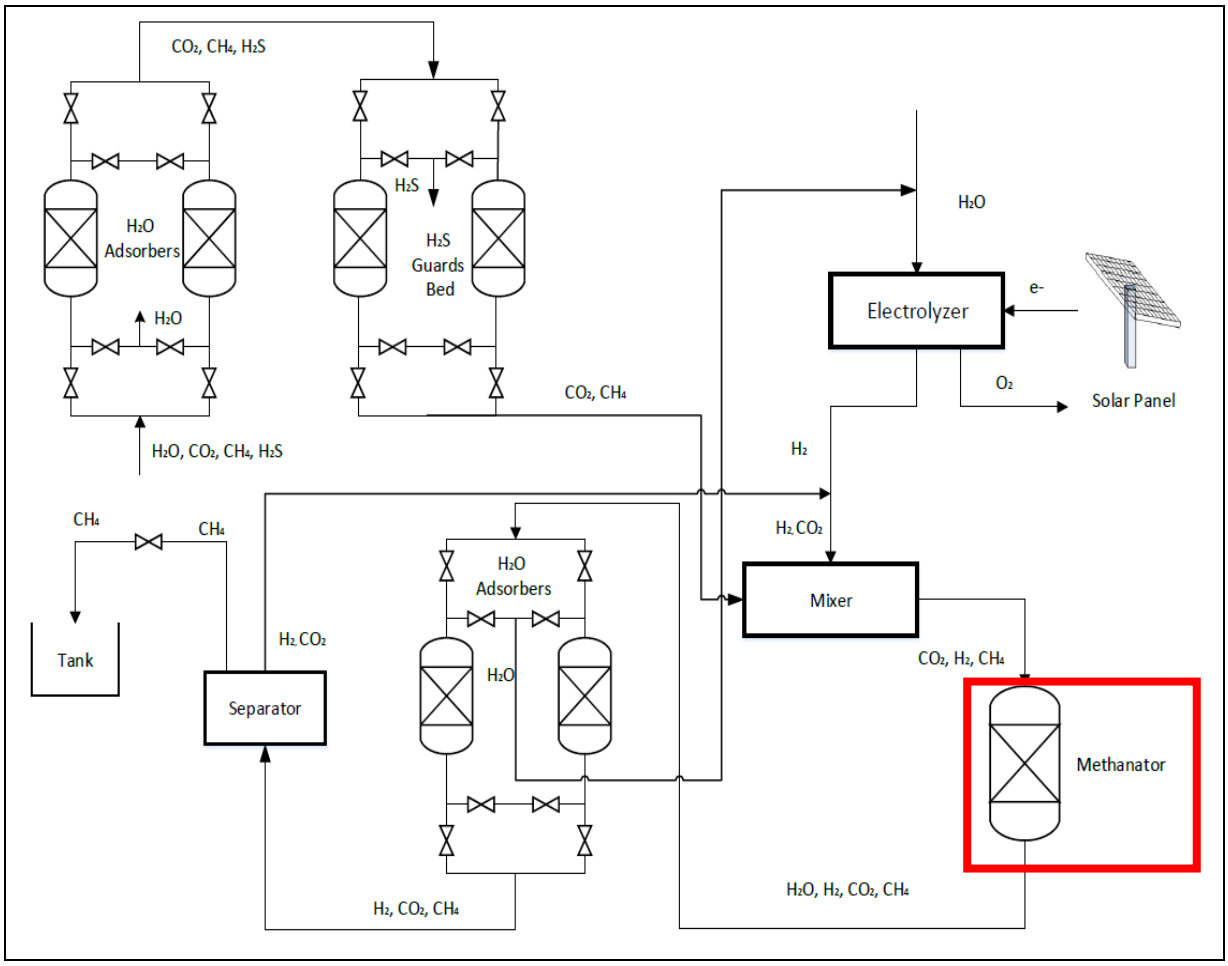


**Figure 3.1. Process designed for carbon dioxide conversion to solar fuels emphasizing the methanation reactor**

For this reason, it is important to find the important conditions according to the proper restrictions stipulated from the beginning, so that is why it is needed to determine the state of the art to know how have been the previous studies done by some investigators throughout the world, focusing their investigations in a similar way.

# 3.1 State of the art

Gao et al.[7] in 2011 did a comprehensive thermodynamic analysis of reactions that occurred in the methanation of carbon oxides (carbon monoxide and carbon dioxide) using the Gibbs free energy minimization method. This method can answer several doubts that commonly came up by the investigators, such as the type of thermodynamic stable reaction, the impact of reaction parameters like temperature, pressure or reactant ratios and at the same time whether observed reaction temperatures are thermodinamicaly appropriate.[7]

These investigators prepared optimized calculations for both kind of methanation, but in this case it is shown what they obtained for carbon dioxide and hydrogen reaction. It has been

demonstrated through this methanation that it is a particularly promising technique for reducing this atmospheric gas concentration and producing energy carrier.[8,9,10] In their study, they considered a feed gas with a stoichiometric molar ratio $H_2/CO_2 = 4$.

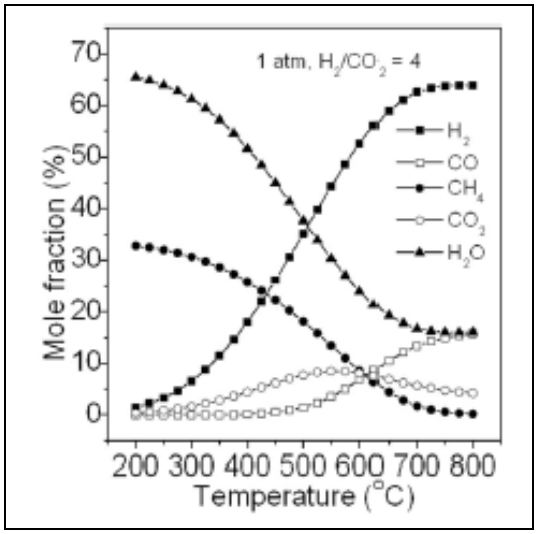


**Figure 3.2. Simulation results obtained by Gao et al. of mole fraction for each compound against temperature.[7]**

In Figure 3.2, it is shown that due to the strongly exothermic reaction existing in this case, the fact of increasing the temperature is not favorable for this. Nevertheless, if the temperature exceeds the value of 550ºC, the mole fraction of carbon dioxide reaches its maximum and then it becomes as a peak, decreasing owing to the reversed water gas shift reaction domination.[7]

Then, in the same figure it is shown the effect of parameters such as pressure and temperature in carbon dioxide conversion, methane selectivity and methane yield. When temperature (at values below 600ºC) and pressure increases, its conversion decreases, looking as a cause the fact of the reducing volume and exothermic reaction in which $CO_2$ methanation is involved. In addition, when the reaction takes place in conditions of 1 atm and beyond 600ºC, the $CO_2$ conversion gradually increases, owing to the reversed reaction of Water Gas Shift and its domination.[7]

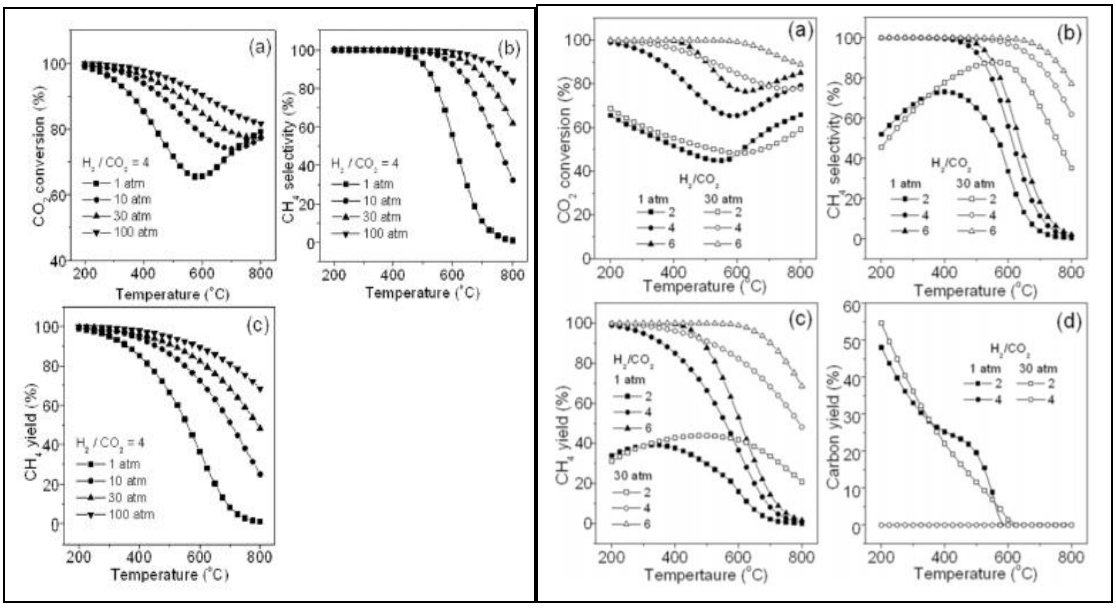


**Figure 3.3. Effect of pressure and temperature in $CO_2$ methanation obtained by Gao et al. in different aspects (left) and Effect of $H_2/CO_2$ molar ratio obtained by Gao et al. in different aspects (right).[7]**

In Figure 3.3, it can be seen the effect of molar ratio from the reactants in aspects like carbon dioxide conversion, methane selectivity, methane yield and carbon yield. From these results, it can be distinguished among all the others that when this ratio is higher, generally it leads to a higher conversion of carbon dioxide and $CH_4$ selectivity.[7] Conclusively, low temperature, high pressure, and proper $H_2/CO_2$ ratio is required for optimized $CO_2$ methanation.[7]

Er-rbib et al.[4] study the design of a methanation reactor considering carbon monoxide and hydrogen as reagents. In 2013, they prepared a project in which syngas entered to the methanation reactor with $H_2/CO$ molar ratio of 3; the reactions considered in the proposed model are CO methanation and Water Gas Shift conversion (WGS).

Modelling and simulation for this catalytic reactor was accomplished employing the Aspen Plus™ software through an isothermal fixed bed reactor (Plug Flow Reactor) with steam recovery, considering $Ni/Al_2O_3$ (50 wt% $Ni/Al_2O_3$, BET surface area = 183 $m^2/g$)[5] as a catalyst with the correspondent kinetics, that was defined for each reaction, shown in the next equations.[4]

$$\left(-r_{reaction\ 1}\right) = \frac{k_1 * K_C * P_{CO}^{0,5} * P_{H2}^{0,5}}{(1 + K_C * P_{CO} + K_{OH} * P_{H2O} * P_{H2}^{-0,5})^2} \qquad (1)\ ^4$$

$$\left(-r_{reaction\ 2}\right) = \frac{k_2 * (K_\alpha * P_{CO} P_{H2O} P_{H2}^{-0,5} - \frac{P_{CO2} * P_{H2}^{0,5}}{K_{eq}})}{\left(1 + K_C * P_{CO} + K_{OH} * P_{H2O} * P_{H2}^{-0,5}\right)^2} \qquad (2)\ ^4$$

Where $k_1$ and $k_2$ (rate constants); $k_{eq}$ is the equilibrium constant for the Water Shift reaction; $k^{\alpha}$ is refered to a combination of the adsorption constants of each of the compounds that participated

in the reactions and finally the constants which related the surface adsorption in equilibrium that are a function of temperature ($k_{OH}$ and $k_C$).[4] This kinetics worked in a temperature range of 473-673 K and high pressure.

In the simulation for this reactor, it was found in the Figure 3.4 the gas concentration profiles compared with the experimental obtained by Kopyscinski[5] in one of his previous investigations with the same methodology at a bench scale at 593 K, 2 bar and a molar ratio of $H_2/CO = 5$.[4]

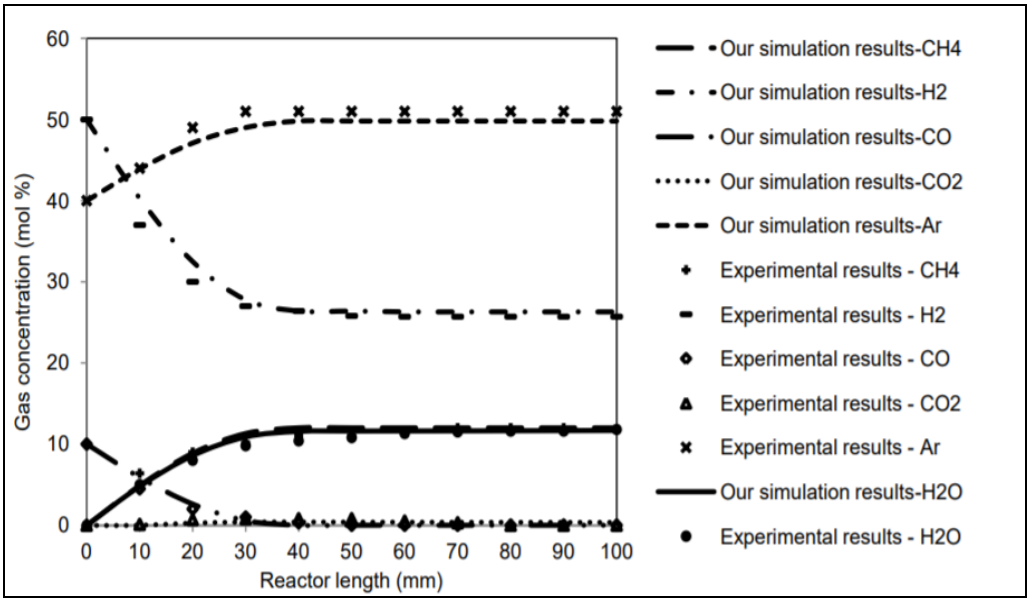


**Figure 3.4. Simulation results obtained by Er-rbib et al. Compared to the experimental data obtained by Kopyscinski (2010).**[4]

In concrete, the reactor had the next dimensions: a length of 10.57m, an inner diameter of 2.44 m and an outside diameter of 2.64 m; working at a temperature of 560.77 K and a high pressure of 62 bar. It was found that at higher temperatures, the rate of disappearance of reactants and the rate of formation of products increase. At the same time, it was assumed that as the concentration of $H_2O$ increases, the water gas shift reaction becomes important.[4]

In 2017, Granitsiotis[6] used Aspen Plus to model and simulate the reaction. He considered that owing to the lack of kinetics for the catalyst he had used (Ni-$Al_2O_3$), the conversion rate of the reactants was calculated based on the thermodynamic equilibrium data of the reaction.[6] He employed a Gibbs reactor module, as it can be seen in Figure 3.5, regarding the no kinetics data available.[6]

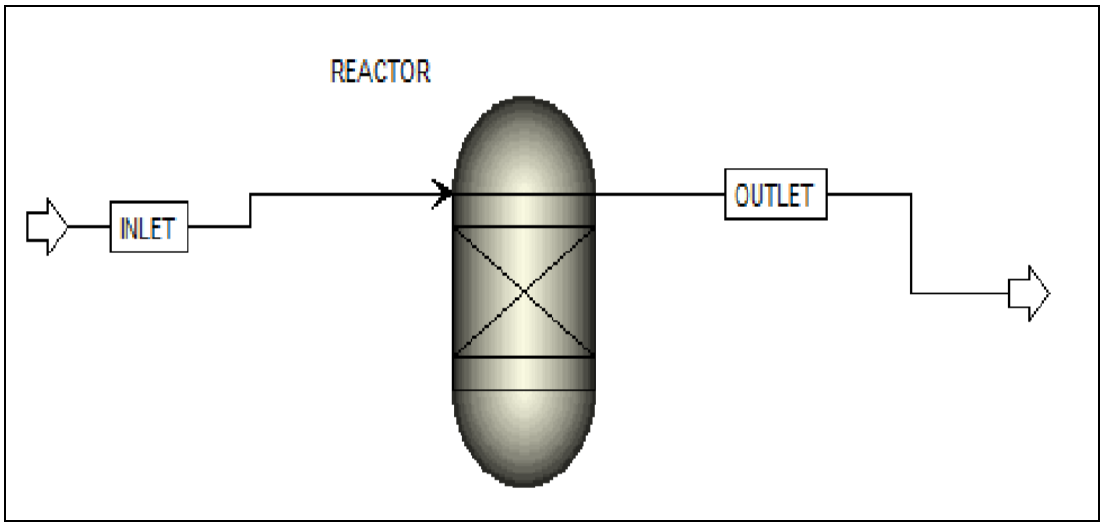


**Figure 3.5. Gibbs reactor model ellaborated in Aspen Plus [6]**

Therefore, it was done a sensitivity analysis in order to understand the conversion of carbon dioxide considering a pressure of 1 bar of the reactor, with multiple temperatures and with a composition of 76,19% $N_2$, 19,05% $H_2$ and 4,76% of $CO_2$.

Granitsiotis[6] obtained in his results that carbon dioxide conversion decreases from 120ºC and onwards. In the second simulation he had done, he obtained, for the same variation of temperature, but for several different values of pressure of the reactor, that the influence of the latter affects significantly in the development of the reaction, considering that for elevated pressures the conversion rises in higher values in comparison with those reactors working at lower pressures (1 bar, for example). Hence, industrial applications for methanation according to Granitsiotis[6] must take place at reactors of more than 20 bar of pressure, with the aim of converting as much as possible the carbon dioxide that is desired to be used in other ways.[6] In Figure 3.6, it is possible to see the result of his analysis graphically.[6]

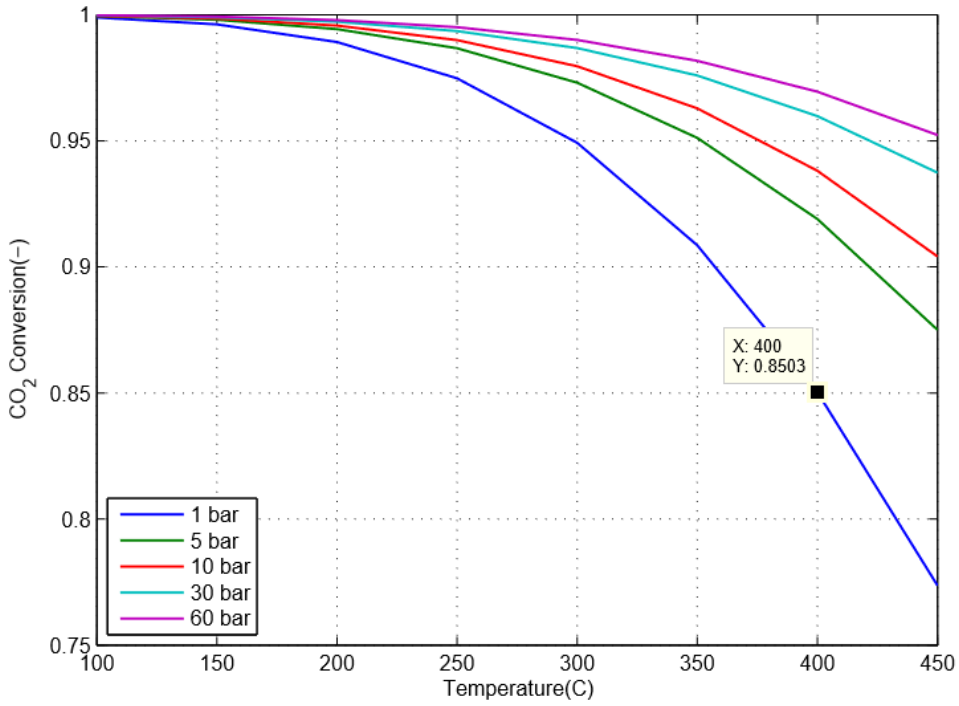


**Figure 3.6. Theoretical conversion of $CO_2$ for different values of pressure.[6]**

# 3.2 References


1. Čuček L, Varbanov P. S, Klemeš J. J and Kravanja Z, *AIDIC*, 2012, **29**, 61-66.
2. Gahleitner, G, *International Journal of Hydrogen Energy*, 2013, **38**, 2039-2061.
3. Sudiro, M & Bertucco, A. (2010). *Synthetic Natural Gas (SNG) from Coal and Biomass: a Survey of Existing Process Technologies, Open Issues and Perspectives, Natural Gas*. DOI: Padova.
4. H. Er-rbib and C. Bouallou, *AIDIC*, 2013, **35**, 541-546.
5. Kopyscinski, J. (2010). *Production of synthetic natural gas in a fluidized bed reactor: Understanding the hydrodynamic, mass transfer, and kinetic effects*. Villigen: Paul Scherrer.
6. Granitsiotis, G. (2017). *Methanation of Carbon Dioxide: Experimental research of separation enhanced methanation of $CO_2$.* Estocolmo: Delft.
7. J. Gao, Y. Wang, Y. Ping, D. Hu, G. Xu, F. Gu and F. Su. RSC Advances, 2012, **2**, 2358–2368.
8. J. L. Li, N. Fu, G. X. Lu and Chin. J. *Inorg. Chem*, 2010, **26**, 2175–2181.
9. T. Abe, M. Tanizawa, K. Watanabe and A. Taguchi, *Energy Environ. Sci*, 2009, **2**, 315–321.
10. J. N. Park and E. W. McFarland, *J. Catal*, 2009, **266**, 92–97.

# Chapter 4
# Methods

Computational programs have been used to design and study some of the $CO_2$ utilization catalytic processes. In this chapter, the computational methods applied for this project are shown. From one hand, the method involved for the catalysis of the reductive coupling of carbon dioxide with ethylene to produce acrylic acid is studied through Gaussian. For this reason, it is explained how is the program used, the thermodynamics involved for the Gibbs free energy calculations and the ligands used for this study. From the other hand, Aspen Plus is applied to study the carbon dioxide methanation process in this mathematical tool, starting from the initial conditions and looking for the best design of this reactor taking into the consideration as a main variable the molar ratio between the reactants.

## 4.1 Method for reductive coupling of carbon dioxide with ethylene

### 4.1.1 Description

The program used to do the geometry optimization is Gaussian 16. Using this one, it is possible to obtain the molecular structure and thermodynamic data of each of the steps created for the reaction mechanism proposed by Hollering et al, shown in Figure 4.1.

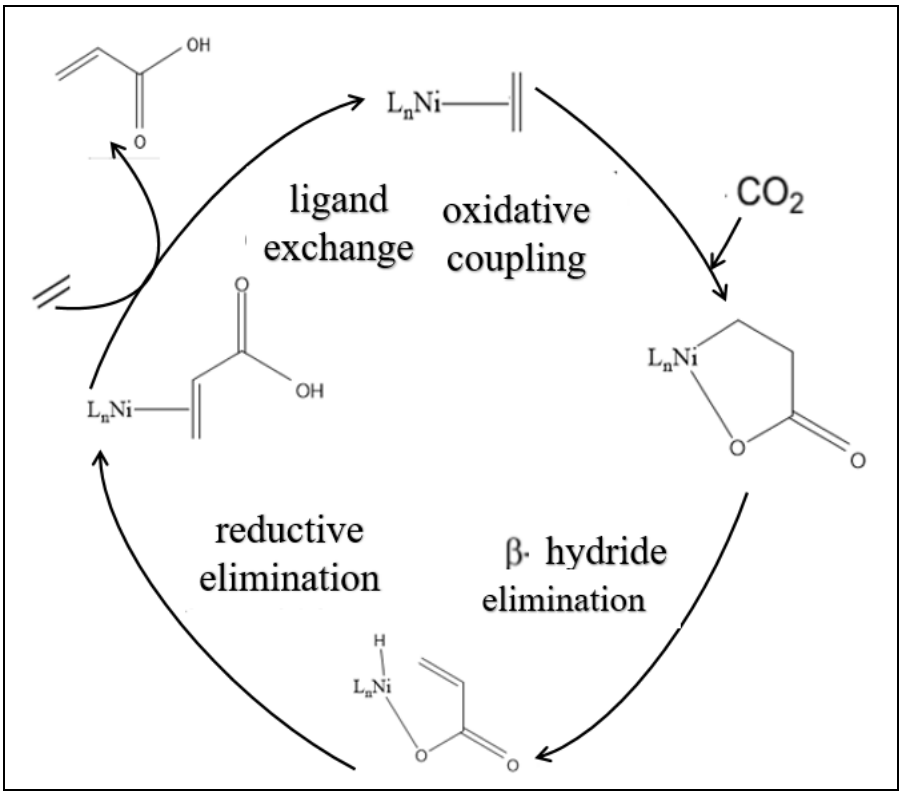


**Figure 4.1. Reaction mechanism used in this project, proposed by Hollering et al.[1]**

The internal ring has been chosen from the literature. Being one of the most common type of NHCs for organometallic chemistry and metal-mediated catalysis[2,3]: imidazol-2-ylidene. This specie, shown in Figure 4.2, has two important considerations to know how it could be altered during a reaction: backbone & ring side modications and N-substituted modifications.[4]

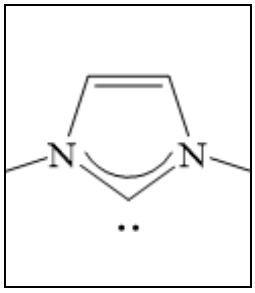


**Figure 4.2. Imidazol-2-ylidene ring**

Percent buried volume concept shows how high volume occupied by the ligand in comparison with others, and this will be an important parameter to consider at the time of study the mechanism. For this reason, the following ligands have been taken to study this reaction.

There have been chosen nine ligands according to their electronic and steric properties[4], and having different type of substituents: from one hand, there are IPr, SIPr, IPr*, SIPr*, IHept, ISO and Isoqui, as ligands with N-aryl substituents. From the other hand, they have been chosen IAd and IDD

as N-alkyl substituents, which names have been used from the literature to simplify their study throughout the project.[4,5]

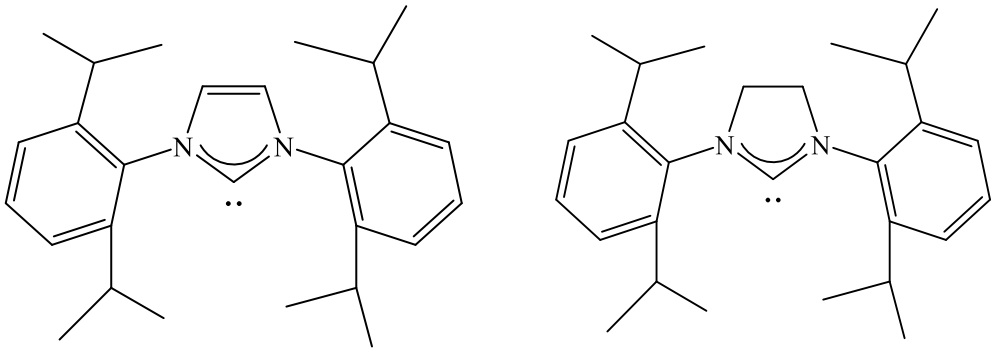

**Figure 4.3. Ligands IPr (left) and SIPr (right)**

From Figure 4.3, they are shown the following ligands: IPr (1,3-Bis(2,6-di-iso-propylphenyl)imidazol-2-ylidene) and SIPr (1,3-Bis(2,6-di-iso-propylphenyl-4,5-dihydroimidazol-2-ylidene).

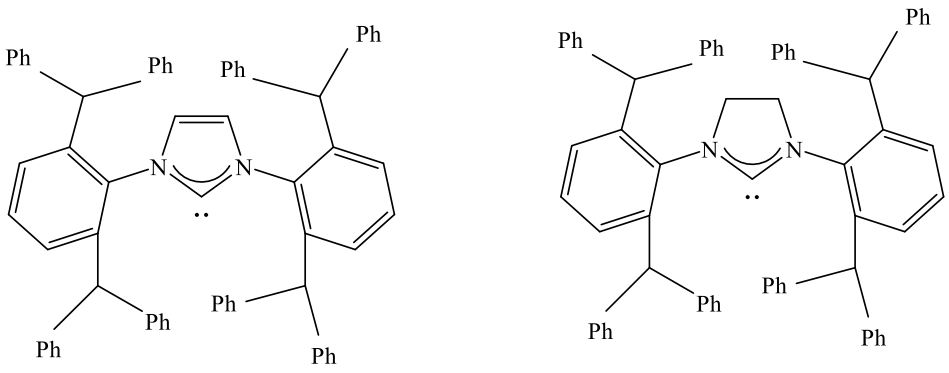

**Figure 4.4. Ligands IPr* (left) and SIPr* (right)**

Then, from Figure 4.4, being also N-aryl NHC, the previous ligands, which are conformed by isopropyls as substituents in each benzene, might be changed for phenyls. In the same study mentioned previously, IPr* (1,3-Bis(2,6-bis(diphenylmethyl)-4-methylphenyl)imidazol-2-ylidene). At the same time, the saturated form of this compound, renamed SIPr* (1,3-Bis(2,6-bis(diphenylmethyl)-4,5-dihydroimidazol-2-ylidene) have been taken in account.

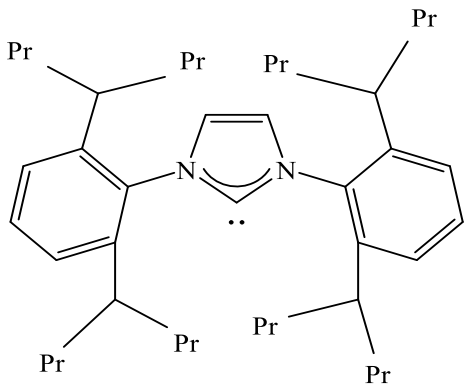


**Figure 4.5. Ligand IHept**

Belonging to the same group, it is desired to regard other substituents such as propyls. This is the case of IHept (1,3-Bis(2,6-di(4-heptyl)phenyl)imidazol-2-ylidene).

At the same time, according to Huynh[5] there are other N-aryl substituents also considered by Gómez-Suárez et al.[4] that represent species bearing less common NHC ligands. This is the case of the one conformed by isoquinolin substituents shown in the Figure 4.6. The aim of employing this kind of structure is increasing the available data in the literature and provide for further investigations more information about the catalytic activity of this ligand.[4] This one is abbreviated Isoqui (2-Benzyl-5-(2-methylnaphthalen-1-yl)imidazo[1,5-b]-isoquinolinium) for this project, but it is not found with this name in the literature, shown in Figure 4.6.

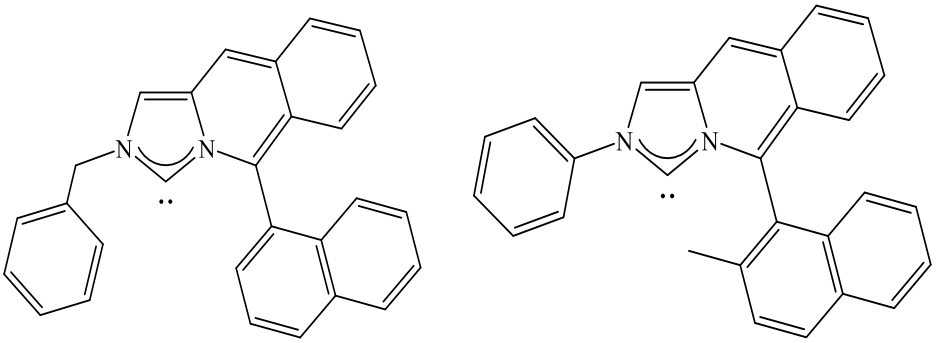


**Figure 4.6. Ligand Isoqui (left) and ISO (right)**

Besides, it is considered another ligand that counts with the same structure than Isoqui, but with the difference that the benzyl linked to one of the nitrogens of the ylidene ring is changed for a phenyl and from this it is possible to determine another comparison afterwards between both ligands and learn their catalytic behavior through this reaction. This is called ISO (2-phenyl-5-(2-methylnaphthalen-1-yl)imidazo[1,5-b]-isoquinolinium) shown in Figure 4.6.

From the second group mentioned by Gómez-Suárez et al.[4], there are the N-alkyl substituents. In the previous [AuCl(NHC)] study[4] there were studied different cases of this type, and there were found IDD (1,3-Dicyclododecylimidazol-2-ylidene) and IAd (1,3-Diadamantylylimidazol-2-ylidene), shown in Figure 4.7.

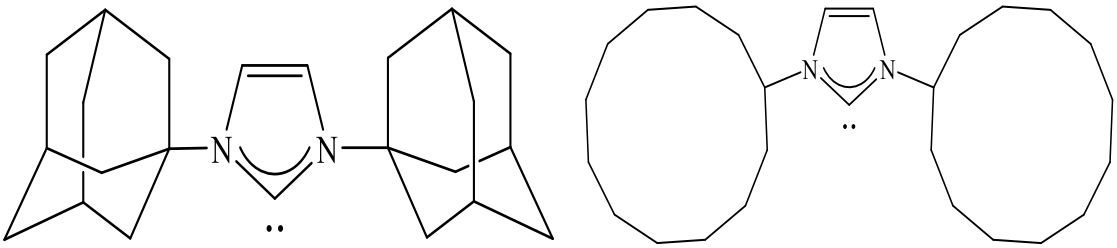

**Figure 4.7. Ligand IAd (left) and IDD (right)**

Then, each intermediate has been built in Gaussian 16, it is sent to optimize, and after it has converged, it is done a rotational scan study through a 360º rotation in a dihedral scan, consisting in 36 steps of 10º to complete the turn, with the aim of studying the conformer with the lowest energy and from this obtaining the structure the most stable as possible. Once each of them has been obtained, then there have been done diverse types of bond scans to look for possible transition states for the oxidative coupling (the approaching of $CO_2$ carbon to each of the ethylene carbons) and for the β-hydride elimination (the approaching of the β-hydrogen to the metallic atom).

Using these scans, when it has been found a possible result, it is sent to optimize as a TS and if it shows an imaginary frequency associated with the reaction mechanism and it converges in all the aspects, an IRC is performed (Intrinsic Reaction Coordinate) in both directions (forward and reverse) to determine that it is precisely the searched transition state.

Then, based on this energy values, the Gibbs free energy diagrams have been built for each ligand used and from this fact, it is determined how these ligands participate in the mechanism steps such as the oxidative coupling and the most limiting step: β-hydride elimination.

For these calculations, it has been applied the functional PBE1BE, based on the functional PBE. Besides, the polarized divided valence (SVP) has been applied too through the base Def2SVP considering the equations that approximate to the Schrödinger equation according to Koch et al.[6] The functional and the base equations were chosen due to the good performance and results obtained by Peverati et al.[7]

Gaussian 16 employs different equations in order to do all the calculations required. They are shown in the following part.

### 4.1.2 Gibbs free energy change

Previously to know how to calculate the Gibbs free energy in Gaussian, it is necessary to stablish all the parameters related for each of the motion that appear for it: translation, electronic, rotation and vibration must be considered individually.[8]

First, it is important to define the contributions from translation, defining the next equations for the entropy $S_t$, internal thermal energy $E_t$ and heat capacity $C_t$:

$$q_t = \left(\frac{2\pi m k_B T}{h^2}\right)^{\frac{3}{2}} * \left(\frac{m k_B T}{P}\right) \quad (4.1)$$

$$S_t = R * (\ln q_t + 1 + \frac{3}{2}) \quad (4.2)$$

$$E_t = \frac{3}{2} RT \quad (4.3)$$

$$C_t = \frac{3}{2} R \quad (4.4)$$

Where

| | |
|---|---|
| $T$ | Reaction temperature (K), default is 298.15 K |
| $R$ | Gas constant (8.31441 J/(mol*K)) |
| $m$ | Mass of the molecule |
| $P$ | Pressure (as default its value is 1 atmosphere) |
| $k_B$ | Boltzmann constant = 1.380662x $10^{-23}$ J/K |
| $h$ | Planck´s constant = 6.626176x$10^{-34}$ J s |
| $q_t$ | Transitition partition function |

Another aspect than be considered is the entropy due to electronic motion $S_e$ can be calculated as it follows: [4]

$$S_e = R * (\ln q_e + T * \left(\frac{\partial \ln q_e}{\partial T}\right)_V = R * \ln q_e \quad (4.5)$$

Where

| | |
|---|---|
| $V$ | Volume |
| $q_e$ | Electronic partition function |

In comparison with the previous criteria, there must be mentioned that the electronic heat capacity and the internal thermal energy are equal to zero.

In reference for the rotational contribution to the entropy is shown in the next formulations:[8]

$$q_r = \frac{1}{\sigma_r} * \left(\frac{T}{\Theta_r}\right) \quad (4.6)$$

$$S_r = R * (\ln q_r + T * \left(\frac{\partial \ln q_r}{\partial T}\right)_V = R * \left(\ln q_r + 1\right) \quad (4.7)$$

Where

$\sigma_r$ Symmetry number for rotation

$\ominus_r$ Characteristic temperature for rotation (referred to the moment of inertia)

$q_r$ Rotational partition function

At the same time, it´s possible to know the contribution to the internal thermal energy $E_r$ and the contribution to the heat capacity $C_r$.

$$E_r = RT^2\left(\frac{\partial \ln q_r}{\partial T}\right)_V = RT^2 * \left(\frac{1}{T}\right) = RT \quad (4.8)$$

$$C_r = \left(\frac{\partial E_r}{\partial T}\right)_V = R \quad (4.9)$$

For a nonlinear molecule, the rotational partition function must be calculated in a separate way, according to the following parameters:

$$q_r = \frac{\pi^{1/2}}{\sigma_r} * \left(\frac{T^{\frac{3}{2}}}{(\ominus_{r,x} \ominus_{r,y} \ominus_{r,z})^{1/2}}\right) \quad (4.10)$$

Where

$\ominus_{r,x} \ominus_{r,y} \ominus_{r,z}$ Characteristic temperature for rotation (referred to the moment of inertia in the x, y and z plane)

Then, for the rest of parameters it changes in the following way:

$$S_r = R * (\ln q_r + T * \left(\frac{\partial \ln q_r}{\partial T}\right)_V = R * \left(\ln q_r + \frac{3}{2}\right) \quad (4.11)$$

$$E_r = RT^2\left(\frac{\partial \ln q_r}{\partial T}\right)_V = RT^2 * \left(\frac{3}{2T}\right) = \frac{3}{2}RT \quad (4.12)$$

As a last parameter that must be mentioned is the vibrational motion and its important variables for the geometry optimization, including the $q_v$ which is the vibrational partition function,

entropy due to vibrational motion $S_V$, the internal thermal energy referred to the $E_V$ and finally the heat capacity $C_V$.

$$q_v = \prod_K \frac{e^{-\frac{\Theta_{v,K}}{2T}}}{1 - e^{-\frac{\Theta_{v,K}}{T}}} \tag{4.13}$$

$$S_V = R * \sum_K \left( \frac{\frac{\Theta_{v,K}}{T}}{e^{\frac{\Theta_{v,K}}{T}} - 1} - ln(1 - e^{-\frac{\Theta_{v,K}}{T}}) \right) \tag{4.14}$$

$$E_V = R * \sum_K \Theta_{v,K} \left( \frac{1}{2} + \frac{1}{e^{\frac{\Theta_{v,K}}{T}} - 1} \right) \tag{4.15}$$

$$C_V = R * \sum_K e^{\frac{\Theta_{v,K}}{T}} * \left( \frac{\frac{\Theta_{v,K}}{T}}{e^{-\frac{\Theta_{v,K}}{T}} - 1} \right)^2 \tag{4.16}$$

Where

$\frac{\Theta_{v,K}}{T}$ Characteristic temperature for vibration K

After these expressions, now it is possible to define the total energy $E_{tot}$, enthalpy $H_{corr}$, entropy $S_{tot}$ and finally Gibbs free energy $G_{corr}$, considering the previous contributions.

$$E_{tot} = E_{tran} + E_{rot} + E_{vib} + E_{el} \tag{4.17}$$

$$H_{corr} = E_{tot} + k_B * T \tag{4.18}$$

$$S_{tot} = S_{tran} + S_{rot} + S_{vib} + S_{el} \tag{4.19}$$

$$G_{corr} = H_{corr} - T * S_{tot} \tag{4.20}$$

# 4.2 Method for carbon dioxide methanation

Carbon dioxide methanation reactor has been designed applying Aspen Plus as the mathematic tool to obtain a simulation changing different variables that have been helpful to determine how the different linked parameters must be taken into account.

Previously at the design of a reactor, it is important to stablish that CATCO2RE have already defined some initial conditions from it which are seen it follows:

- **Methanation Catalysts**: supported Ni, Ru or Co
- **Conditions**: pressure of 1 atmosphere and a temperature equals or higher than 550 K, to prevent the formation of volatile Ni-carbonyls.
- **Selectivity**: 100% for stoichiometric feeds (will depend on feed composition)
- **Conversion**: as higher as possible, but it is better if it is 100%.
- **Reactor Dimensions & Catalyst Amount**: 1 cm diameter, ~0.5 g of 15 wt.% Ni on y-$Al_2O_3$ (75% conversion, No Heat or Mass Transfer Limitations and negligible pressure drop).
- **Catalyst Stability**: Sulfur, water and so more on.

Besides these conditions already known, there are others found in the following table referred to the components and its possible waste in different perspectives.

**Table 4.1: Conditions for the reactor according to components and its possible waste**

| ***Components*** | **Household waste** | **Wastewater treatment plants sludge** | **Agricultural wastes** | **Waste of agrifood industry** |
|---|---|---|---|---|
| $CH_4$ % vol | 50-60 | 60-75 | 60-75 | 68 |
| $CO_2$ % vol | 38-34 | 33-19 | 33-19 | 26 |
| $N_2$ % vol | 5-0 | 1-0 | 1-0 | - |
| $O_2$ % vol | 1-0 | < 0,5 | < 0,5 | - |
| $H_2O$ % vol | 6 (at 40 ° C) | 6 (at 40 ° C) | 6 (at 40 ° C) | 6 (at 40 ° C) |
| Total % vol | 100 | 100 | 100 | 100 |
| $H_2S$ mg/m$^3$ | 100 – 900 | 1000 - 4000 | 3000 – 10 000 | 400 |
| $NH_3$ mg/m$^3$ | - | - | 50 - 100 | - |
| Aromatic mg/m$^3$ | 0 – 200 | - | - | - |
| Organochlorinated or organofluorated mg/m$^3$ | 100-800 | - | - | |

Using values in Table 4.1, Table 4.3 shows which have been the compositions employed for the different simulations done in Aspen Plus, where the terms of higher or lower refers to $CO_2$ composition.

**Table 4.2: Specifications and conditions for L and H-gas network[14]**

| Feature | Specification for L gas-network | Specification for H gas-network |
|---|---|---|
| **Calorific upper value (incineration conditions 25 ° C and 1.01325 bara)** | 9,52 to 10,75 kWh/m³ | 10,81 to 12,79 kWh/m³ |
| **Wobbe index (combustion conditions 25 C and 1.01325 bara)** | 12,09 to 13,03 kWh/m³ | 13,65 to 15,78 kWh/m³ |
| **Density (relative)** | Between 0,555 and 0,700 | |
| **$C_3H_8$** | <3% (Current maxim measured value in GN) | |
| **T on injection** | in MD-C : 2°C < T < 38°C<br>in MD-C : 2°C < T < 38°C | |
| **Water content** | < 110 mg/m³(n) | |
| **Total sulfur content for odorization** | < 20 mgS/m³(n) | |
| **Total sulfur content after odorization** | < 30 mgS/m³(n) | |
| **Content of sulfur mercaptans for odorization** | < 6 mgS/m³(n) | |
| **Sulfur content of $H_2S$ + COS for odorization** | < 5 mgS/m³(n) | |
| **$CO_2$ content** | < 6 % (molar) | < 4 % (molar) |
| **$N_2$ + $CO_2$ content** | < 15 % (molar) | |
| **$O_2$ content** | < 1 % (molar) | |

**Table 4.3: Feed composition for several types of waste**

| Compound | Household Waste (average) (feed molar fraction %) | Household Waste (higher) (feed molar fraction %) | Household Waste (lower) (feed molar fraction %) | Wastewater treatment (average) (feed molar fraction %) | Wastewater treatment (higher) (feed molar fraction %) | Wastewater treatment (lower) (feed molar fraction %) | Waste of agrifood industry (feed molar fraction %) |
|---|---|---|---|---|---|---|---|
| **$CH_4$** | 55,27 | 50,5 | 60,00 | 67,50 | 60,00 | 75,00 | 68,00 |
| **$CO_2$** | 36,19 | 38,38 | 34,00 | 26,00 | 33,00 | 19,00 | 26,00 |
| **$N_2$** | 2,51 | 5,05 | 0,00 | 0,50 | 1,00 | 0,00 | 0,00 |
| **$H_2O$** | 6,03 | 6,06 | 6,00 | 6,00 | 6,00 | 6,00 | 6,00 |

After having already taken into consideration all these rules, in Aspen Plus the fact of having chosen the choice of Gibbs reactor comes from the idea of minimizing the Gibbs Free Energy for the reactions involved in the process: the proper methanation and the Water Gas Shift. However, in comparison with the Equilibrium reactor, another case found in Aspen Plus for which it is needed to determine the kinetic previously at the moment of defining the parameters for the calculations, the simulation results in both cases are completely similar, due to the fact that Gibbs reactor does not consider the kinetics as in the second case is realized, but this does not avoid obtaining the same values. This study has been done in isotherm conditions in order to have the same defined temperature in the feed and product flows.

One of the most important aspects that might be chosen cautiously is the thermodynamic model in Aspen Plus, according to the components used in the simulation, in Figure 4.8 there is shown a tool that help significantly to find the property model.[10]

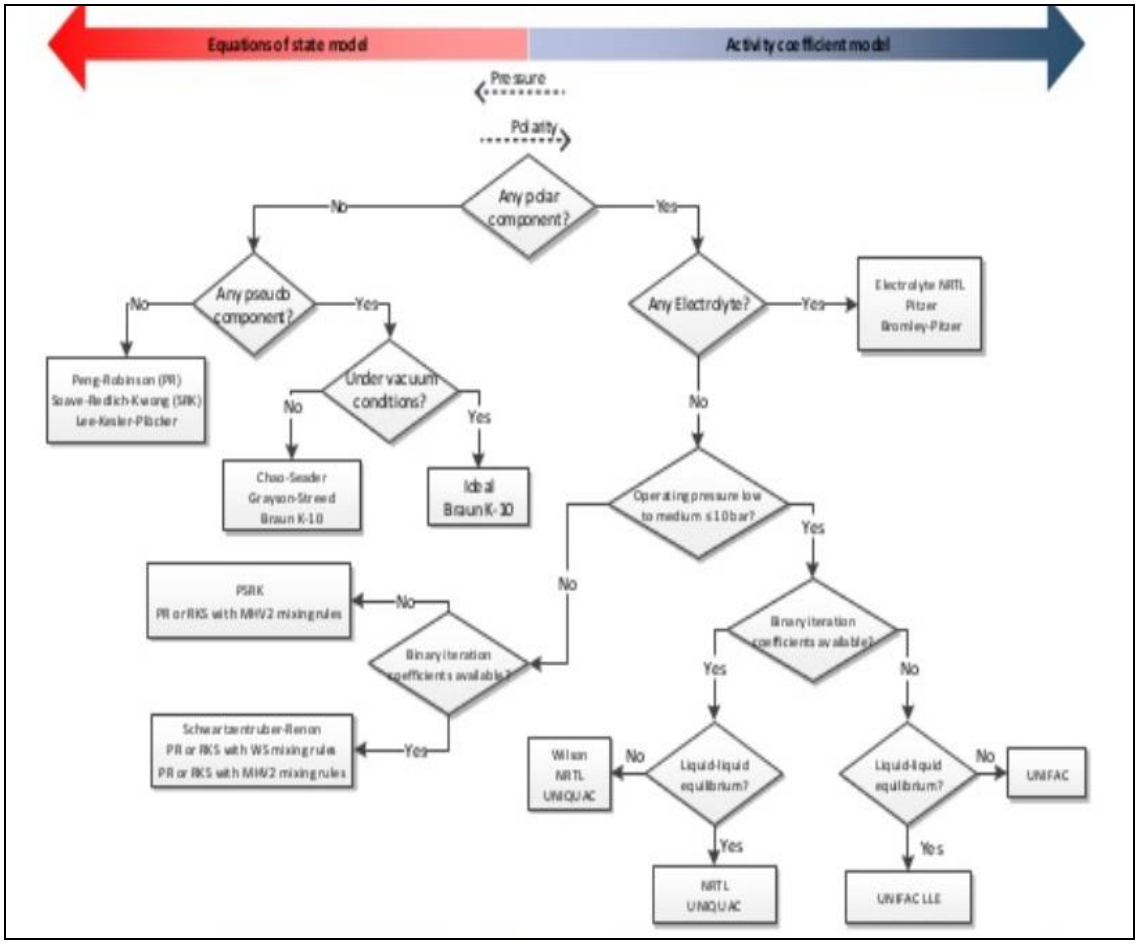


**Figure 4.8. Tool to obtain the ideal thermodynamic model for a simulation in Aspen Plus[10]**

The components participating in this simulation are: carbon dioxide, carbon monoxide, hydrogen, water and methane. According to Granitsiotis[9] and Kopyscinski[11] this process consists in a mixture of gases, in which most of them are non-polar, so that allows to choose as a thermodynamic model: Peng-Robinson (PR).

This decision allows to simulate all the calculations in Aspen Plus, considering the different gases participating and their correspondent chemical properties.

After this, it is necessary to do a sensitivity analysis to obtain different representations for the desired conditions in the products and to study the influence of some variables such as: the molar ratio between hydrogen and carbon dioxide, reactants conversion, methane production, methane molar fraction, methane yield and carbon monoxide production. The mathematic formulas for these parameters are shown in Table 4.4.

**Table 4.4: Mathematic formulas for parameters calculated in Aspen Plus**

| Parameter | Formula |
|---|---|
| **$H_2$ conversion (4.21)** | $\frac{H_2\ feed\ flow - H_2\ productflow}{H_2\ feed\ flow} * 100$ |
| **$CO_2$ conversion (4.22)** | $\frac{CO_2\ feed\ flow - CO_2\ productflow}{CO_2\ feed\ flow} * 100$ |
| **$H_2/CO_2$ molar ratio (4.23)** | $\frac{H_2\ feed\ flow}{CO_2\ feed\ flow}$ |
| **$CH_4$ molar fraction (4.24)** | $\frac{CH_4\ productflow}{\sum each\ component\ product\ flow} * 100$ |
| **$CH_4$ yield (4.25)** | $\frac{CH_4\ productflow}{H_2\ or\ CO_2\ feed\ flow} * \frac{1}{stoich.coefficient}$ |

In some cases, molar fractions have been estimated in dry basis (without considering water), due to the fact that this compound is not important at the time of analyze certain aspects that will be shown in the results. Then, an energy balance has been done to study which are the best conditions using these parameters. There have been considered the following relations:

$$Duty\ in\ the\ reactor = Duty_{products} - Duty_{feed} \quad (4.26)$$

This formula considers the energy from both exothermic reactions in cal $s^{-1}$.

$$Separation\ energy_{gases} = -R * T * \sum x_i * \ln(x_i) \quad (4.27)$$

Where[13]

| | |
|---|---|
| *T* | Reaction temperature (K) |
| *R* | Gas constant (8.31441 J/(mol*K)) |
| $x_i$ | Molar fraction in dry basis for a compound |
| Energy | J $mol^{-1}$ |

*4.27* considers ideal gases behaviour that for this study would help to obtain an idea on how much energy is necessary to apply in diverse conditions.

Then, in Figure 4.9, it is shown a capture from a Sensitivity Analysis done in Aspen Plus.

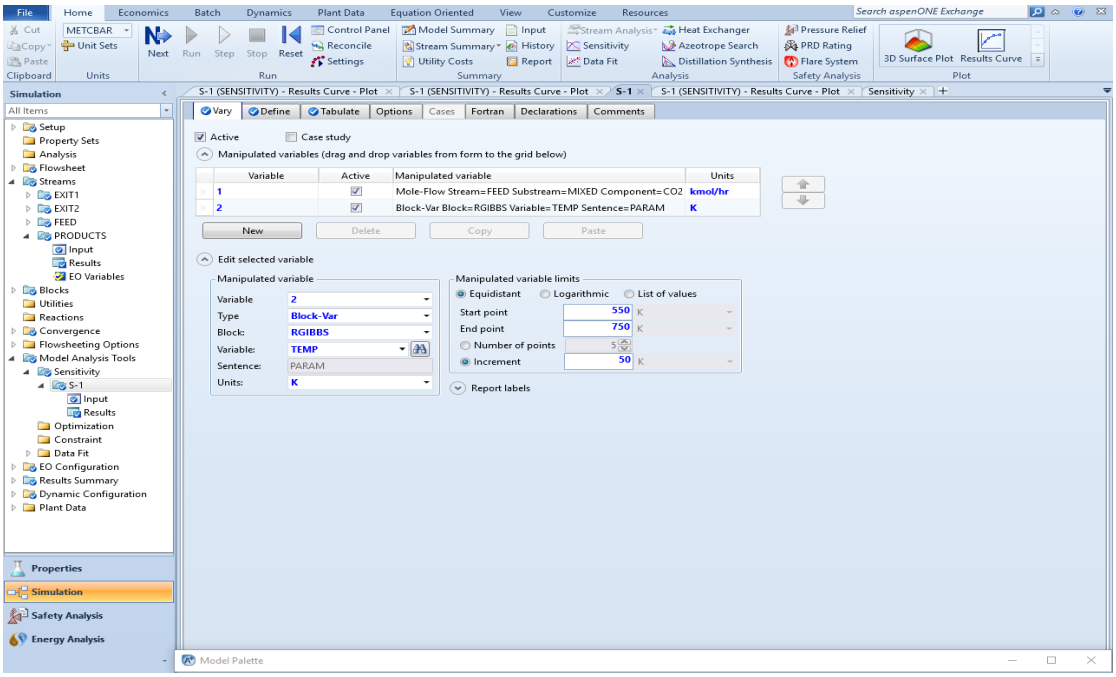


**Figure 4.9: Sensitivity analysis in Aspen Plus.**

# 4.3 References


1. M. Hollering, B. Dutta and F. Kühn, *Coordination Chemistry Reviews*, 2016, **309,** 51-67.
2. M. N. Hopkinson, C. Richter, M. Schedler and F. Glorius, Nature, 2014, **510**, 485–496
3. S. Díez-González, N. Marion and S. P. Nolan, Chem. Rev., 2009, **109**, 3612–3676.
4. A. Gómez-Suárez, D. J. Nelson and S. P. Nolan, *Chem. Commun*, 2017, **53**, 2650.
5. H.V. Huynh. *Chem. Rev*, 2018.
6. Koch, W., & Holthausen, M. (2015). *A Chemist's Guide to Density Functional Theory*. Weinheim: Wiley-VCH.
7. Peverati, R., & Truhlar, D. G. (2014*). Quest for a universal density functional: the accuracy of density functionals across a broad spectrum of databases in chemistry and physics*. *Philosophical Transactions of the Royal Society*.
8. Ochterski, J. (2000). *Thermochemistry in Gaussian.* Help Gaussian.
9. Granitsiotis, G. (2017). *Methanation of Carbon Dioxide: Experimental research of separation enhanced methanation of* $CO_2$. Estocolmo: Delft.
10. A. Carrero, N.Quirante & J. Javaloyes (2016). *Introduction to Chemical process simulators: DWSIM Chemical Process Simulator. ConCEPT.*
11. Kopyscinski J. (2010). *Production of synthetic natural gas in a fluidized bed reactor: Understanding the hydrodynamic, mass transfer, and kinetic effects*. Villigen: Paul Scherrer.
12. http://www.biogas-renewable-energy.info/biogas_composition.
13. S. Satter, 2000. *Thermodynamics of Mixing Real Gases*. J. Chem. Educ. **77**, 1361-1365.
14. http://www.synergrid.be/download.cfm?fileId=G5_42_NL_Voor_consultatie_20171201.pdf

# Chapter 5
# Gaussian results

In this chapter the different results that have been obtained for the study of the reductive coupling between carbon dioxide and ethylene will be discussed. There are considered two reaction mechanisms depending on the initial step: if it is done with one ethylene or two ethylenes. Then, there are shown the different partial energy diagrams for the ligands chosen for this investigation, considering a comparison among them.

Thus, there is presented a comparison between the intermediates and the important properties coming from their structure. Finally, the ideal mechanism and ligand are mentioned in the discussion.

Gómez-Suárez et al.[1] have studied several N-heterocyclic carbenes according to their electronic and steric properties. Basing on their study, the different ligands used for this investigation have been divided into three groups considering the decreasing buried volume obtained by these authors: IHept, IPr* and SIPr* (first group), IPr, SIPr and IAd (second group) and finally IDD, ISO and Isoqui (third group). For the latter, the last two ligands have not been studied in the literature with this type of reaction yet, so that is why both will be studied with the ligand found with the lowest $\%V_{bur}$ among them.[1]

Therefore, it will be presented the study for one ethylene and its correspondent reaction mechanism starting from the previous idea.

## 5.1 Reaction mechanisms

### 5.1.1 Ethylene study

The corresponding reaction mechanism for one ethylene begins with the attack of the carbon dioxide to carry out the oxidative coupling.[6] This way, the carbon of the latter joins with any of the ethylene carbons (α or β).

Then, a transition state is obtained between the ethylene and the lactone formed, subsequently obtaining two different reaction paths depending on which carbon bond has been formed in the previous step.

From the lactones, the β-elimination might take place from the lactone and then, another intermediate has been found: the hydride acrylate. In the following Figures, there are shown the reaction mechanism and the partial energy diagrams obtained for the different ligands.

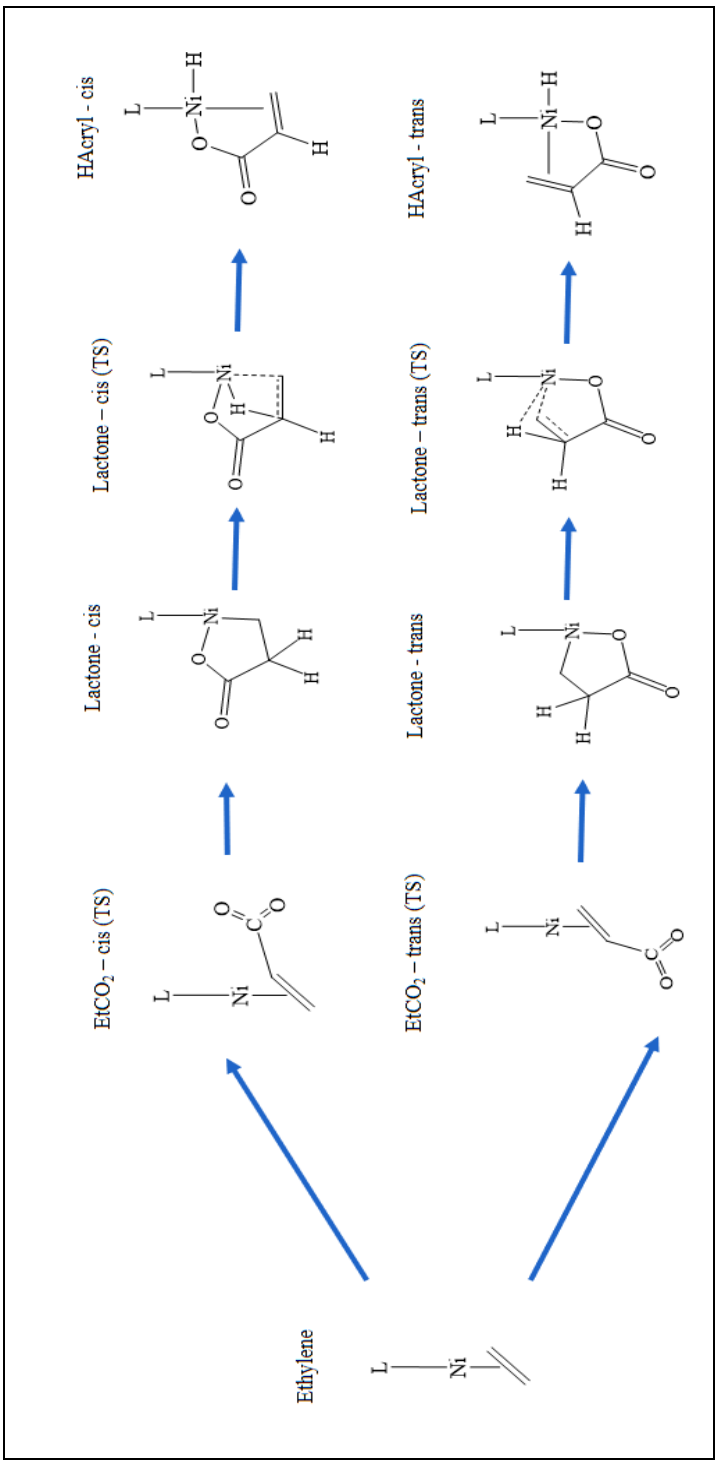


**Figure 5.1. First reaction mechanism**

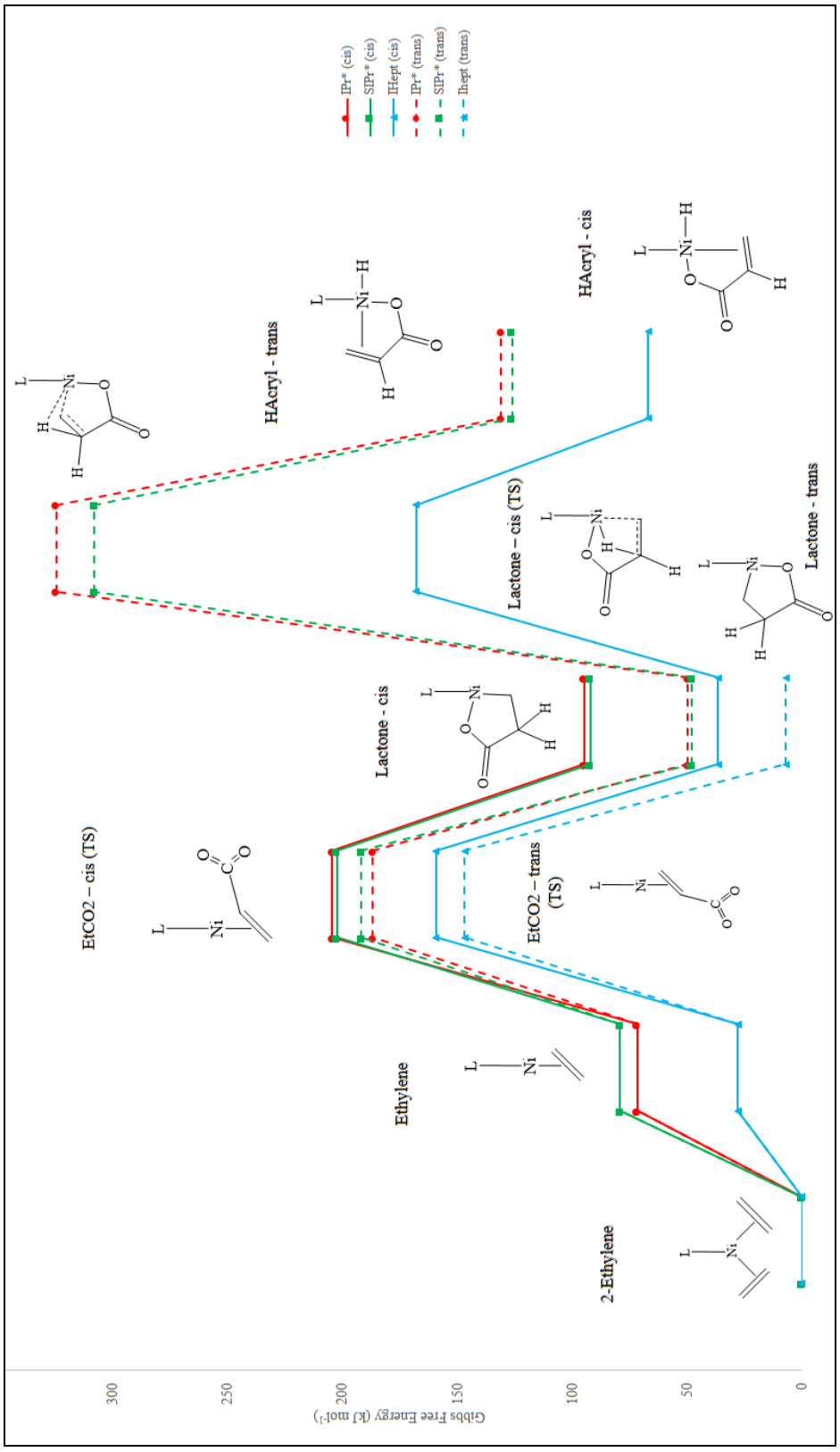


**Figure 5.2. Diagram energy for ligands IPr*, SIPr* and IHept with the first reaction mechanism**

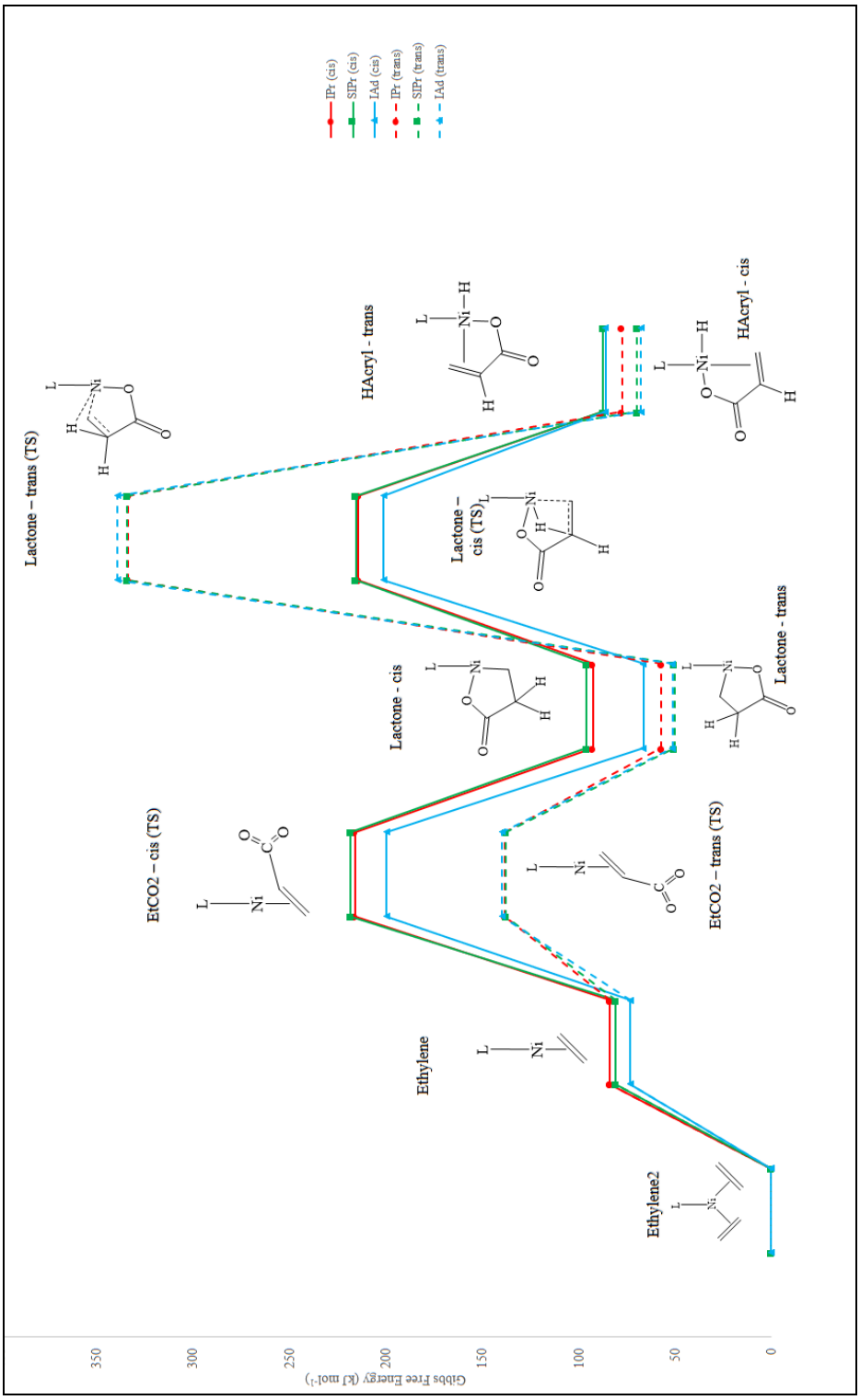


**Figure 5.3. Partial diagram energy for ligands IPr, SIPr and IAd with the first reaction mechanism**

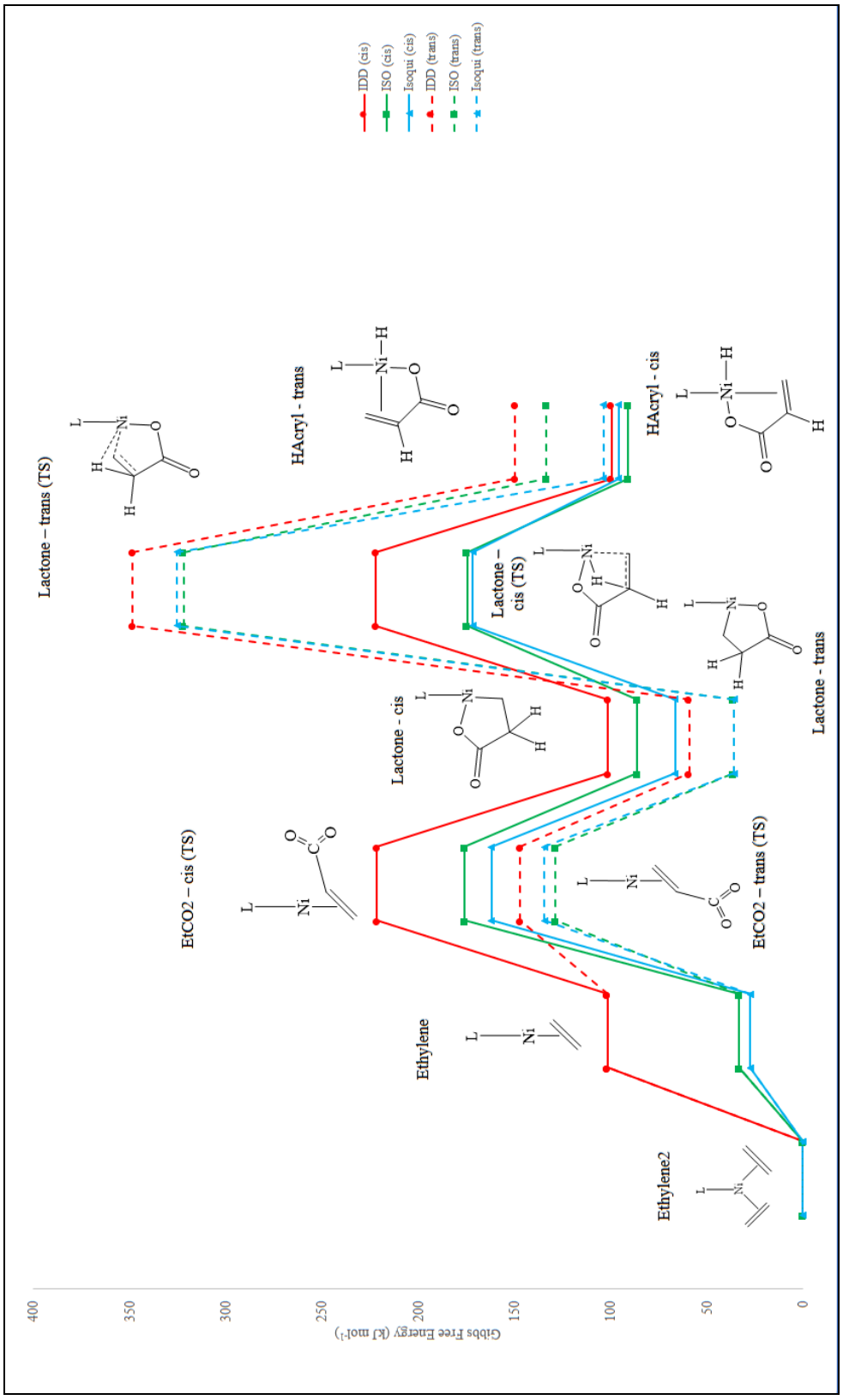


**Figure 5.4. Partial diagram energy for ligands IDD, ISO and Isoqui with the first reaction mechanism**

The first aspect that may be discussed is referred to the presence of the two ethylenes bound to the organometallic compound in the diagrams. The latter is more stable than the one with just one ethylene, so that is why it has been used as the reference to estimate the Gibbs Free energy for each step in the mechanism.

From the three groups, it can be seen from Figures 5.2 to Figure 5.4 how the energy changes according to the ligand. In the first step (the oxidative coupling) it has been obtained that the β-coupling gets higher energies than the α-coupling, due to the high energetic cost it takes to obtain the *cis*-lactone in comparison with the *trans*-lactone, which at the same time are more stable than the other.

Regarding to the β-coupling, during the bond scan done for each ligand to look for the transition state, it has been obtained that for the ligands from Group 3, the attack of the carbon dioxide is produced in the inner zone of the ligand, while for the rest it is produced in the external zone, as it is shown in Figure 5.5. However, according to the IRC studied for this transition state, the mechanism keeps being the same in both cases.

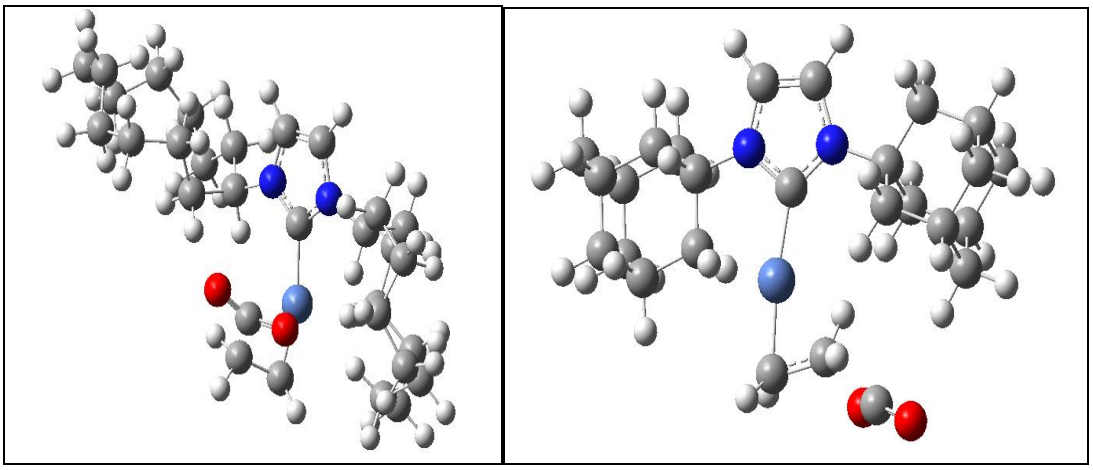

**Figure 5.5. Inner attack of $CO_2$ to IDD (left) and external attack to IAd (right)**

After the mechanism mentioned above, the limiting step in the proposed mechanism is the β-elimination, as it has been stablished by Buntine et al.[7] due to the high kinetic barrier that it might be beaten. The transition state from the *trans*-lactone to the *trans*-hydride acrylate is too high, taking values of almost 350 kJ $mol^{-1}$, which is practically undesired and impossible to develop in real life. Nevertheless, while it is true that the *cis*-lactone (transition state) is more stable but with high energies too, at the time of looking for the ideal mechanism, this becomes the key step to choose between one or the another.

IDD represents the ligand with the highest Gibbs Free energies in almost all the steps, which coincides with the study done by Gómez et al.[1] and the definition of this ligand as the one with less steric control among the studied in this investigation.

Thus, IHept represents the ligand with more stability, mentioned by Gómez et al.[1] as the bulkiest, which can be seen through Figure 5.2 with lower energies in comparison with IPr* and SIPr*. At the same time, the ligands not study by them, Isoqui and ISO have shown a favorable result for this reaction, due among other reasons to the electronic cloud coming from the aromatic rings that provides greater stability to the reagent.

In this way, it is continued with the study of the mechanism with two ethylenes.

## 5.1.2 Two ethylenes study

Once it has been shown the proposed mechanisms with one ethylene, it is important to know that the metallic center: nickel, located in the 10th group of the periodic table, have 14 electrons counted according to the covalent model from the 18 electron rule stablished for organometallic compounds. This metal represents an exception to this rule, because its stability can be found with 16 electrons instead of the number this method mentions.[2]

For this reason, it is proposed to add another ethylene coordinated with the metallic center to obtain 16 electrons and from this it will be possible to study how the reaction takes place in a more stable molecule than the one with just one ethylene. This structure has been used as the reference to calculate the rest of energies for intermediates and transitition states shown in Figure 5.6.

This mechanism starts with the ligand and the metallic center bound to two ethylenes. The first step consists in the reductive coupling with carbon dioxide, which attacks directly one of them. Then, depending on which ethylene carbon is joined to the $CO_2$ carbon, a transition state is found for α and β positions. It is formed an intermediate: a lactone and ethylene coordinated at the same time after this step.

Then, the β-elimination might occur as it happens with the previous mechanism. However, it has been found that it is not possible to produce this step with another ethylene, so this means the one not forming part of the lactone might be dissociated, as it was found by Grubbs et al.[3] and the necessary structure for which the β-elimination takes place, where the β carbon of the alkyl must have a hydrogen as a substituent and. The M–C–C–H unit must be able to take up a roughly syn-coplanar conformation, which brings the β hydrogen close to the metal.[2]

In addition, the mechanism continues the same route as the previous case, starting from the lactone in *cis* or *trans* position, followed by a transition state between this intermediate and a hydride acrylate with the same type of isomers.

The ligands have been divided in the three groups mentioned in the beginning, according to the classification of the steric control reflected by Gómez et al.[1] in their study. The correspondent partial energy diagrams appear in the Figures below.

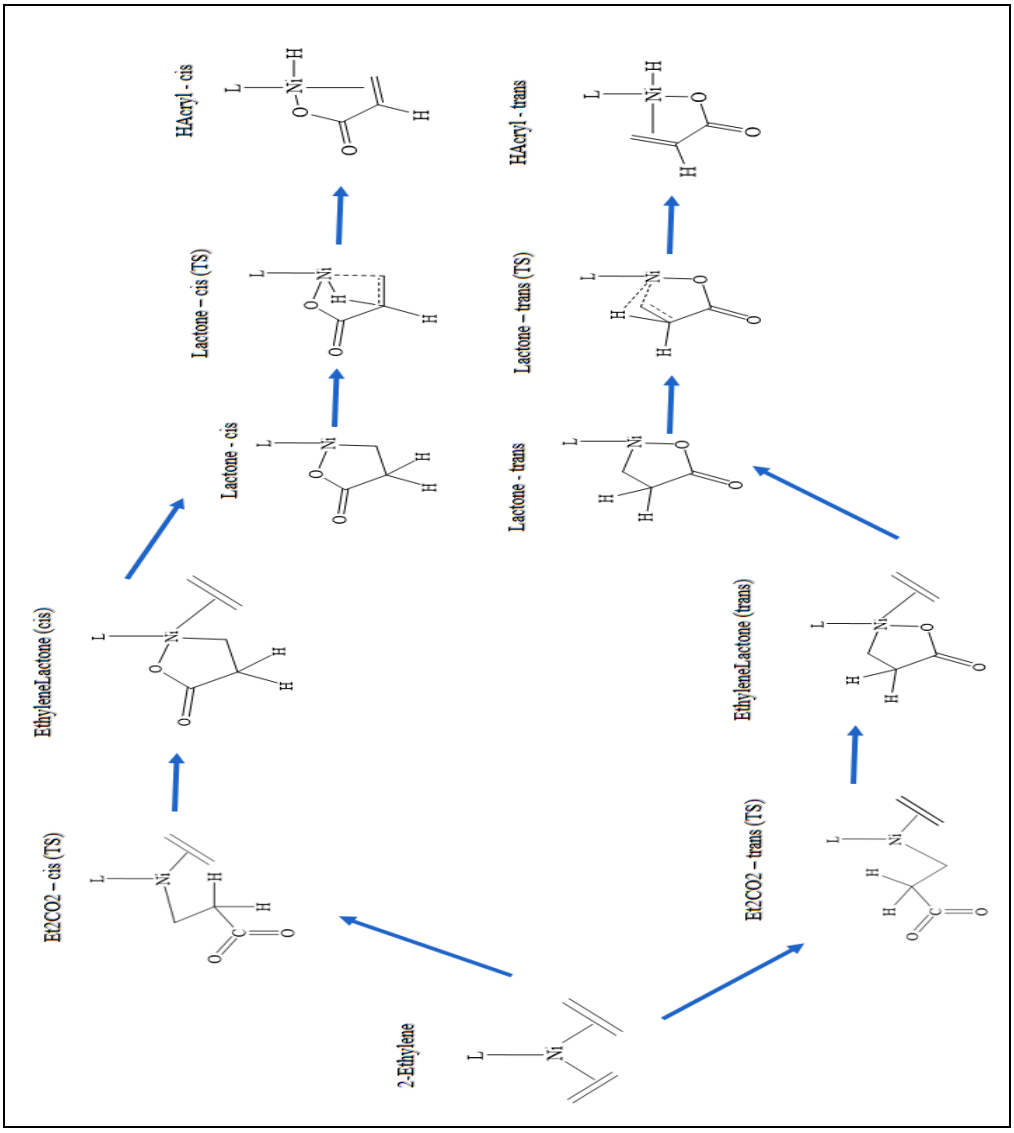


**Figure 5.6. Second reaction mechanism**

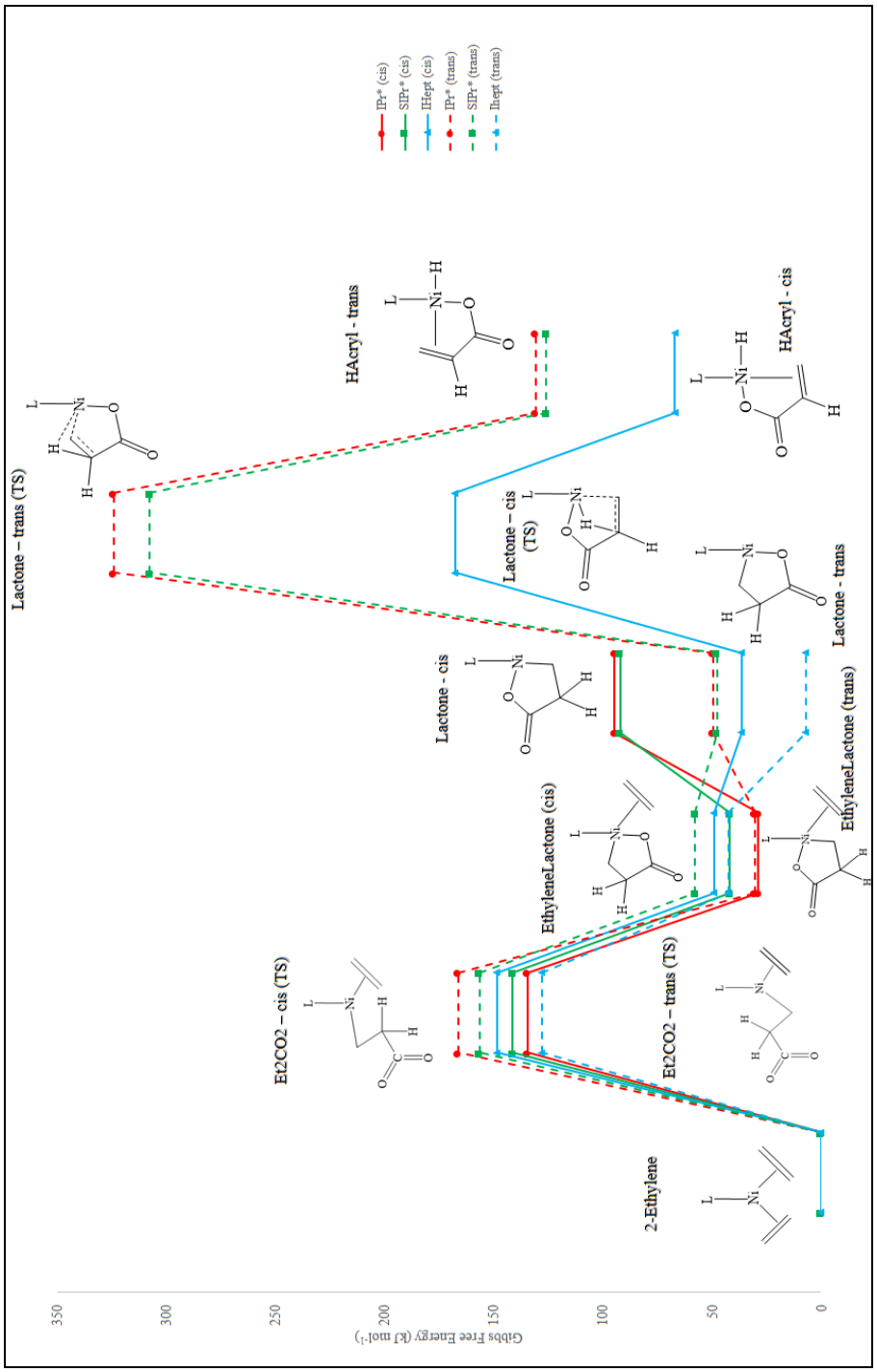


**Figure 5.7. Partial diagram energy for ligands IPr*, SIPr* and IHept with the second reaction mechanism**

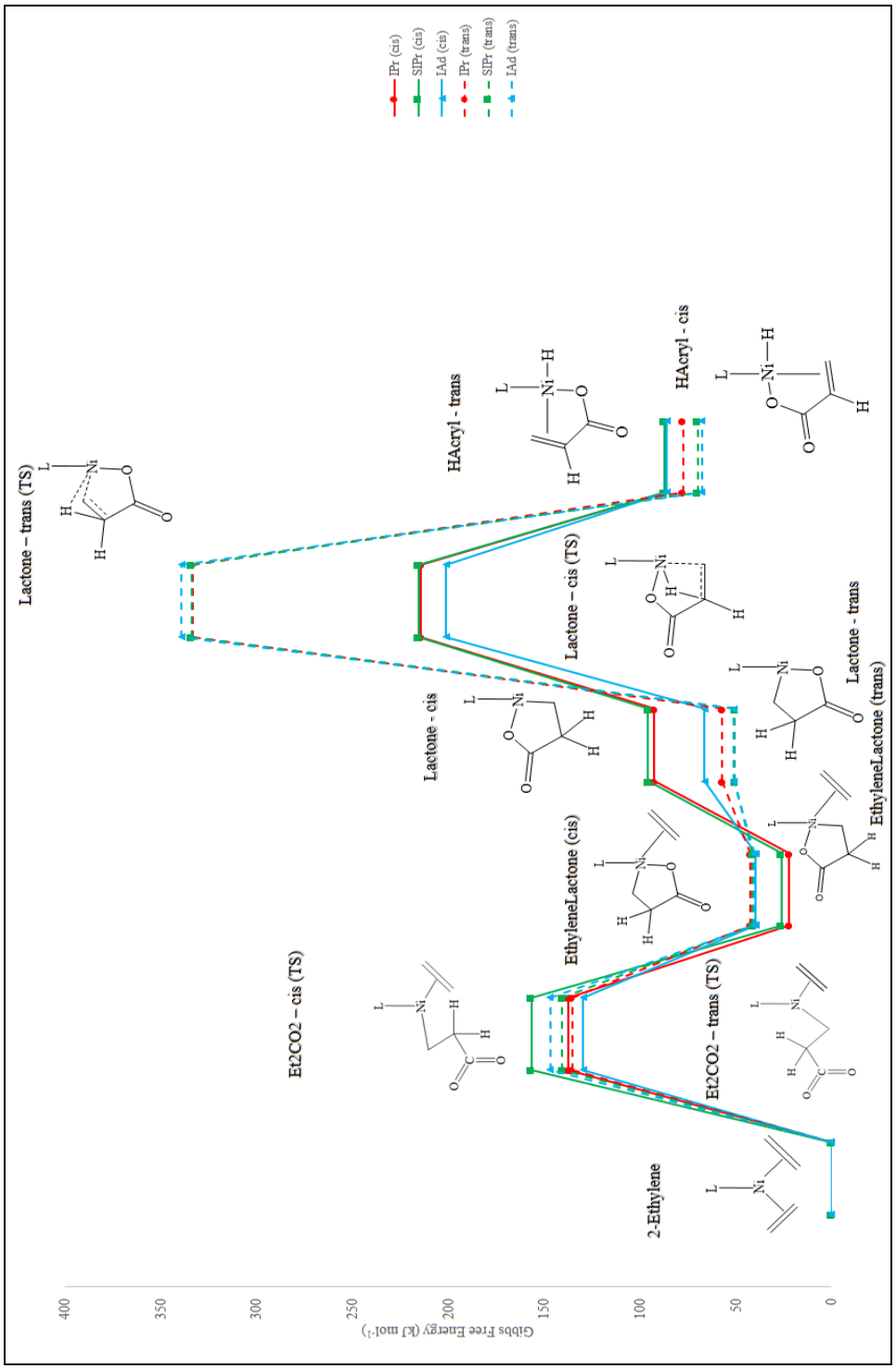


**Figure 5.8. Partial diagram energy for ligands IPr, SIPr and IAd with the second reaction mechanism**

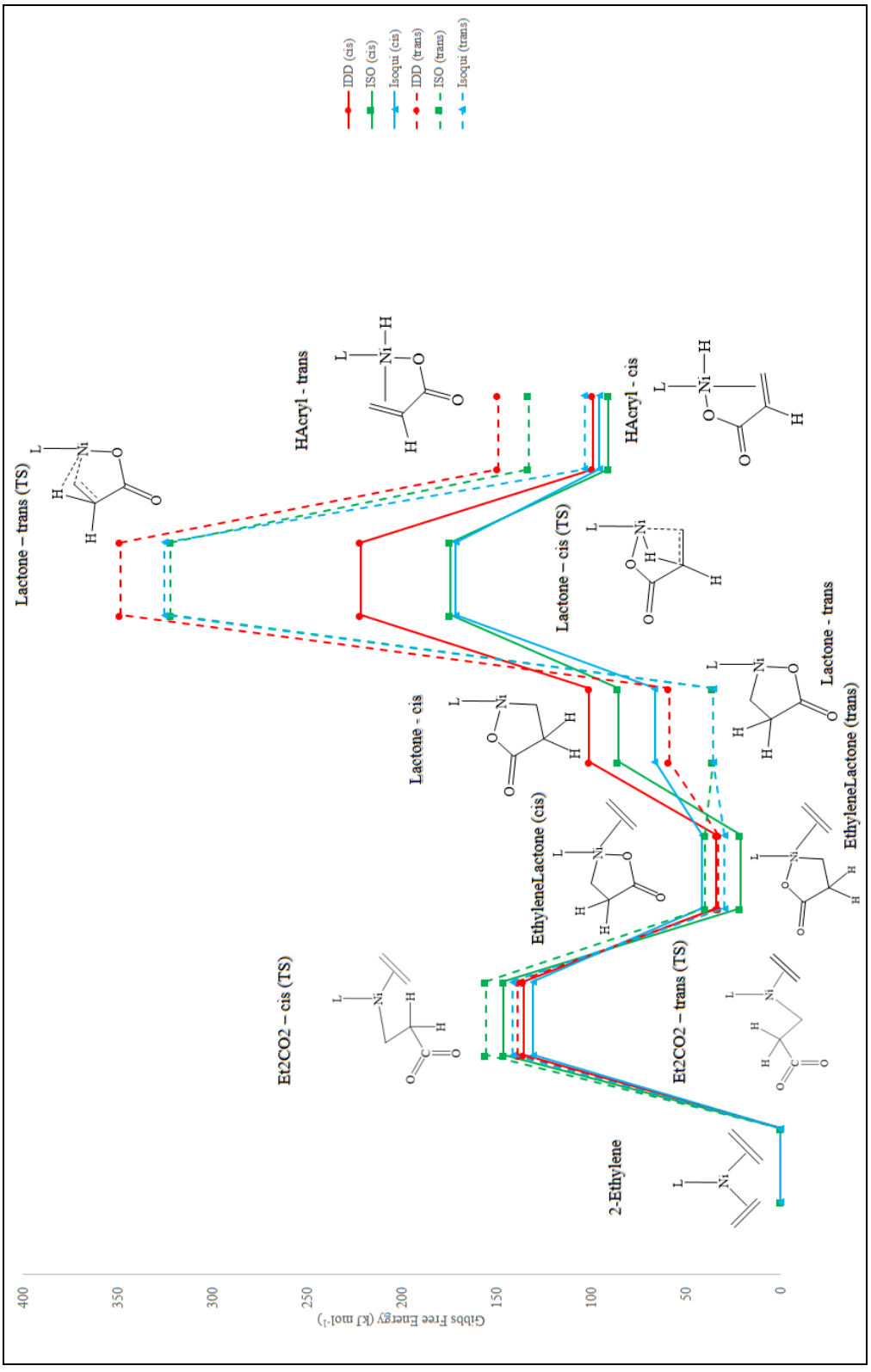


**Figure 5.9. Partial diagram energy for ligands IDD, ISO and Isoqui with the second reaction mechanism**

As it has been shown in the previous Figures, the mechanism with two ethylenes has been determined for all the ligands. The transition states for the reductive coupling have been found according to a scan bond starting from the approaching of the $CO_2$ to one of the ethylenes, looking for a step in which it was found a maximum between two minimums which are the correspondent intermediates.

Their validity must be proved through the IRC (Intrinsic reaction coordinate) to determine they really are the searched transition state in both senses (forward and reverse), because in this investigation there have surged some mistakes at the time of looking for them which solution have not been found.

In correspondence to this transition state, it is not possible to affirm which type of coupling (α or β) is more convenient, due to the fact that each ligand has presented a difference trend with one of another. However, this mechanism becomes important when the following intermediate conformed by an ethylene and lactone is more stable than the proper lactones, owing to the electrons the ethylene could contribute (2 electrons) to the compound, that brings more stability, besides the geometry that the metallic center acquires.

It is important to mention that all the ligands are symmetric except ISO and Isoqui. For this reason, the reductive coupling transition state have been studied in the two ethylenes, showing the lowest energy in the diagram. It has not been found a transition state for each ethylene in each case, so it is not to possible to determine which ethylene is more beneficial in the reaction for these ligands in terms of energy.

At the same time, the kinetic barriers for the reductive coupling between the reference and the lactone after having dissociated the ethylene, have shown the lowest energies for the bulkiest ligand: IHept, obtaining for the *cis*-conformation (36.44 kJ $mol^{-1}$) and for the *trans*-conformation (6.98 kJ $mol^{-1}$). The kinetic barrier becomes lower with ligands that accomplish a greater bulking in the metallic center for the *trans*-lactone.

### 5.1.3 Comparison between both mechanisms

The reaction mechanism between one ethylene and two ethylenes differ practically in the way the oxidative coupling takes place. As it has been mentioned before, the β-coupling in the first reaction mechanism requires high energies in comparison with the α-coupling. The energies found for the second mechanism in this step are significantly lower, without a key parameter that expresses which type of coupling is more favorable. For this reason, the kinetic barrier that might be beaten in this step to obtain the lactones seems more convenient through the second case.

Nevertheless, the dissociation of the ethylene not bound to the carbon dioxide for the second reaction mechanism supposes a high energy cost that has not been determined in this investigation, but that is important to consider at the time of choosing between these mechanisms.

N-aryl substituents[1] in both mechanisms show a better trend to design the catalyst in view of the energies they register, because IDD and IAd (the N-alkyl substituents) have less stability owing to their worse steric control executed on the reagent. Then, Isoqui and ISO, not study in the literature yet, show a favorable reaction behavior in terms of stability, as it has been exposed in the previous description.

The importance of having lower energies in the oxidative coupling is given due to the high energies in the β-elimination. As it has been already shown, both proposed mechanisms follow the same steps after the dissociation. Energetically, the transition state after the *trans*-lactone involves an unattainable way that would not take place easily, and it also results unreal to develop in the laboratory. At the same time, the transition state after the *cis*-lactone, despite of having high energies, allow to produce the hydride acrylate that is necessary to continue to the following steps to produce acrylic acid.

# 5.2 Intermediates comparison

After the dihedral scan coordinate done for all the intermediates in order to obtain the conformer with the lowest energy and from this study the rest of the steps of each mechanism, it is important to compare them as it follows.

## 5.2.1 *Cis*-Lactone vs. *Trans*-Lactone

**Table 5.1. Gibbs Free Energies for *Cis*-Lactone and *Trans*-Lactone in all ligands**

| Ligand | *Cis*-Lactone | *Trans*-Lactone |
|---|---|---|
| | Gibbs Free Energy [kJ mol$^{-1}$] | Gibbs Free Energy [kJ mol$^{-1}$] |
| **IPr** | 92.43 | 57.00 |
| **SIPr** | 95.67 | 50.19 |
| **IAd** | 66.19 | 50.99 |
| **IDD** | 101.14 | 58.82 |
| **ISO** | 85.85 | 35.83 |
| **Isoqui** | 66.35 | 35.54 |
| **IHept** | 36.44 | 6.98 |
| **IPr*** | 94.68 | 49.65 |
| **SIPr*** | 92.00 | 47.67 |

As it is shown in Table 5.1, all ligands registered that the *trans*-lactone is more stable than *cis*-lactone, owing to the bound formed by C-Ni-O in the first case, which bond energy is higher than the C-Ni-C bond present in the second case, and this means while the higher the bond energy is, the more stable is the compound.[5]

According to the molecules and their steric control[1], it has been found that the ones having a major shielding, have lower energies, so that is why ligands as IHept, IPr* and SIPr* show low values in this intermediate. Nevertheless, asymmetric ligands as ISO and Isoqui show stable molecules for both cases, due to the electronic cloud that provide a better stability to this lactone.

Then, in Figure 5.10 it is shown the structure found for the ligand that provides the most stable lactones, IHept.

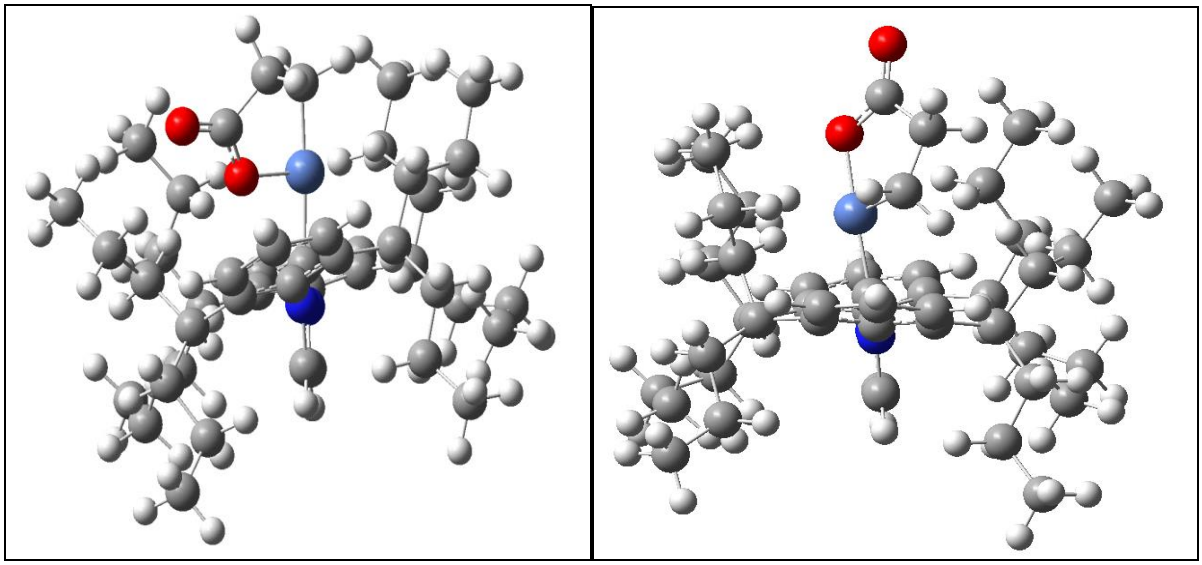

**Figure 5.10. *Cis*-lactone (left) and *Trans*-lactone (right) for ligand IHept**

Through the Figure 5.10, it is possible to detail the C-Ni-C bond present in the *cis*-lactone, while the C-Ni-O bond, energetically more stable than the another.

In addition, it has been found possible agostic interactions between the metallic center and one of the hydrogens present in the substituents. This type of interactions provides a higher stability to the molecules, as it happens with other cases as hydrogen bonds and intermolecular strengths. In Figure 5.11, it is shown an example with ligand IDD and *trans*-lactone, where the bond length between nickel and the hydrogen is 1.96 Å, which is characteristic of the agostic interactions and the angle ring-Ni-O is 92.2º. However, to ensure their existence, it is necessary to do a proper study in Gaussian, because this has just been studied qualitatively.

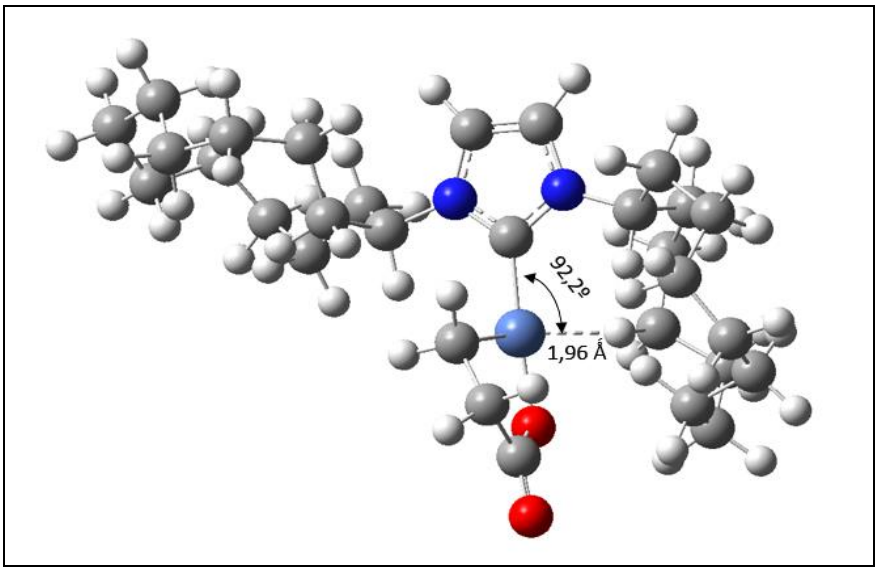


**Figure 5.11. Possible agostic interaction found for *Trans*-Lactone in IDD**

At the same time, it is studied the same intermediate, but including the ethylene that it has been mentioned in the second proposed reaction mechanism.

## 5.2.2 *Cis*-EthyleneLactone vs. *Trans*-EthyleneLactone

**Table 5.2. Gibbs Free Energies for *Cis*-EthyleneLactone and *Trans-Ethylene*Lactone-trans in all ligands**

| Ligand | *Cis*-EthyleneLactone | *Trans*-EthyleneLactone |
|---|---|---|
| | **Gibbs Free Energy [kJ mol$^{-1}$]** | **Gibbs Free Energy [kJ mol$^{-1}$]** |
| **IPr** | 21.89 | 42.24 |
| **SIPr** | 26.09 | 41.06 |
| **IAd** | 39.38 | 40.20 |
| **IDD** | 33.84 | 32.94 |
| **ISO** | 21.40 | 39.96 |
| **Isoqui** | 41.50 | 29.79 |
| **IHept** | 49.12 | 42.61 |
| **IPr*** | 28.65 | 30.43 |
| **SIPr*** | 41.78 | 57.81 |

In Table 5.2, it is possible to denote that there is not a complete coincidence among all the ligands about which is more stable between EthyleneLactone *cis* and *trans*, because for some of them the cis is more stable while for others it happens the opposite effect.

This fact can be attributed to how close is the ethylene not bound with the carbon dioxide to the metallic center. For the *trans* case, the distance becomes longer, which promotes a loss in the stability for the nickel. It has been seen the same type of interactions with the lactones that bring more

stability. In comparison with the latters, EthyleneLactones are more stable due to the stability that acquires the organometallic compound accomplishing 16 electrons around the metallic center, including the fact of having a squared planar geometry.[2] In the Figures below, there are shown both intermediates for ligand ISO.

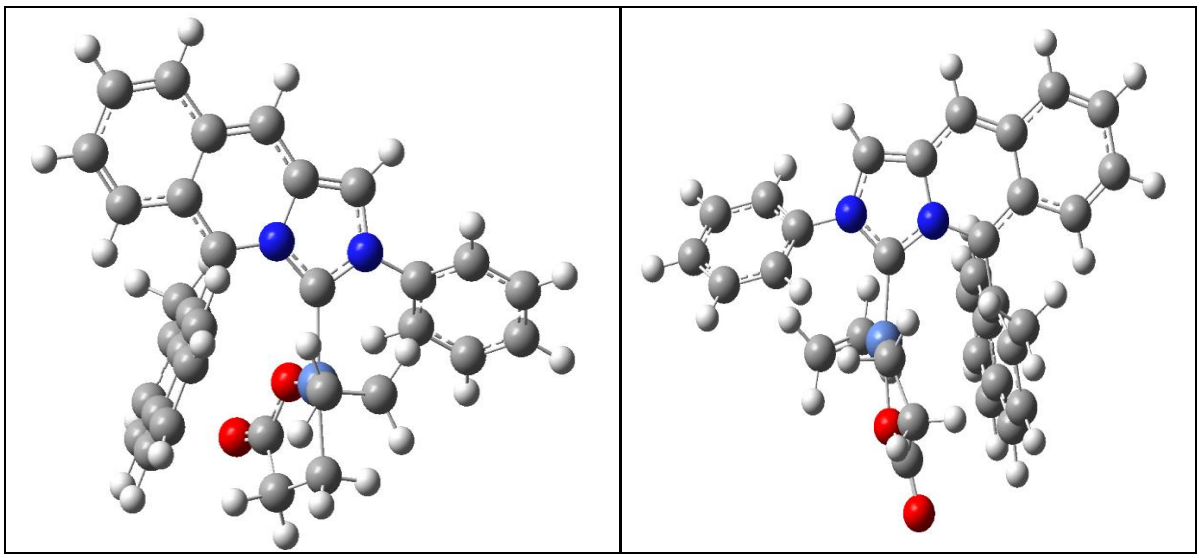

**Figure 5.12. *Cis*-EthyleneLactone (left) and *Trans*-EthyleneLactone (right) for ligand ISO**

Another intermediate that might be considered is the hydride acrylate, shown in the following sector.

## 5.2.3 *Cis*-Hydride acrylate vs. *Trans*-Hydride acrylate

**Table 5.3. Gibbs Free Energies for *Cis*-Hydride acrylate and *Trans*-Hydride acrylate in all ligands**

| Ligand | *Cis*-Hydride acrylate | *Trans*-Hydride acrylate |
|---|---|---|
| | Gibbs Free Energy [kJ mol$^{-1}$] | Gibbs Free Energy [kJ mol$^{-1}$] |
| **IPr** | 87.17 | 77.28 |
| **SIPr** | 87.14 | 69.59 |
| **IAd** | 85.76 | 67.54 |
| **IDD** | 99.23 | 149.28 |
| **ISO** | 90.76 | 133.10 |
| **Isoqui** | 95.63 | 103.60 |
| **IHept** | 66.92 | -- |
| **IPr*** | -- | 130.75 |
| **SIPr*** | -- | 125.93 |

Through Table 5.3, it is possible to denote the presence of the two types of hydride acrylate. It is found that the *trans*-hydride acrylate shows high energies for most of the ligands, being more stable the *cis*-hydride acrylate. The main reason of this fact comes from the high energy the transition state for the *trans* mechanism has, so this implies a higher barrier to break in front of the another. At the same time, in comparison with the lactones, the hydride acrylates present less stability considering the bonds Ni-O and Ni-H, which need to be dissociated for further steps in the entire mechanism, as it was established by Hollering et al.[7] In the Figure 5.13, it is shown the case for ligand IDD.

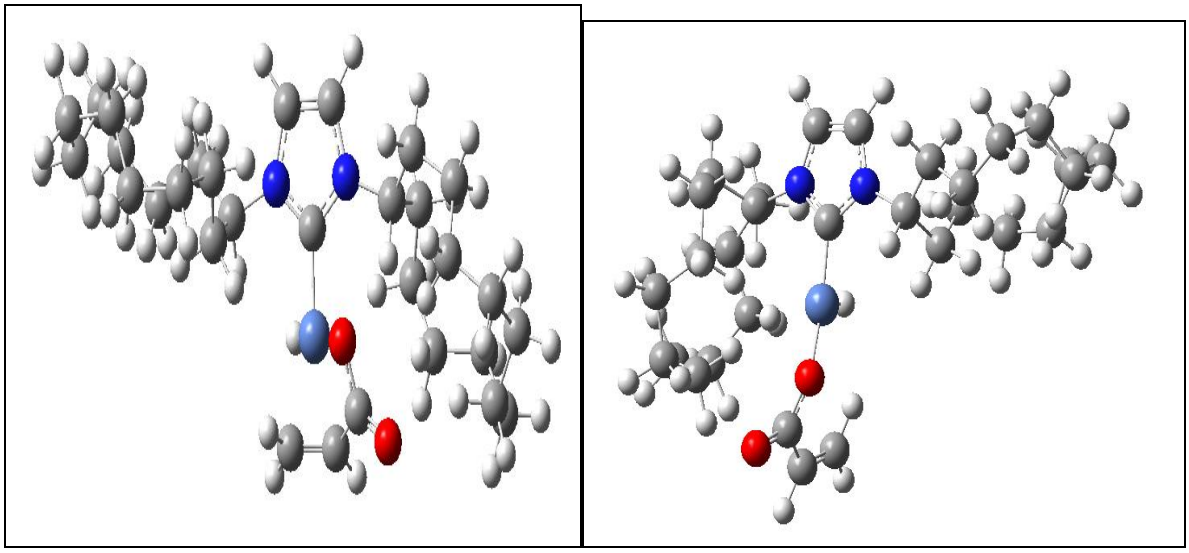

**Figure 5.13. *Cis*-Hydride acrylate and *Trans*-Hydride acrylate for ligand IDD**

# 5.3 Most favorable mechanism and ligand

According to what it has been already mentioned, the β-elimination through the *trans*-lactone involves the necessity of high energies. For this reason, it would be suggested to take the mechanism via the β-coupling (producing *cis*-lactone). At the time of deciding between the first or second reaction mechanism, the criteria that has been determinant to choose among them is the dissociation of one of the ethylenes for the latter, because it might be done to continue with the mechanism. It has not been studied in this investigation, but it might consider the dissociation energy of the Ni-C bonds with the proper method. The possible ligands that are more favorable are IHept, Isoqui and ISO, which have got more stability and they allow to break the different barriers, while the others take more energetic cost until this step of the reaction.

# 5.4 Conclusions

The study of the reductive coupling of carbon dioxide with ethylene has been done through Gaussian 16. According to the chemical properties of the metallic center – Ni, they have been proposed two different mechanism reactions: the first starting with one ethylene and the second with two ethylenes, to complete the stability of 16 electrons in nickel complex. The studied steps, the oxidative coupling and the β-elimination have been considered following two different pathways depending on which $CO_2$ carbon is bound: *cis* (for β-ethylene carbon) and *trans* (for α-ethylene carbon).

It has been studied using nine ligands classified in three groups according to their steric control found in the literature. The limiting step is the β-elimination, due to the high energies it requires to be done, and besides it might be preceded by a step for which the kinetic barrier should not be too high to continue with the mechanism. Both mechanisms differ in the transition state coming from the oxidative coupling, and the second mechanism has an intermediate conformed with one lactone and one ethylene that need to be dissociated, owing to the impediment to produce the β-elimination when this gas is presented.

*Trans*-lactone has been found more stable than the *cis*-lactone in all the ligands in view of the C-Ni-O bond the first intermediate has that brings higher energy bonds and hence a better energetic behavior, including the possible agostic interactions that have been found in the structure. However, in the Ethylenelactones and Hydride acrylates, for some ligands the correspondent *cis* structure has been more stable, while for others it happens with the *trans* isomer. From one hand, in the first case the result has been obtained due to how close the ethylene is from the metallic center. From the other hand, hydride acrylates derive from the highest energy in the mechanism, which result to be more convenient for the *cis* conformer.

The transition state that exists between the *trans*-lactone and *trans*-hydride acrylate has been found practically impossible to put in practice, because the Gibbs Free Energy have resulted to be even 350 kJ $mol^{-1}$, which is unattainable in the experimental design. For this reason, the pathway considered for the reaction to take place starts from the β-coupling through the first reaction mechanism, because it has not been determined how it would be the ethylene dissociation for the second mechanism that could involve higher energetic costs. Finally, the most optimal ligands according to the results have been IHept, Isoqui and ISO, which have registered favorable energies in the process and this is desired in terms of the reaction.

# 5.5 References


1. A. Gómez-Suárez, D. J. Nelson and S. P. Nolan, *Chem. Commun*, 2017, **53**, 2650.
2. Crabtree, R. (2007). *The organometallic chemistry of the transition metals*, Yale University: Wiley.
3. R. Grubbs, A. Miyashita, M. Liu and P. Burk, *J. Am. Chem. Soc*, 1978, **100**, 2418–2425.
4. I. Vidal, S. Melchor and J. A. Dobado, *J. Phys. Chem. A*, 2005, **109**, 7500-7508.
5. Luo, Y. (2007). *Comprehensive Handbook of Chemical Bond Energies*, CRC Press: Florida.
6. H. Hoberg, K. Sümmermann, A. Milchereit, *Angew. Chem*, 1985, **97**, 320–321.
7. M. Hollering, B. Dutta and F. Kühn, *Coordination Chemistry Reviews*, 2016, **309,** 51-67.

# Chapter 6
# Methanation results

Aspen Plus has been applied to obtain different results according to the conditions mentioned in the methodology. The process simulated consists in a Gibbs reactor working at a temperature of 298 K and atmospheric pressure. There have been taken into consideration the four compounds that participate in the $CO_2$ methanation: carbon dioxide, hydrogen, methane and water. However, literature has already determined that carbon monoxide could be a product depending on the conditions for which the reaction takes place. In this chapter it will be discussed distinct aspects extracted from Aspen Plus.

The following results have been acquired due to the use of the Sensitivity analysis tool that belongs to this simulation program where it has been used a $H_2$ molar flow of 10 mol $day^{-1}$ and for carbon dioxide of 2.5 mol $day^{-1}$, but these values have just been important to establish the stoichiometric ratio as the boundary to do the calculations.
It is desired to obtain the maximum $H_2$ conversion and the higher production flow for $CH_4$ as possible, and depending on this data it will be determined which are the most optimal values for the reaction parameters.

For this reason, there will be analyzed several study cases: reaction temperature, reactants molar ratio, conversion and molar flows from determined compounds, to expose the conditions previously indicated. At the same time, there will be analyzed diverse types of waste and the influence of their properties for the carbon dioxide molar fraction in the product flow.

Then, the exothermic behavior of this reaction will be considered through an energy balance for the most favorable case found in the previous results.

## 6.1 Study of temperature and pressure

### 6.1.1 Influence of the reaction temperature

There are different parameters that must be studied to generate a complete decision about which would be the ideal properties of the methanation process considering the initial conditions, among it is found the reaction temperature.

#### 6.1.1.1 Reactants conversion

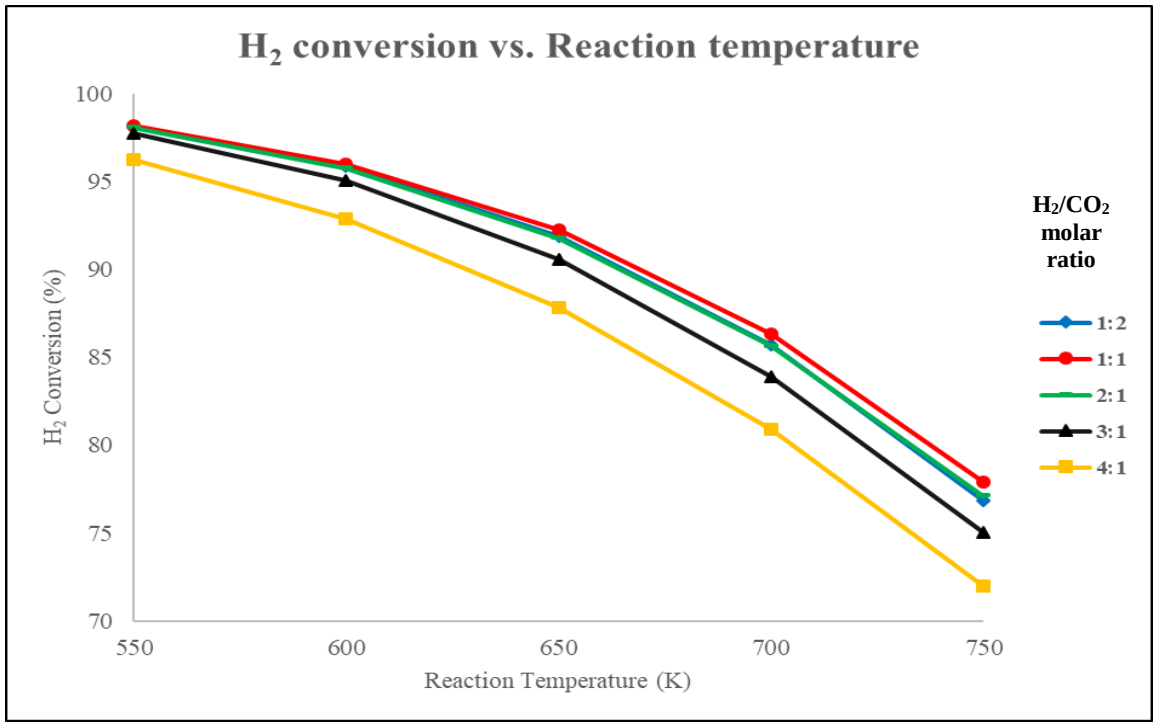


**Figure 6.1. Graphic representation of the hydrogen conversion vs. reaction temperature**

From one hand, as it has been mentioned in the methanation design conditions, the minimum temperature estimated for this reaction is 550 K. It is desired to have as high as possible conversion of hydrogen with the aim of having the product current free of hydrogen. It is shown in Figure 6.1 that for a molar ratio of reactants of $H_2/CO_2$=1 and with the minimum temperature, there is a conversion of 98.21%, in comparison with lower molar ratios that reflect how this conversion decreases. These results coincide with the ones obtained by Gao et al.[1], showing that the cause of this result (the higher the reaction temperature is, the lower will be the conversion for the same molar ratio) is due to the fact that when the temperature increases, the equilibrium constant decreases and the equilibrium reaction moves to the left, producing higher reactants flow and having a lower conversion. At the same time, the fact of increasing more the molar ratio could generate the same effect for this parameter.

A complete conversion (100%) has not been found, so it means that hydrogen would be as a component in the products, and if it is not wanted in a small proportion in this current, it must be considered any type of industrial equipment to give an use to the remaining gas, such as absorbers, separators and so on, as it would be explained in the energy balance.

To specify the maximum $H_2$ conversion found for the initial conditions of temperature and pressure and the different molar ratios, these values are shown in the Table below.

**Table 6.1: Maximum $H_2$ conversion found for each molar ratio at T=550 K and P=1 atm**

| Molar ratio ($H_2$:$CO_2$) | $H_2$ conversion (%) |
|---|---|
| **1:2** | 98.13 |
| **1:1** | 98.21 |
| **2:1** | 98.08 |
| **3:1** | 97.73 |
| **4:1** | 96.24 |

Despite of the fact that the equimolar ratio gets the highest value, it is important to know that it is also the one producing a high $CO_2$ flow that would become a problem at the time of separating the gas mixture, due to their chemical properties and the difficulty to separate gases as $CH_4$ and $CO_2$, so this ratio is not directly the best option so far.

Studying the carbon dioxide conversion with the same variable, it is possible to determine the next analysis according to the Figure 6.2.

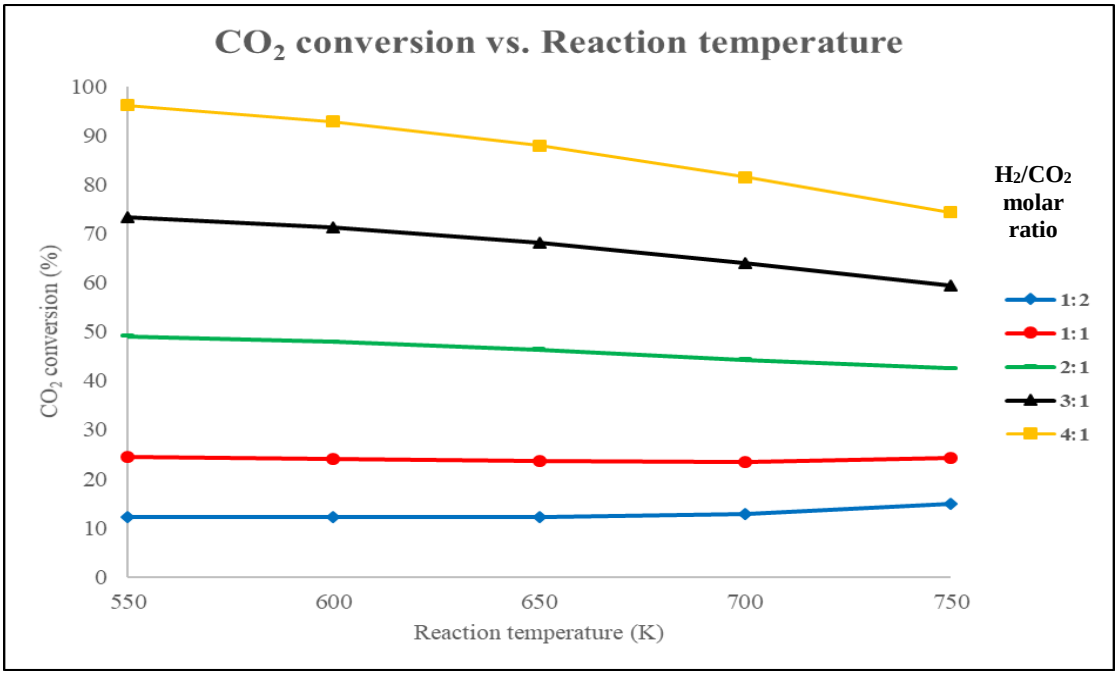


**Figure 6.2. Graphic representation of the carbon dioxide conversion vs. reaction temperature**

From the other hand, corresponding to the results obtained for the carbon dioxide conversion, it is shown in Figure 6.2 that for a higher molar ratio, the conversion would be higher, due to the fact that the equilibrium gets affected for having more reactants flow (leaving $CO_2$ fixed and considering an amount of hydrogen flow) stablishing a displacement of this reaction to the right, as it has been determined by Gao et al.[1] and resulting in a major production of $CH_4$ and $H_2O$. However, for the same

molar ratio, the temperature has the same effect that the one mentioned for hydrogen conversion, owing to the exothermic effect that promotes the decreasing of this conversion, creating a displacement of the equilibrium to the left for which $CO_2$ is less converted.

However, it is important to detail that these authors mentioned[1] in their project that starting from a stoichiometric ratio and lower values, when a certain temperature is obtained, another reaction implicated in this process, the Water Gas Shift (WGS), takes place. The latter consists in the reaction between carbon monoxide and water to obtain the methanation reactants.

It has been found through the simulation that WGS occurs at lower molar ratios (1:1 and 1:2) starting at a temperature of 650 K approximately. It is shown in Figure 6.2 that $CO_2$ conversion increases, because being $CO_2$ a product of this reaction and at the same time a reagent of the main reaction, thus this will cause at the end a displacement of the equilibrium to the right, for which the conversion will increase slightly. For this reason, these molar ratios register the opposite effect in comparison with the rest.

In addition, considering the result obtained for $H_2$ conversion about the most optimal molar ratio (1:1) according to the desired conditions in the process, and supposing that the reaction was not reversible, the maximum conversion of carbon dioxide at the design temperature (550 K) at this molar ratio would be 25%. In comparison with the reversible case, the maximum conversion is 24.59%, which means the difference between both is not high and it would depend on all the parameters involved in the process.

Other important aspects to analyze for the methanation are the production of methane and carbon monoxide.

### 6.1.1.2 Molar aspects

The aim that $CATCO_2RE$ proposes is emphasized in the production of biogas (methane), so that is why it acquires more importance to study this compound shown in Figure 6.3.

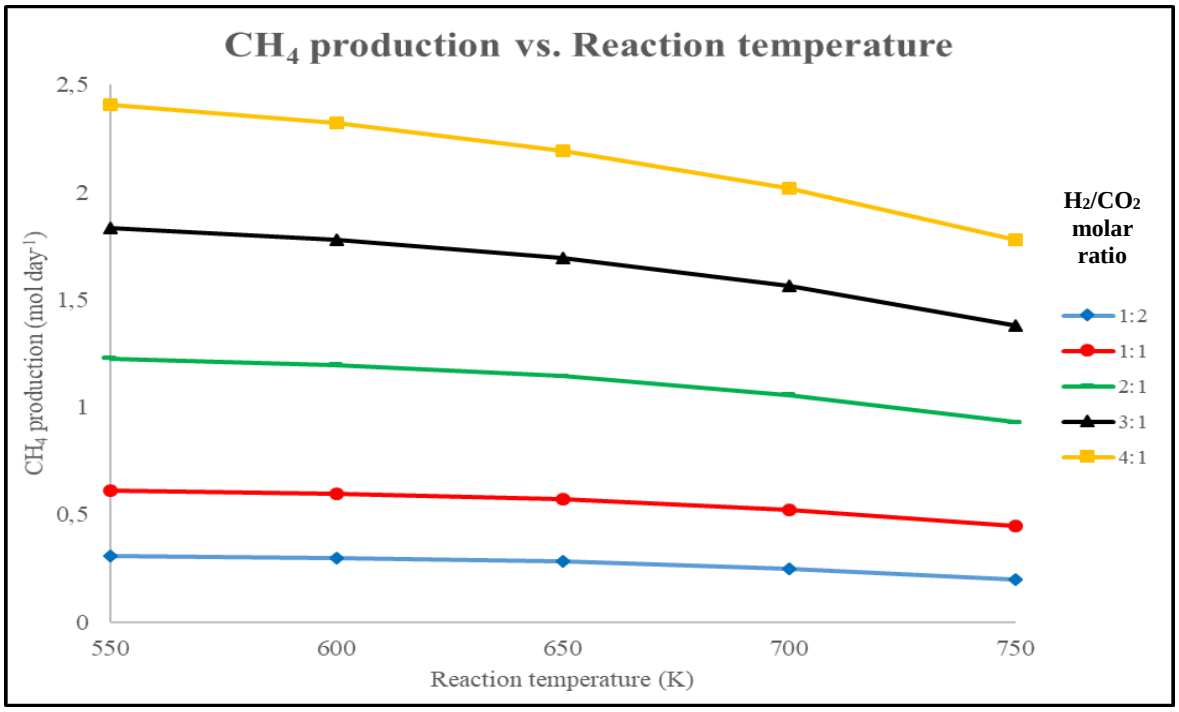


**Figure 6.3. Graphic representation of the methane production vs. reaction temperature**

Kopyscinski[2] and Gao et al.[1] determine in their projects that a higher molar ratio would promote a higher production of methane, while a higher temperature determines the inverse effect: its decreasing for the exothermic behavior of the reaction. When the molar ratio is equals to 0.5, at 550 K the production is 0.122 mol $day^{-1}$ and when this value is equals to 4 at the same temperature, 2.41 mol $day^{-1}$ are produced, owing to the previous theory stablished by the authors. It is important to highlight how the flow production changes when the reaction takes place with a higher amount of hydrogen, e.g. a higher ratio. There are variations of approximately 0.6 mol $day^{-1}$ when for the same temperature, the molar ratio increases a unit. The preference to compare one or another ratio completely depends on how high the production is wanted to be, and to make a choice of which factor, hydrogen conversion or methane production, is more important.

Nevertheless, being the main product, it is necessary to visualize how much methane is produced according to the product flow, so that is why this molar fraction is represented versus the reaction temperature, shown in Figure 6.4.

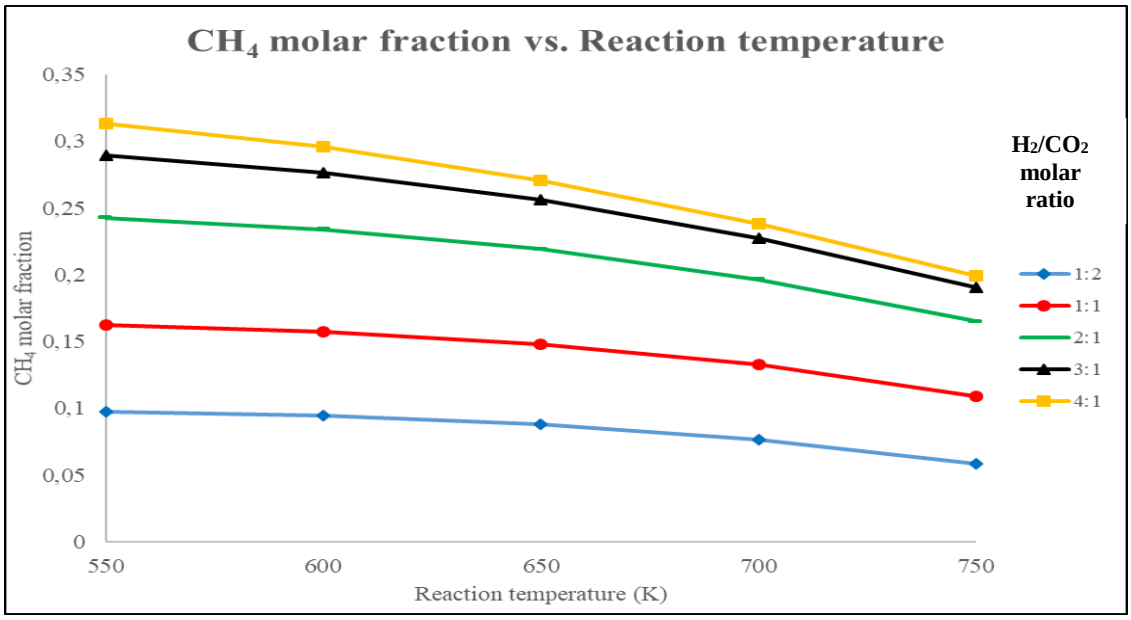


**Figure 6.4. Graphic representation of the methane production vs. reaction temperature**

The results show a high similarity with the correspondent curves for each molar ratio in Figure 6.3, having a major molar fraction when the ratio is 4, due to the fact that besides being the stoichiometric conditions, both products are formed without any limitant or excess reagent involved in the reaction, and this provides the best scenario to produce methane.

In addition, another variable that might be important to detail for this study is the carbon monoxide production to understand how the secondary reaction occurs (Water Gas Shift) throughout the process.

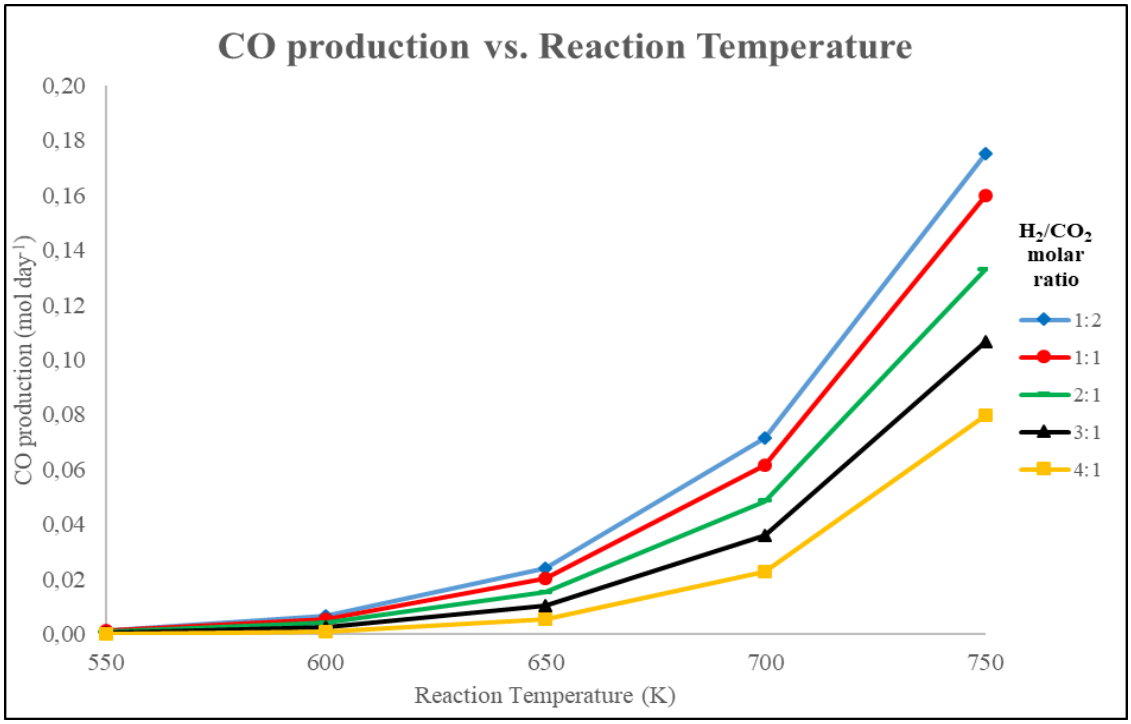


**Figure 6.5: Graphic representation of the carbon monoxide production vs. reaction temperature**

At the same time, the Water Gas Shift reaction takes place at elevated temperatures according to Granitsiotis[3]. In this case, it is shown in Figure 6.5 how carbon monoxide starts to appear more rapidly over 600 K and even faster after 650 K. This has been found with the study of carbon dioxide conversion, where after 700 K, this reaction takes place simultaneously with the methanation one. The highest value found has been 0.175 mol $day^{-1}$ at a molar ratio 0.5:1, so it means that if it is considered to work with this relation to have a higher conversion of hydrogen at atmospheric pressure, it would be a higher carbon monoxide production in comparison with other molar ratios. In addition, the slope of the line that form two points increases faster with the temperature value, which indicates that much more carbon monoxide is produced with this rapid variation.

### 6.1.1.3 Methane yield

Then, methane yield is estimated regarding both reactants, shown in the following Figures.

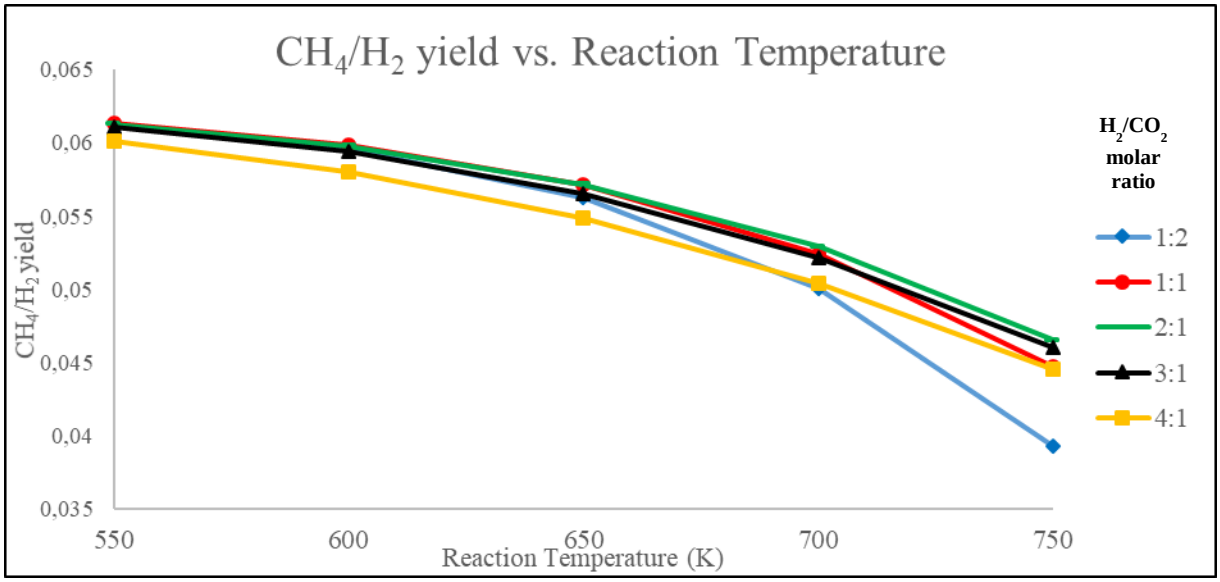


**Figure 6.6. Graphic representation of methane yield regarding $H_2$ vs. reaction temperature**

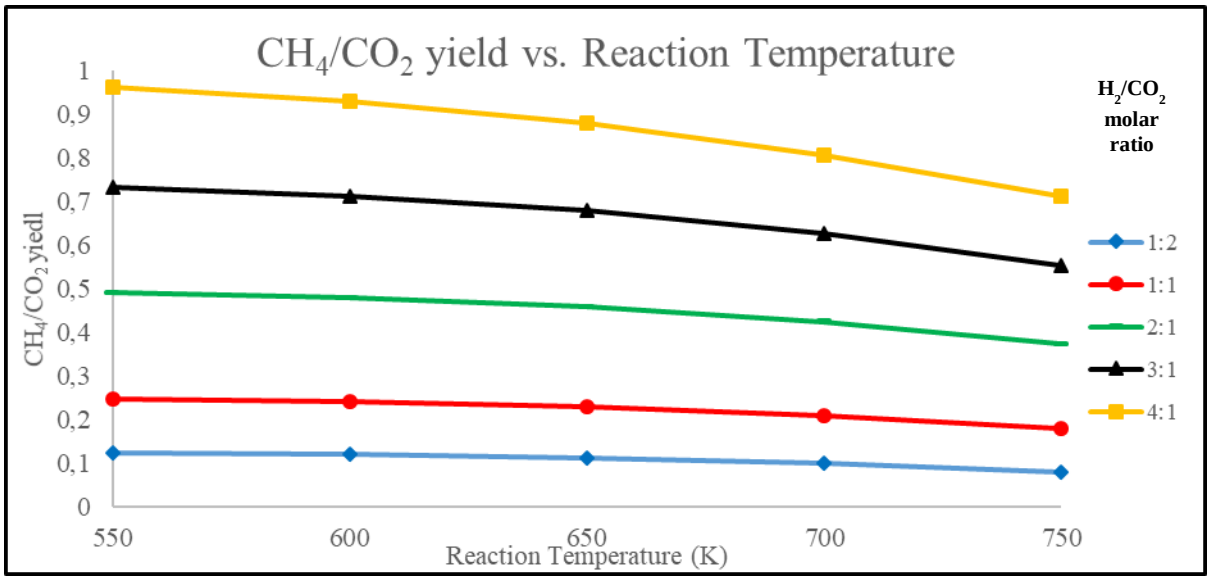


**Figure 6.7. Graphic representation of methane yield regarding $CO_2$ vs. reaction temperature**

Through Figures 6.6 and 6.7, it is shown that for both reactants, there are opposite effects in terms or yield, because while for $H_2$ the best condition is the 1:1 molar ratio, for $CO_2$ is the stoichiometric case. The higher the yield is, the more adequate is $CH_4$ production for this process, because at this point the economic cost will be lower when more reactive is profited to produce methane, as it will be shown in the energy balance.

For this reason, at this point it is known that the best temperature in which the reaction would take place according to the stablished goals is 550 K, the minimum value from the design. However, the molar ratio can not be decided yet without doing a study of the influence of the pressure in the methanation reactor and an energy balance for the process, that will provide a better judgement to estimate the best design conditions.

## 6.1.2 Influence of the pressure in the methanation reactor

As it has been done for the reaction temperature, there will be discussed also the same parameters that has been studied with the latter to provide another conclusion from this magnitude.

### 6.1.2.1 Reactants conversion

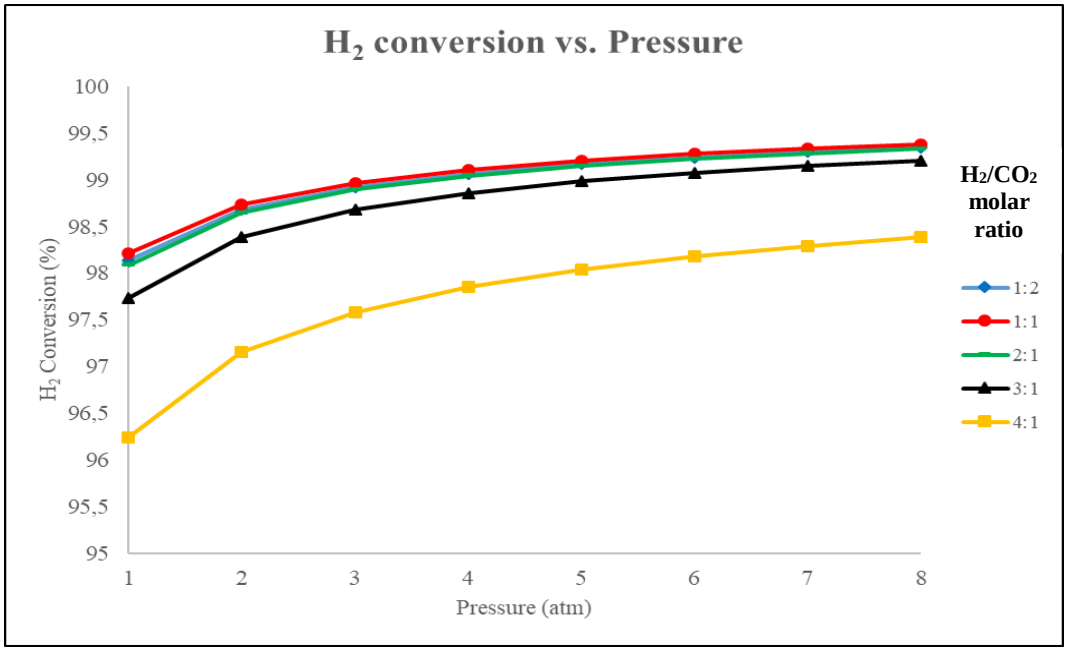


**Figure 6.8. Graphic representation of the hydrogen conversion vs. methanation reactor pressure**

Granitsiotis[3] discussed in his project that the influence of the pressure in the hydrogen conversion implies a higher value when the pressure increases, owing to the effect produced in the equilibrium: when there is an amount of this parameter, the reaction displaces to the side in which there is a minor quantity of gaseous moles. In this case, there are three moles in the right side in comparison with the five moles found in the reagents side, so that is why it displaces to the right. This conclusion has been found in the previous figure. At the same time, it has been calculated that for a

molar ratio equals to 1, the maximum conversion is found at the pressure of 8 atm: 99.37%. However, it is necessary to study the rest of parameters to verify how beneficial would be high pressures in the process.

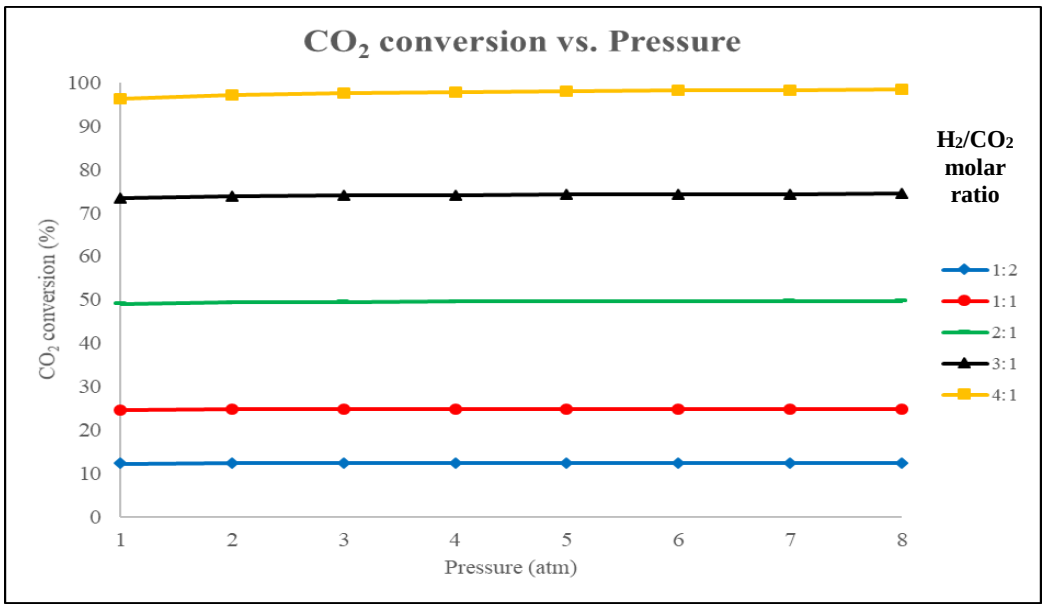


**Figure 6.9. Graphic representation of the carbon dioxide conversion vs. methanation reactor pressure**

In Figure 6.9 it is shown that for the same molar ratio, the increasing of pressure does not affect significantly carbon dioxide conversion, so this indicates the major influence of the reagents proportion over the pressure in terms of equilibrium, that is displaced to the right as it has been mentioned for the reaction temperature.

### 6.1.2.2 Molar aspects

As it has been discussed for the reaction temperature, it will be shown the results obtained from the influence of the methanation reactor pressure for methane production and its molar fraction, and carbon monoxide production in Figures 6.10 and 6.11.

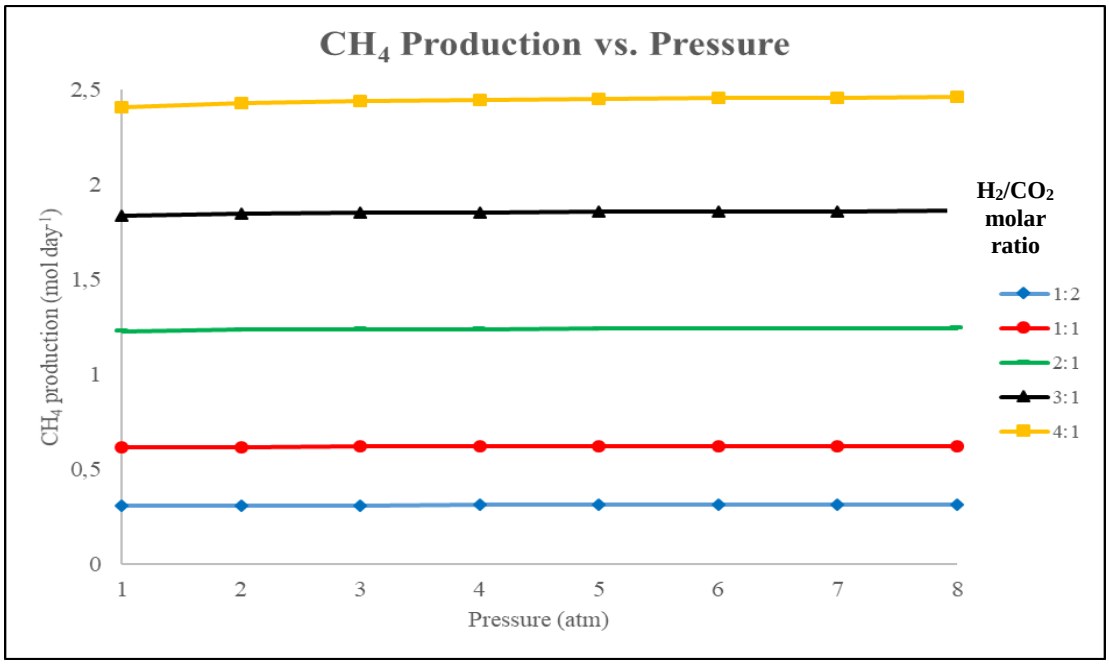


**Figure 6.10. Graphic representation of the methane production vs. methanation reactor pressure**

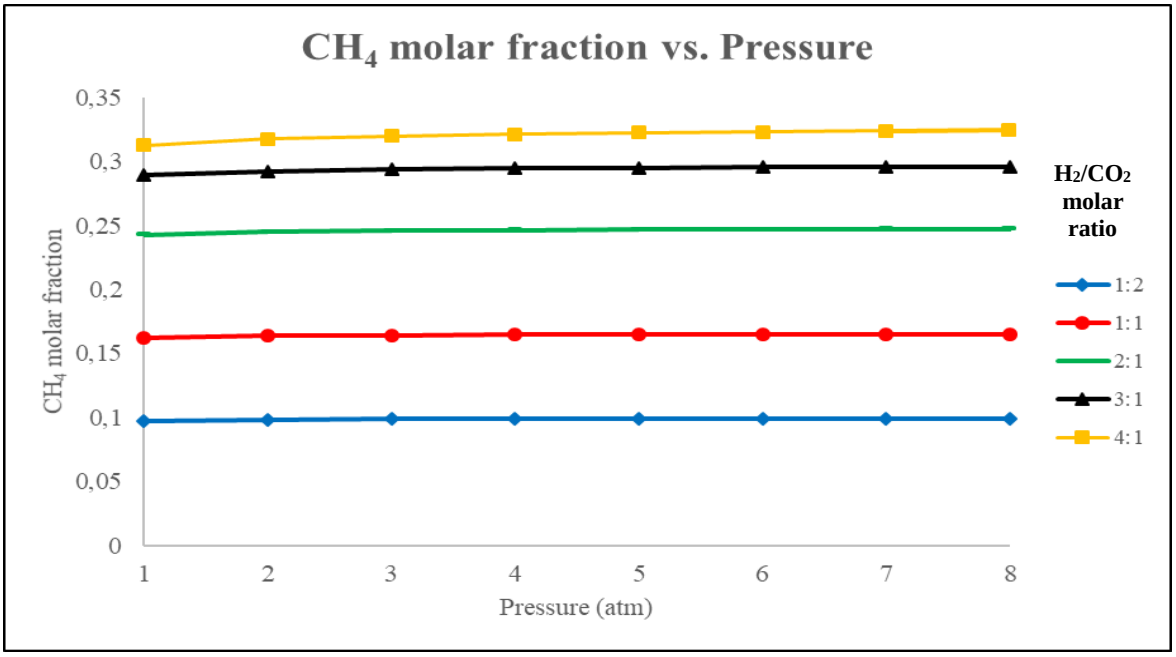


**Figure 6.11. Graphic representation of the methane molar fraction vs. methanation reactor pressure**

It can be appreciated that the major methane production and molar fraction occurs at 8 atm when the molar ratio is 4, taking a value of 2,45 mol $day^{-1}$ (32,44%). For all these cases, with a higher pressure, these values do not change significantly, as it has been exposed for carbon dioxide conversion. It is understood that the equilibrium displaces to the right, where there is a minor quantity of moles to counter the effect of the pressure. However, in a range between 0 and 8 atm, it is not truly important to analyze this variable.

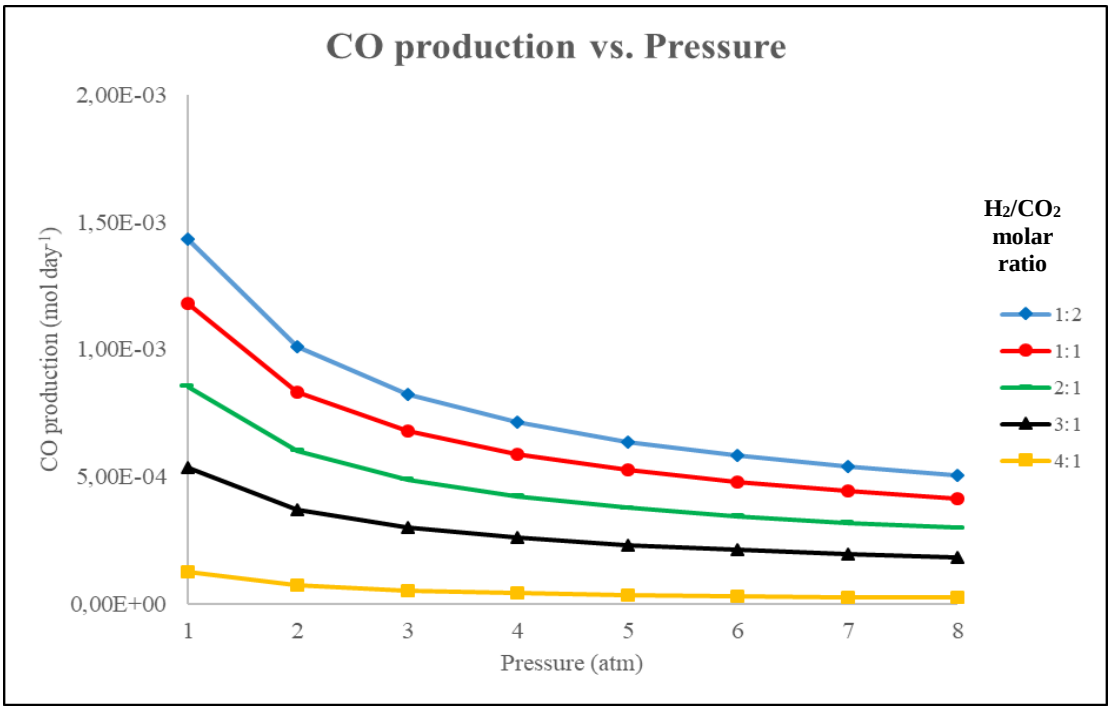


**Figure 6.12. Graphic representation of the carbon monoxide production vs. methanation reactor pressure**

Comparing Figure 6.12 and Figure 6.5 allow to affirm that the increasing of the pressure affects significantly the carbon monoxide production that is almost one thousand times lower than the production affected by the increasing effect of temperature, due to the fact that in terms of equilibrium, Water Gas Shift reaction does not seem affected due to the same number of moles at each side of the reaction, so this does not provide a major production.

Thus, the cause of the decreasing of CO production with higher pressures is attributed directly to the exothermic behavior already mentioned and the fact of the best conditions found in the simulation for which WGS occurs (low pressures and high temperatures).

### 6.1.2.3 Methane Yield

In this case, methane yield study for this magnitude is present in the Figures below.

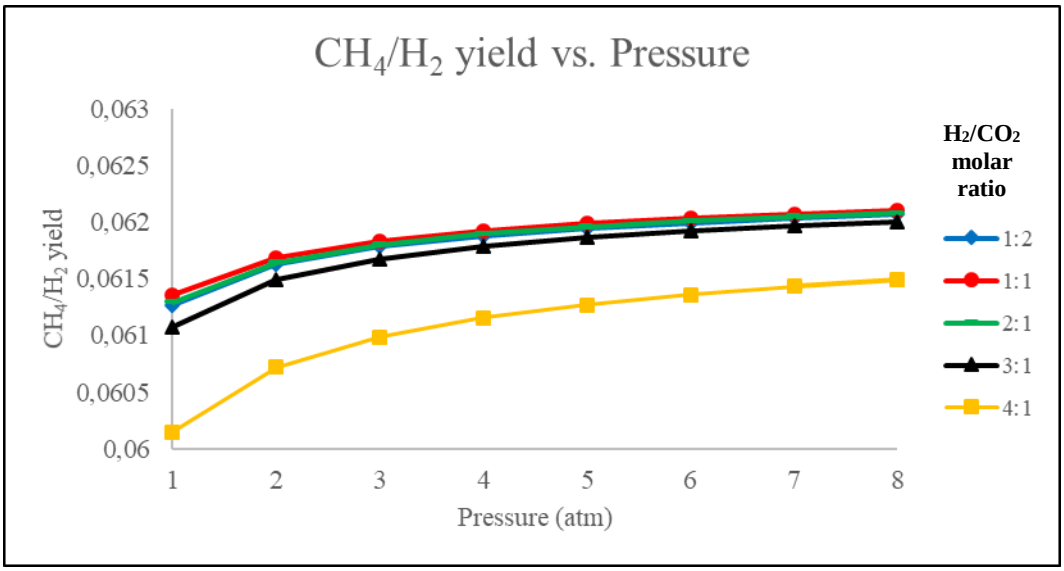


**Figure 6.13. Graphic representation of methane yield regarding $H_2$ vs. pressure**

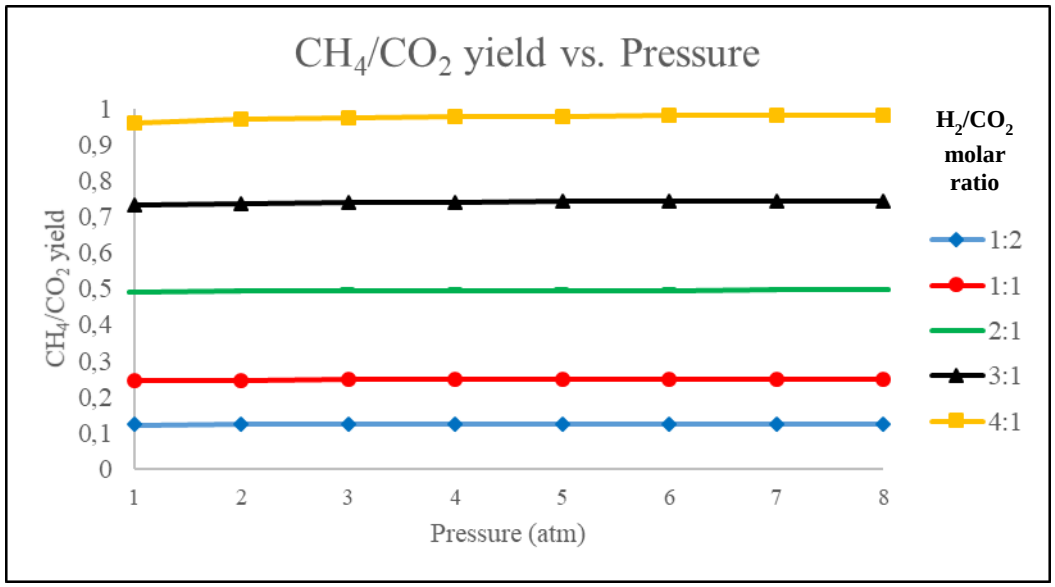


**Figure 6.14. Graphic representation of methane yield regarding $CO_2$ vs. pressure**

As it has been down with the reaction temperature, methane yield according to the pressure shows a proper result when there are high pressures, as it has been obtained by Gao et al.[1] Nevertheless, the most adequate ratio would depend in the type of separation expected after the reaction, due to the fact that the stoichiometric ratio would bring more hydrogen, which is easier to separate in comparison with the equimolar ratio, where there is a higher $CO_2$ flow, as it has been mentioned before.

After the study of the influence of both variables, it is possible to affirm that the best conditions to obtain the higher $H_2$ conversion and the higher $CH_4$ production without compromising other factors significantly in the process as the economic one, is produced working at high pressures and low temperatures (even the minimum 550 K seems to be the best option). The election of the best

$H_2$:$CO_2$ molar ratio for this design can not be determined exclusively with the previous analysis, because there are other important factors that might be considered too as the energy balance.

## 6.2 Energy balance

The energy balance in the Gibbs reactor has been calculated considering the feed and product flow, whereby the value of Duty corresponds to the heat formed by both exothermic reactions. Now, as the temperature necessary to carry out the methanation has already been chosen, the value acquired for the Duty is estimated for different pressures and molar ratios and they have been studied to determine how the process is more viable energetically.

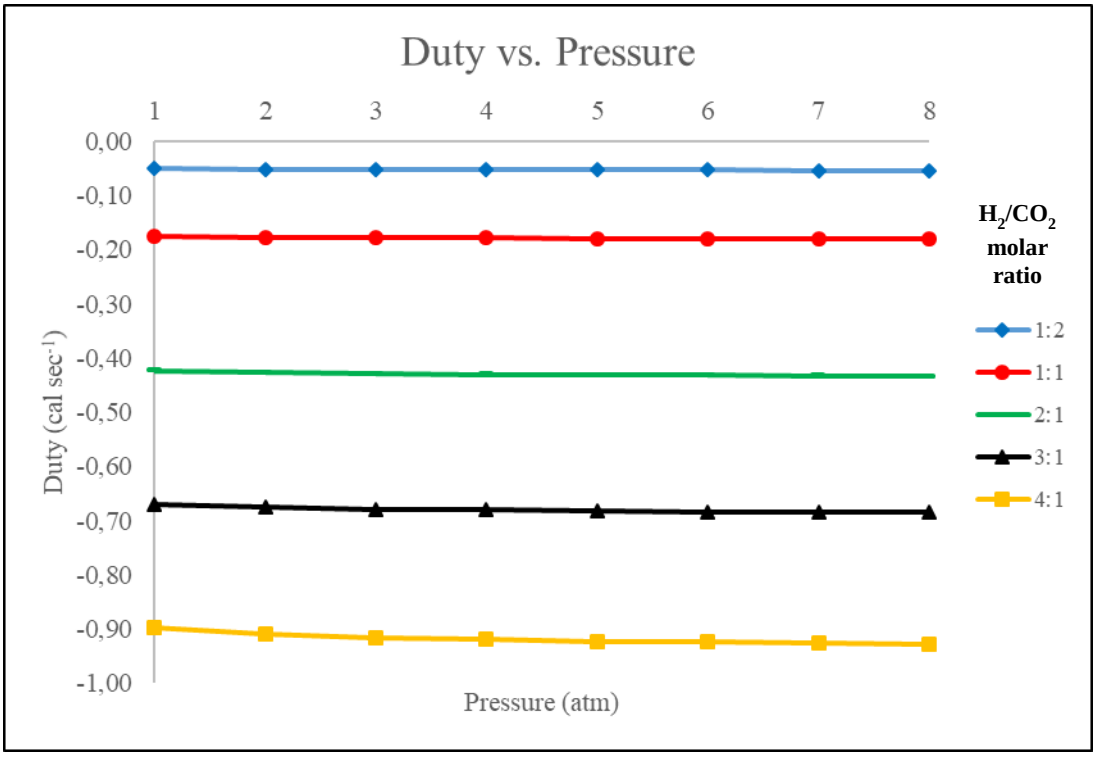


**Figure 6.15. Graphic representation of reactor duty vs. pressure**

Figure 6.15 shows that the Gibbs reactor produces a higher duty when there are high pressures and the molar ratio increases, due to the two effects already mentioned (the increasing of reagents flow and an amount in the pressure, which generate a displacement in the reaction to the right, promoting the formation of products). Nevertheless, the meaning of having more heat in the reaction could be beneficial if it is employed for other processes and it would avoid looking for other sources to obtain energy and hence higher costs.

According to the objectives already mentioned, this energy balance should not be focused exclusively in the reactor, because at the end it is preceded and followed by other machines and equipment which are extremely important due to the energy they use or produce in the process. This

fact means that the election of any specific pressure or molar ratio basing just on the previous Figure is not enough to rule out other conditions.

Therefore, it has been created a flow diagram considering a compressor, two heat exchangers and a separator as it has been done by Porubova et al.[4], to indicate how the energy may be estimated for different cases. The compressor has been considered to compress the feed flow from the atmospheric pressure to a higher pressure. This current comes at room temperature where it might be heated until 550 K before going into the reactor using a refrigerant and working isothermally. After the product flow could be cooled before going into a separator in which the gases start to separate.

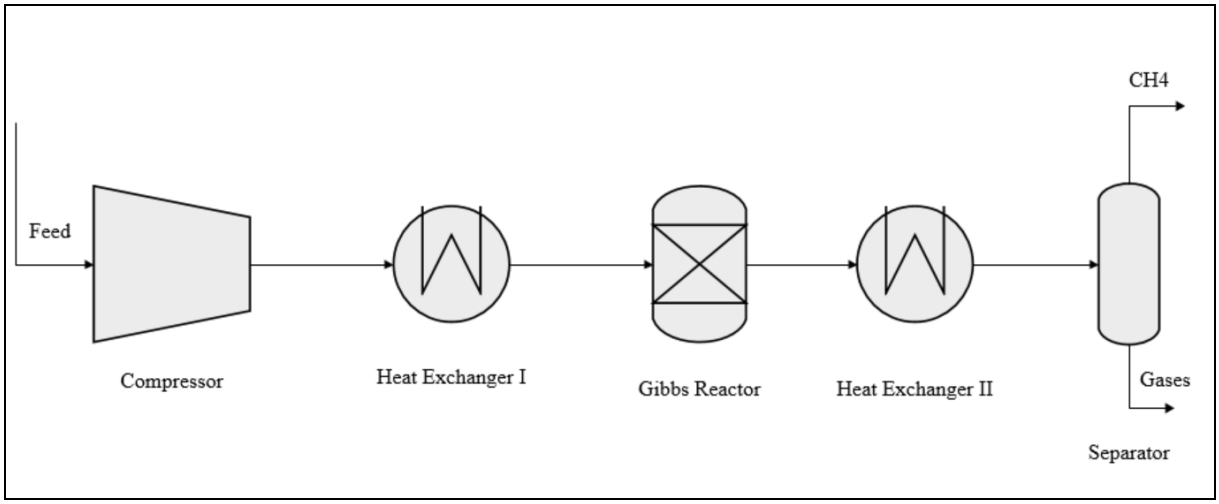


**Figure 6.16. Flow diagram for methanation process**

In terms of energy, it is desired to have low costs, so that is why in this design it might be considered the compression energy, heating and cooling energy and separation energy. In the methods, it is presented the mathematic relation for the latter.

Compression energy increases when the final pressure is higher, so that is why the feed flow may not be compressed until extremely high pressures because it would represent a high energy cost, even more when this energy might be imposed by external factors. In the case of heating and cooling, it is important to understand that the main variables to get a certain temperature would depend directly on the flows and the current compositions, so qualitatively this energy is harder to estimate.

Thus, the energy separation has been estimated using the Gibbs energy of separation, which works for ideal gases using molar fractions in dry basis, because water is easier to separate in comparison with the rest of gases and that is why it has been discarded. This is not the exactly case, but it brings an idea on how the energetic behavior is. As it has been done for the exothermic energies, in Figure 6.17, it is shown a hypothetical case for this magnitude.

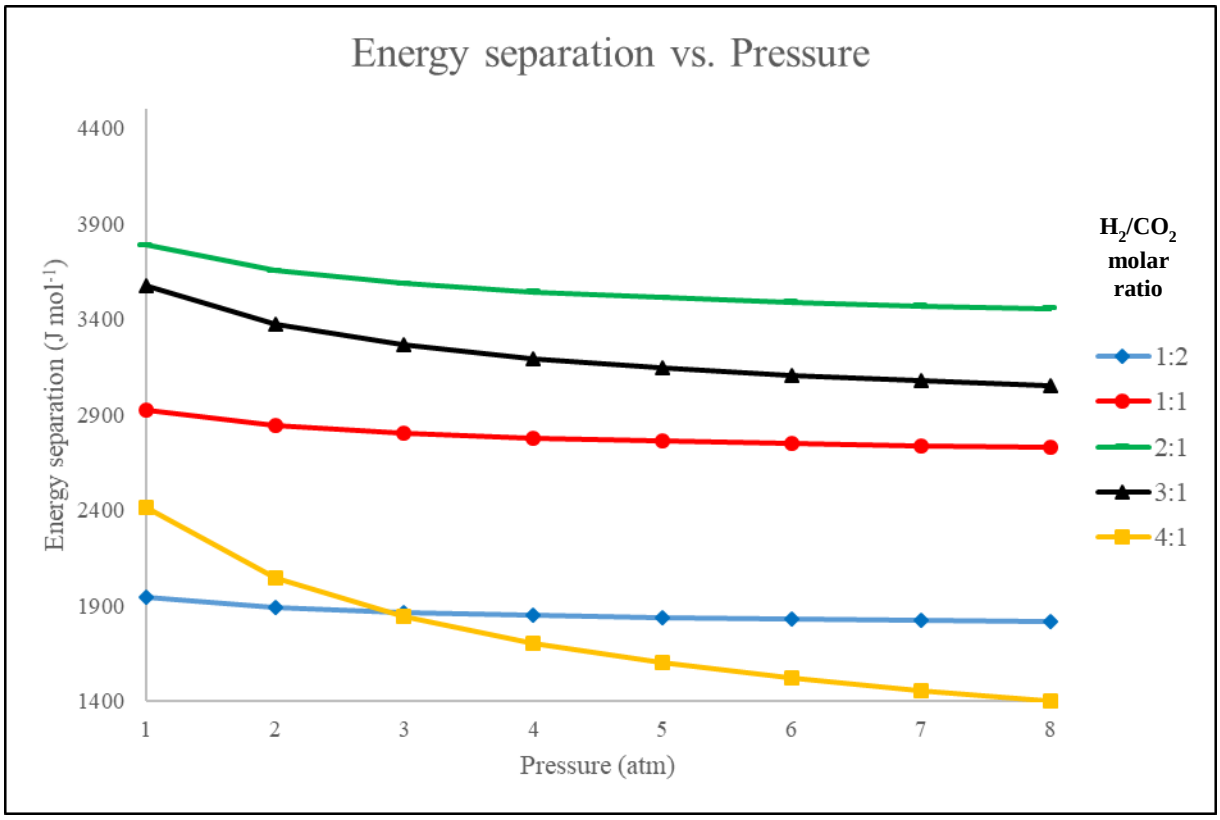


**Figure 6.17. Graphic representation of energy separation vs. pressure**

Differing from the previous case, energy separation seems to acquire the lowest values at high pressures and a stoichiometric ratio. For this reason, it is needed to do a total energy balance considering each energy to stablish a final judgement about the optimal conditions, because energy separation is just a part of the entire calculation.

Considering these analysis, the conditions from Figure 6.17 are the best option to design the methanation process so far. From one hand, when the molar ratio gets lower values than the stoichiometric, $CO_2$ has a major composition in the product, which means it would be harder to separate from methane and the rest of gases, in comparison with $H_2$. From the other hand, working at higher molar ratios would be the opposite case, but producing less methane with a better yield.

Then, it will be studied several types of waste for the methanation reaction in the following sector.

# 6.3 Types of waste for methanation reaction

Starting from Table 4.1 in Chapter 4, there have been created distinct simulations for each type of waste depending on the feed composition. Household waste, wastewater treatment and waste of agrifood industry have been considered according to three cases for which the term of higher or lower refers to the $CO_2$ composition; the average case refers to the middle value that each compound has in their correspondent range of concentrations. In the methods, it is possible to denote the molar fractions used for each simulation at 550 K and atmospheric pressure.

At the same time, it is important to mention three aspects:

1. Oxygen has not been considered in the simulations, because the mixture between hydrogen and this gas at elevated temperatures is hazardous.
2. Agricultural wastes have not been simulated, due to the fact that their compositions are exactly the same than wastewater treatments.
3. Molar fractions have been calculated in dry basis to facilitate the study.

Then, these simulations have been created to determine how is the behavior when there is present a low (L-) or high (H-) gas network, and how it is possible for each of them to accomplish one of the conditions stablished in the methodology: 6% (L-gas network) or 4% (H-gas network) for $CO_2$ molar fraction in the product flow.

### 6.3.1 L-gas network study

L-gas network has been studied through the following tables that show all simulation results obtained for product composition, hydrogen and methane flows, reactants conversion and a summary for three parameters for this network.

**Table 6.2: Product composition in dry basis for L-gas network according to the types of waste**

| Compound | Household Waste (average) (feed molar fraction %) | Household Waste (higher) (feed molar fraction %) | Household Waste (lower) (feed molar fraction %) | Wastewater treatment (average) (feed molar fraction %) | Wastewater treatment (higher) (feed molar fraction %) | Wastewater treatment (lower) (feed molar fraction %) | Waste of agrifood industry (feed molar fraction %) |
|---|---|---|---|---|---|---|---|
| **$CH_4$** | 85,86 | 83,09 | 88,61 | 89,03 | 87,69 | 90,40 | 89,54 |
| **$CO_2$** | 5,95 | 5,98 | 5,92 | 5,95 | 5,99 | 5,99 | 5,95 |
| **$N_2$** | 2,52 | 5,06 | 0,00 | 0,05 | 1,00 | 0,00 | 0,00 |
| **CO** | 0,00 | 0,00 | 0,00 | 0,00 | 0,00 | 0,00 | 0,00 |
| **$H_2$** | 5,65 | 5,85 | 5,45 | 4,50 | 5,30 | 3,60 | 4,50 |

**Table 6.3: $H_2$ and $CH_4$ flows for L-gas network according to the types of waste**

| Compound | Household Waste (average) (feed molar fraction %) | Household Waste (higher) (feed molar fraction %) | Household Waste (lower) (feed molar fraction %) | Wastewater treatment (average) (feed molar fraction %) | Wastewater treatment (higher) (feed molar fraction %) | Wastewater treatment (lower) (feed molar fraction %) | Waste of agrifood industry (feed molar fraction %) |
|---|---|---|---|---|---|---|---|
| **$H_2$ feed flow (mol $day^{-1}$)** | 12,67 | 13,55 | 11,78 | 8,50 | 11,34 | 5,61 | 8,50 |
| **$CH_4$ production flow (mol $day^{-1}$)** | 8,55 | 8,29 | 8,81 | 8,76 | 8,70 | 8,81 | 8,81 |

**Table 6.4: $H_2$ and $CO_2$ conversion for L-gas network according to the types of waste**

| Compound | Household Waste (average) (feed molar fraction %) | Household Waste (higher) (feed molar fraction %) | Household Waste (lower) (feed molar fraction %) | Wastewater treatment (average) (feed molar fraction %) | Wastewater treatment (higher) (feed molar fraction %) | Wastewater treatment (lower) (feed molar fraction %) | Waste of agrifood industry (feed molar fraction %) |
|---|---|---|---|---|---|---|---|
| **$H_2$ conversion** | 95,55 | 95,69 | 95,40 | 94,79 | 95,36 | 93,74 | 94,78 |
| **$CO_2$ conversion** | 83,62 | 84,44 | 82,68 | 77,47 | 81,96 | 69,25 | 77,47 |

All these values have been chosen because they belong to the maximum case in which it is found that there is a molar fraction lower than 6% for $CO_2$. As it is shown in Table 6.3, CO content in the product flow is basically null, due to its extremely low composition that could be also negligible. However, the rest of compounds show a considerable molar fraction in dry basis, among it is important to mention how hydrogen is present in this current: it is remarked in the previous conditions that this gas should have a molar fraction lower than 0.5%, but all simulations show a content higher than 4%, meaning that it is not possible to accomplish this rule and it would be necessary to add any equipment to the process to decrease $H_2$ concentration.

Then, methane shows a high molar fraction in dry basis due to the high content coming from all the feed flows, which is desirable following the goal referred to its production.

Table 6.5 shows a summary for three parameters to decide which is the best waste flow according to the hydrogen ratio in front the rest of gases, its conversion and its molar fraction.

**Table 6.5: Summary for parameters for L-gas network according to the type of waste**

| Type of waste | Ratio $H_2$/rest of gases | $H_2$ conversion (%) | $H_2$ molar fraction (%) |
|---|---|---|---|
| **Household water (average)** | 1,267 | 95,55 | 5,65 |
| **Household water (higher)** | 1,355 | 95,69 | 5,85 |
| **Household water (lower)** | 1,178 | 95,40 | 5,45 |
| **Wastewater treatment (average)** | 0,850 | 94,79 | 4,50 |
| **Wastewater treatment (higher)** | 1,134 | 95,36 | 5,30 |
| **Wastewater treatment (lower)** | 0,561 | 93,74 | 3,60 |
| **Waste of agrifood industry** | 0,850 | 94,78 | 4,50 |

It is shown in Table 6.5 that the higher the ratio $H_2$: rest of gases is, the higher is $H_2$ conversion, due to the fact that this would promote an equilibrium displacement to the right as it has been mentioned before, and it would promote a higher conversion. Nevertheless, a greater amount of

hydrogen would signify at the same time a higher molar fraction in the product flow, what it is not wanted for this process.

The highest hydrogen conversion is found in the household water (higher $CO_2$ feed molar fraction). Nevertheless, this current shows the highest molar fraction for this gas in the product flow, so that is why it is not considered to be the best option for the L-gas-network. Looking for an intermediate situation, wastewater treatments take values for these parameters which are enough feasible to design the process.

## 6.3.2 H-gas network study

H-gas network has been studied through the following tables that show all simulation results as it has been done for the low case.

**Table 6.6: Product composition in dry basis for H-gas network according to the types of waste**

| Compound | Household Waste (average) (feed molar fraction %) | Household Waste (higher) (feed molar fraction %) | Household Waste (lower) (feed molar fraction %) | Wastewater treatment (average) (feed molar fraction %) | Wastewater treatment (higher) (feed molar fraction %) | Wastewater treatment (lower) (feed molar fraction %) | Waste of agrifood industry (feed molar fraction %) |
|---|---|---|---|---|---|---|---|
| **$CH_4$** | 87,05 | 84,29 | 89,75 | 90,28 | 88,90 | 91,73 | 90,77 |
| **$CO_2$** | 3,93 | 3,97 | 3,99 | 3,98 | 3,96 | 3,98 | 3,98 |
| **$N_2$** | 2,50 | 5,01 | 0,00 | 0,50 | 1,00 | 0,00 | 0,00 |
| **CO** | 0,00 | 0,00 | 0,00 | 0,00 | 0,00 | 0,00 | 0,00 |
| **$H_2$** | 6,51 | 6,71 | 6,26 | 5,23 | 6,13 | 4,28 | 5,24 |

**Table 6.7: $H_2$ and $CH_4$ production flow for H-gas network according to the types of waste**

| Compound | Household Waste (average) (feed molar fraction %) | Household Waste (higher) (feed molar fraction %) | Household Waste (lower) (feed molar fraction %) | Wastewater treatment (average) (feed molar fraction %) | Wastewater treatment (higher) (feed molar fraction %) | Wastewater treatment (lower) (feed molar fraction %) | Waste of agrifood industry (feed molar fraction %) |
|---|---|---|---|---|---|---|---|
| **$H_2$ flow (mol $day^{-1}$)** | 13,55 | 14,43 | 12,63 | 9,34 | 12,22 | 6,45 | 9,34 |
| **$CH_4$ flow (mol $day^{-1}$)** | 8,75 | 8,49 | 9,00 | 8,96 | 8,90 | 9,00 | 9,00 |

**Table 6.8: $H_2$ and $CO_2$ conversion for H-gas network according to the types of waste**

| Compound | Household Waste (average) (feed molar fraction %) | Household Waste (higher) (feed molar fraction %) | Household Waste (lower) (feed molar fraction %) | Wastewater treatment (average) (feed molar fraction %) | Wastewater treatment (higher) (feed molar fraction %) | Wastewater treatment (lower) (feed molar fraction %) | Waste of agrifood industry (feed molar fraction %) |
|---|---|---|---|---|---|---|---|
| **$H_2$ conversion** | 95,17 | 95,31 | 95,03 | 94,44 | 94,98 | 93,49 | 94,43 |
| **$CO_2$ conversion** | 89,07 | 89,58 | 88,23 | 84,82 | 87,97 | 79,41 | 84,82 |

The results for this case are similar to the previous one in terms of composition and variables. CO is found to be also practically null, methane presents high values for the same feed composition reason, $N_2$ as it is inert in the reaction, have a higher or lower concentration depending on the one this gas in the feed, and $CO_2$ has been studied in the maximum case in which it is obtained a molar fraction equals to 4% in dry basis. Hydrogen values might be lower if there is considered another process design in order to decrease its concentration.

**Table 6.9: Summary for parameters for H-gas network according to the type of waste**

| Type of waste | Ratio $H_2$/rest of gases | $H_2$ conversion (%) | $H_2$ molar fraction |
|---|---|---|---|
| **Household water (average)** | 1,355 | 95,17 | 6,51 |
| **Household water (higher)** | 1,443 | 95,31 | 6,71 |
| **Household water (higher)** | 1,263 | 95,03 | 6,26 |
| **Wastewater treatment (average)** | 0,934 | 94,44 | 5,23 |
| **Wastewater treatment (lower)** | 1,222 | 94,98 | 6,13 |
| **Wastewater treatment (higher)** | 0,645 | 93,49 | 4,28 |
| **Waste of agrifood industry** | 0,934 | 94,43 | 5,24 |

According to the Table 6.9, the result is the same found for L-gas network, household water feeds have high conversions but also high molar fractions for $H_2$, that are not desired for the process.

However, wastewater treatments have a more adequate result for the methanation, owing to the kinetics and thermodynamics involved in the reaction that is favorized when $H_2$ molar ratio:the rest of gases is necessary to not exceed the determined boundaries shown in the methods (hydrogen molar fraction is even higher for household water treatments).

# 6.4 Conclusions

The study of the $CO_2$ methanation done through the design of a Gibbs reactor in Aspen Plus has allowed to determine that mainly changes in pressure and temperature influence significantly on different parameters such as the conversion of reagents, the production of methane and the production of carbon monoxide, for being involved in a secondary reaction as the Water Gas Shift, produced from 650 K and low pressures. At the same time, in terms of the goals outlined by CATCO2RE, it is necessary to have the maximum conversion of $H_2$ and the major methane production which are achieved when it is worked at a temperature of approximately 550 K, minimum established from the beginning in the methods.

Pressure is a magnitude that would favorize this reaction when it acquires higher values than the atmospheric one. Although it is true that they are ideal for the goals already mentioned, in terms of energy it is important to not work with extremely high pressures, because the compression energy promotes a higher cost while there is a higher pressure for the reaction. Regarding the reactants molar ratio, from the beginning it is harder to determine a specific relation according to the goals, in view they have opposite effects if they are taken higher or lower values than the stoichiometric ratio, what leads to do an energy balance. This calculation has shown from the Gibbs reactor through which it is looked for an optimization energy that the stoichiometric ratio produces higher energies coming from the exothermic reactions. However, they could be profited for other processes and this judgement can not be only based in the reactor. For this reason, there have been considered more machines in the study: a compressor, two heat exchangers and the separator.

The separation energy has been estimated from the supposition of working with ideal gases and it just brings an idea on how much energy would be obtained from determined pressures and molar ratios. It is obtained that for the stoichiometric ratio the lowest and the most optimal energy is produced so far. With this result, it is important to carry out a global study of the process with all the components in such a way that the validity of one or the other parameter is fully studied.

Finally, it has been found that wastewater treatments have a more adequate result for the methanation, owing to the kinetics and thermodynamics involved in the reaction that is favorized when $H_2$ molar ratio/the rest of gases is necessary to not exceed the determined boundaries shown in the methods, in comparison with household and agrifood wastes.

# 6.5 References


1. J. Gao, Y. Wang, Y. Ping, D. Hu, G. Xu, F. Gu and F. Su. RSC Advances, 2012, **2**, 2358–2368.
2. Kopyscinski J. (2010). *Production of synthetic natural gas in a fluidized bed reactor: Understanding the hydrodynamic, mass transfer, and kinetic effects*. Villigen: Paul Scherrer.
3. Granitsiotis, G. (2017). *Methanation of Carbon Dioxide: Experimental research of separation enhanced methanation of $CO_2$.* Estocolmo: Delft.
4. J. Porubova, G. Bazbauers and D. Markova, 2011, Scientific Journal of Riga Technical University, 2011, **6**, 79-84.

# Chapter 7
# Conclusions and future work

## 7.1 Conclusions

A design of $CO_2$ utilization catalytic processes has been done and studied for two different cases: the reductive coupling of $CO_2$ with ethylene using Gaussian 16 and its methanation using Aspen Plus.

From one hand, the reductive coupling of $CO_2$ with ethylene has been studied through homogeneous catalysis. This process involves the use of N-Heterocyclic carbenes (NHC) that have become very important in the last years in the organometallic chemistry investigations, in order to study this reaction and its thermodynamics. They have been studied nine ligands classified in three groups according to their steric control found in the literature.

They have been proposed two different mechanism reactions: the first starting with one ethylene and the second with two ethylenes, to complete the stability of 16 electrons in nickel complex. The studied steps, the oxidative coupling and the β-elimination have been considered following two different pathways depending on which $CO_2$ carbon is bound: *cis* (for α-ethylene carbon) and *trans* (for β- ethylene carbon). From this, the limiting step is the β-elimination, due to the high energies it requires. Both mechanisms differ in the transition state, not just because there is one more ethylene in the second mechanism, at the same time the following intermediate for this TS is constituted by one lactone and one ethylene that need to be dissociated, owing to the impediment to produce the β-elimination when this gas is presented.

At the same time, it has been found for several of the structures that there are interactions such as agostic interactions and hydrogen bonds that might be studied with other analysis in this program in order to determine its real existence, repulsions coming from the substituents such as the aromatic rings (benzenes) and the fact of the metallic center (nickel) acquires its most stable geometry (squared planar) throughout the molecule, that bring more stability to a certain ligand in the organometallic compound in comparison with others, besides their electronic and steric properties.

The β-elimination produced via the *trans*-lactone has been found practically impossible to put in practice, because the Gibbs Free Energy have resulted to be even 350 kJ $mol^{-1}$, which is

unattainable in the experimental design. Therefore, the pathway considered for the reaction to take place starts from the α-coupling through the first reaction mechanism, because it has not been determined how it would be the ethylene dissociation for the second mechanism that could involve higher energetic costs. Finally, the most optimal ligands according to the results have been IHept, Isoqui and ISO, which have registered favorable energies in the process and this is desired in terms of the reaction, that might be completed to verify its validity until the acrylic acid production.

On the other hand, the study of the $CO_2$ methanation done through the design of a Gibbs reactor in Aspen Plus has allowed to determine that mainly changes in pressure and temperature influence significantly on different parameters such as the conversion of reagents, the production of methane and the production of carbon monoxide, for being involved in a secondary reaction as the Water Gas Shift, produced from 650 K and low pressures.

The preferred temperature according to the exothermic behaviour of the reactions is 550 K, precisely the one stablished as the minimum, because higher temperatures would imply lower hydrogen conversions and worse methane production. In addition, pressure is a magnitude that would favorize this reaction when it acquires higher values than the atmospheric one. Regarding the reactants molar ratio, from the beginning it is hard to determine a specific relation according to the goals, in view they have opposite effects if they are taken higher or lower values than the stoichiometric ratio, what leads to do an energy balance. This calculation has shown from the Gibbs reactor through which it is looked for an optimization energy that the stoichiometric ratio produces higher energies coming from the exothermic reactions. However, they could be profited for other processes and this judgement can not be only based in the reactor. For this reason, there have been considered more machines in the study: a compressor, two heat exchangers and the separator.

At the same time, the separation energy has been estimated from the supposition of working with ideal gases and it just brings an idea on how much energy would be obtained from determined pressures and molar ratios. It is obtained that for the stoichiometric ratio the lowest and the most optimal energy so far. Finally, it has been found that wastewater treatments have a more adequate result for the methanation, owing to the kinetics and thermodynamics involved in the reaction that is favorized when $H_2$ molar ratio/the rest of gases is necessary to not exceed the determined boundaries shown in the methods, in comparison with household and agrifood wastes.

# 7.2 Future work

The following recommendations are made for future investigations to complete and to improve the conclusions obtained in this project:

**For reductive coupling of $CO_2$ with ethylene:**

- Study the complete reaction mechanism, basing on the results obtained in this investigation.

- Create the IRC that have not been done in this investigation for the correspondent transition state for the second reaction mechanism in the oxidative coupling.
- Verify the transition states obtained in the present investigation, because they might be confirmed by several investigators.
- Work with other N-alkyl and N-aryl substituents to study if there are others found in the literature that show a better stability for this coupling.
- Design the methodology to produce all the ligands in the laboratory and from this, compare the experimental results with the computational data obtained from the literature and this project.

**For $CO_2$ methanation:**

- Study the sensitivity analysis in Aspen Plus for higher pressures.
- Design the simulation for different wastewater treatments, including all the conditions such as pressure and temperature and the entire plant design.
- Simulate the entire process considering 550 K, high pressures and stoichiometric molar ratio, with the aim of analyzing all the parameters that are involved.
- Study the influence of the catalyst chosen for the methanation to measure the different parameters in the hydrogen conversion, carbon dioxide conversion and methane production.
- Design the compressor, heat exchangers and separators mentioned in this investigation and calculate an energy balance considering the energy produced or used for each of them.